

1987

The effects of testing frequency and temperature on the fatigue crack propagation behavior of poly(vinyl chloride) /

Jill Denise Phillips
Lehigh University

Follow this and additional works at: <https://preserve.lehigh.edu/etd>

Recommended Citation

Phillips, Jill Denise, "The effects of testing frequency and temperature on the fatigue crack propagation behavior of poly(vinyl chloride) /" (1987). *Theses and Dissertations*. 4822.
<https://preserve.lehigh.edu/etd/4822>

This Thesis is brought to you for free and open access by Lehigh Preserve. It has been accepted for inclusion in Theses and Dissertations by an authorized administrator of Lehigh Preserve. For more information, please contact preserve@lehigh.edu.

**The Effects of Testing Frequency and Temperature on the
Fatigue Crack Propagation Behavior of Poly(vinyl chloride)**

by

Jill Denise Phillips

A Thesis
Presented to the Graduate Committee
of Lehigh University
in Candidacy for
the Degree of
Master of Science
in
Materials Science and Engineering

Lehigh University

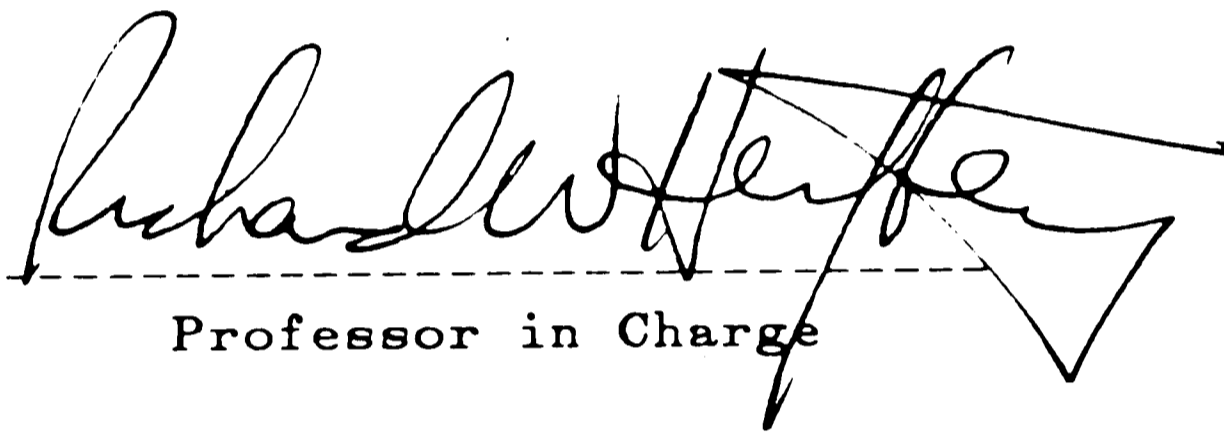
1987

Certificate of Approval

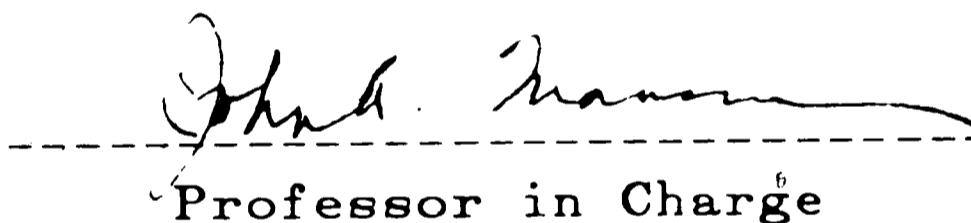
This thesis is accepted and approved in partial fulfillment of the requirements for the degree of Master of Science.

Sept 8, 1987

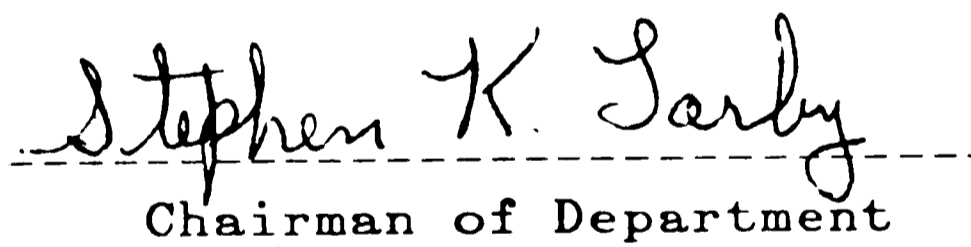
Date



Professor in Charge



Professor in Charge



Chairman of Department

Acknowledgements

The author wishes to express her sincere appreciation to her advisors, Dr. R. W. Hertzberg and Dr. J. A. Manson for their guidance, patience, and support during the course of her research.

Special appreciation is also given to Drs. Crystal Newton and Clare Rimnac, whose help and guidance throughout the author's work has been invaluable. The assistance of the members of the faculty and the staff of the Materials Science Department, in particular Dr. D. A. Thomas and Dr. W. C. Hahn, in this research and in other projects is also deeply appreciated.

The author wishes to thank her friends and fellow graduate students, especially Keith Brown, William Herman, Lisa Auerbach, Deborah Wallach and Jennifer Golub for their understanding and support.

The financial support of the Polymer Division of the National Science Foundation (Grant No. DMR-8412357) is acknowledged.

Finally, the author is indebted to her parents, Lorraine and Darrell Phillips, without whose love and support this manuscript would not have been written.

Table of Contents

Abstract	1
1. Introduction	3
1.1 Background	3
1.2 Objectives	8
2. Experimental Procedure	11
2.1 Materials and Properties	11
2.2 Fatigue Crack Propagation (FCP) Testing	11
2.3 Fractography	19
3. RESULTS AND DISCUSSION	21
3.1 The Effect of Testing Variables on Fatigue Crack Propagation Behavior	21
3.1.1 Fatigue as an Activated Process in PVC	30
3.2 The Effect of Testing Variables on Discontinuous Crack Growth in PVC	38
3.2.1 DGB Macromorphology and Band Size as a Function of ΔK	38
3.2.2 How Testing Conditions Affect DGB Micromorphology	43
3.2.3 The DGB Stretch Zone	61
4. Conclusions	70
REFERENCES	72
Vita	74

List of Figures

Figure 1-1:	Discontinuous Growth Band Morphology at 22°C, 50 Hz, $\Delta K = 0.4 \text{ MPa}\sqrt{\text{m}}$, A) Void Gradient, B) Stretch Zone	7
Figure 1-2:	Schematic of the Relationship of the Stretch Zone to the Crack Opening Displacement	9
Figure 2-1:	The Dynamic Mechanical Spectrum for Trovidur [®]	13
Figure 2-2:	The Yield Strength of Trovidur as a Function of Temperature : + Dynamit Nobel, \square Experimental	14
Figure 2-3:	Diagram of a Single-Edge-Notch Specimen for the Generation of FCP Data (a = crack length, w = specimen width)	15
Figure 2-4:	Diagram of a Compact Tension Specimen for the Generation of FCP Data (a = crack length, w = specimen width)	17
Figure 2-5:	The Fatigue Testing and Temperature Control Apparatus	18
Figure 3-1:	The Effect of Testing Frequency on PVC at 22°C	22
Figure 3-2:	The Effect of Testing Frequency on PVC at 55°C	23
Figure 3-3:	The Effect of Testing Frequency on PVC at 0°C	24
Figure 3-4:	The ΔK Level Required to Maintain a Constant Growth Rate at 1, 10, & 100 Hz as a Function of Temperature	25
Figure 3-5:	The Effect of Temperature on FCP of PVC Fatigue Tested at 100 Hz	26
Figure 3-6:	The Effect of Temperature on FCP of PVC Fatigue Tested at 10 Hz	27
Figure 3-7:	The Effect of Temperature on FCP of PVC Fatigue Tested at 1 Hz	28
Figure 3-8:	The Effect of Temperature on FCP of Polystyrene Fatigue Tested at 0.15 Hz ¹⁰	29
Figure 3-9:	The Variation of the Frequency Sensitivity Factor with $T - T_{\beta}$ for Several Polymers	31
Figure 3-10:	The Variation of the Frequency Sensitivity Factor with $T - T_{\beta}$ and $T - T_{\alpha}$	32
Figure 3-11:	The Variation of Growth Rate With the Inverse of Temperature, $\Delta K = 0.5 \text{ MPa}\sqrt{\text{m}}$	33
Figure 3-12:	The Variation of Growth Rate With the Inverse of Temperature, $\Delta K = 0.7 \text{ MPa}\sqrt{\text{m}}$	34
Figure 3-13:	DG Band Size as a Function of ΔK and Frequency at Room Temperature (Slopes: 100 Hz - 1.1, 10 Hz & 1 Hz - 1.35)	39
Figure 3-14:	DG Band Size as a Function of ΔK and Temperature at 100 Hz	40
Figure 3-15:	DG Band Size as a Function of ΔK and Temperature	41

	at 10 Hz	
Figure 3-16:	DG Band Size as a Function of ΔK and Temperature at 1 Hz	42
Figure 3-17:	DGB Morphology With Increasing Temperature (22°C and Above) at 10 Hz, $\Delta K = 0.5 \text{ MPa}\sqrt{\text{m}}$ a) 22°C, b) 55°C	46
Figure 3-18:	Fracture Surface Morphology at 0°C, 100 Hz $\Delta K = 0.7 \text{ MPa}\sqrt{\text{m}}$	47
Figure 3-19:	Fracture Surface Morphology at -30°C, 100 Hz, $\Delta K = 0.7 \text{ MPa}\sqrt{\text{m}}$	48
Figure 3-20:	Fracture Surface Morphology at -30°C, 10 Hz $\Delta K = 0.7 \text{ MPa}\sqrt{\text{m}}$	49
Figure 3-21:	Fracture Surface Morphology at 0°C, 10 Hz a) $\Delta K = 0.7 \text{ MPa}\sqrt{\text{m}}$, b) $\Delta K = 1.1 \text{ MPa}\sqrt{\text{m}}$	51
Figure 3-22:	Fracture Surface Morphology at -30°C, 1 Hz a) $\Delta K = 0.6 \text{ MPa}\sqrt{\text{m}}$, b) $\Delta K = 0.7 \text{ MPa}\sqrt{\text{m}}$	52
Figure 3-23:	Fracture Surface Morphology at 0°C, 1 Hz a) $\Delta K = 0.7 \text{ MPa}\sqrt{\text{m}}$, b) $\Delta K = 0.8 \text{ MPa}\sqrt{\text{m}}$	53
Figure 3-24:	The Effect of Temperature on the Impact Behavior of Neat PVC : UN = Unnotched Specimens, IS(2), IS(1), IS(1/4) = Notch Tip Radius of 2, 1, 1/4 mm, VS = Very Sharp Notches ($\sim 10 \mu\text{m}$)	57
Figure 3-25:	The Effect of Frequency on DGB Morphology at 22°C $\Delta K = 0.5 \text{ MPa}\sqrt{\text{m}}$, a) 1 Hz, b) 100 Hz	59
Figure 3-26:	DGB Morphology as a Function of ΔK at 35°C a) 1 Hz, $\Delta K = 0.5 \text{ MPa}\sqrt{\text{m}}$, b) 1 Hz, $\Delta K = 0.7 \text{ MPa}\sqrt{\text{m}}$	60
Figure 3-27:	Correspondence of Measured and Calculated Stretch Zone Sizes at 100 Hz	62
Figure 3-28:	Comparison of Measured and Calculated Stretch Zone Sizes at 10 Hz	63
Figure 3-29:	Comparison of Measured and Calculated Stretch Zone Sizes at 1 Hz	64
Figure 3-30:	Relationship Between Calculated and Fractographically Inferred Values of the J-integral at 100 Hz	66
Figure 3-31:	Comparison of Calculated and Fractographically Inferred Values of the J-integral at 10 Hz	67
Figure 3-32:	Comparison of Calculated and Fractographically Inferred Values of the J-integral at 1 Hz	68

List of Tables

Table 2-1:	Mechanical Property Specifications of Trovidur [®] 26	12
Table 3-1:	The Influence of Frequency on Apparent Activation Energies	37
Table 3-2:	The Effect of Temperature, Frequency, & ΔK on DG Band Life	56

Abstract

The fatigue crack propagation (FCP) resistance and fracture surface morphology of a commercial grade of poly(vinyl chloride) was studied as a function of test frequency and temperature. Experiments were conducted at -30, 0, 22, 35, 45, and 55°C at testing frequencies of 1, 10, and 100 Hz. The FCP resistance of this grade of PVC improved with increasing frequency and decreasing testing temperature in accordance with time-temperature superposition principles. The FCP behavior of this grade of PVC at various temperatures was found to parallel that observed for polystyrene. In addition, this study revealed that an Arrhenius relationship exists between the crack growth rate, da/dN , and the inverse absolute temperature. This relationship was found to exist at all testing frequencies and ΔK levels examined. Computed apparent activation energy values were observed to be less than the activation energy associated with the glass transition and the beta peak. This implies that segmental main chain motion and side chain motions do not dominate the fatigue process. However, the existence of a single activation energy (Q) value for a given cyclic frequency is consistent with the observed presence of a single fracture mechanism - discontinuous crack extension. The implications of increasing Q with decreasing frequency are discussed.

The effects of testing frequency and temperature on the macro and micromorphology of discontinuous growth bands (DGB's) were also studied. Although the DGB size was observed to increase with decreasing frequency and increasing temperature, the bands exhibited a less than second-power dependence on ΔK . Consequently, the Dugdale model could not be used to infer the yield strength of the material at various temperatures. The fracture surface

appearance of the DGB's was observed to degenerate slightly with each decade drop in frequency, while DGB's formed at the higher temperatures were distinguished by a sharper void gradient and a clearer, more distinct stretch zone. Bands produced at temperatures below 22°C exhibited a void gradient as well, but were unpredictable in size and often did not possess a classical DGB micromorphology.

A comparison was made between the measured width of the stretch zone and the calculated crack opening displacement (COD). Stretch zone width measurements taken from samples tested at 100 Hz and at temperatures between 22 and 55°C were in agreement with calculated values, thereby suggesting that the stretch zone represents the profile of the blunted crack tip. However, measured stretch zone widths were found to be approximately twice those determined for tests conducted at 1 and 10 Hz in the same temperature range. Subsequently, the values of the J-integral computed from the measured stretch zone width and the yield strengths for the 100 Hz condition were compared with those calculated from the Griffith energy criteria. If corrections are made to allow for changes in stress state, good correlation was noted between the J-integral values found by using the two different computational methods.

Chapter 1

Introduction

1.1 Background

Due to the increased usage of engineering plastics in pipe systems and other important structural applications, it is of practical interest to study the mechanical behavior of these materials under a variety of loading and environmental conditions. Fatigue crack propagation studies are particularly significant, as most components probably contain imperfections which can grow to failure under cyclic stresses well below the yield strength. Consequently, for most plastics the majority of a specimen's lifetime is spent in the propagation of a crack.¹ Many investigators^{2, 3} have demonstrated that linear elastic fracture mechanics is useful in the evaluation of the fatigue crack propagation (FCP) response of PVC and other polymeric materials.

The rate of crack extension of a pre-cracked specimen has been found to depend upon the magnitude of the stress intensity factor range, a measure of the stress amplification at the advancing crack tip. The stress intensity factor range is defined as⁴

$$\Delta K = Y\Delta\sigma\sqrt{a} \quad (1.1)$$

where ΔK is the change in the stress intensity factor, Y is a correction factor to account for specimen geometry, $\Delta\sigma$ is the applied stress range, and a is the crack length. Paris⁵ related the quantity ΔK to the rate of crack growth per cycle, da/dN through the equation

$$da/dN = A\Delta K^m \quad (1.2)$$

where A and m are constants and a function of material and test

variables. This relationship describes FCP behavior at intermediate ΔK levels. At low ΔK levels, crack extension is characterized by vanishingly slow growth rates, while at the high ΔK level, crack growth becomes rapid and unstable.

Due to their viscoelastic nature, the FCP behavior of most plastics is sensitive to such test variables as cyclic frequency and temperature. It is known that the fatigue crack growth rate of many plastics, including PVC, decreases with increasing cyclic frequency, although some exceptions have been reported.⁶ This phenomenon has been attributed to crack tip blunting resulting from local hysteretic heating and to the inhibition of molecular motion due to a shortened deformation response time.^{7, 8, 9} While the effect of testing temperature on fatigue crack propagation has not been studied extensively, it has been reported that the fatigue resistance of polystyrene and poly(methyl methacrylate) improves as the testing temperature is decreased.^{7, 10} In this case, the effects of decreasing temperature are similar to that of increasing frequency. From the study of known temperature and frequency behavior, the FCP response of many plastics can be expected to reflect time-temperature equivalence.

Crack formation and growth can be thought of as representing the accumulation of thermally activated breakage of primary and secondary bonds.¹¹ The Zhurkov/Bueche model postulates that one can apply activation energy barrier concepts to physical processes such as fracture, and that the application of a stress will reduce this energy barrier.¹¹ The Arrhenius relationship for this rate controlled process is expressed as^{12, 13, 14}:

$$da/dN = C \exp^{-(Q+v\sigma)/RT} = C \exp^{(Q'/RT)} \quad (1.3)$$

where Q = activation energy
 Q' = apparent activation energy
 v = activation volume
 σ = effective stress
 R = gas constant
 T = absolute temperature

As implied by Equation 1.3, fracture processes which follow the Zhurkov/Bueche model will exhibit a linear relationship between the logarithm of the crack growth rate and the inverse absolute temperature.

Crazing is the dominant deformation mechanism in neat PVC. During craze formation, a lenticular damage zone forms in highly stressed areas and consists of microvoids and polymer fibrils oriented parallel to the tensile axis. Craze growth occurs either by stretching of the existing fibrils or through viscous flow, the latter involving the drawing of fresh polymer into the craze from the bulk material.^{15, 16, 17} During the cyclic growth process, weak fibrils break resulting in a redistribution of the load to the remaining fibrils. Extension and thickening of the craze is then believed to continue until the thickness of the craze approaches the critical value of the crack opening displacement corresponding to a particular stress intensity level.¹⁸ At this point, craze breakdown occurs abruptly and the crack propagates across the craze.

Depending upon the nature of the crack tip deformation process, cyclic loading will generate striations or discontinuous growth bands on the fracture surfaces of engineering plastics. Striations are oriented normal to the direction of crack growth and represent the successive position of the crack front after each loading cycle. Consequently, the striation spacing can be compared to the macroscopic growth rate, which increases with increasing ΔK .¹⁹ Discontinuous growth bands (DGB's) also lie perpendicular to the direction of crack growth, but represent the position of the crack front after hundreds to thousands of

loading cycles. Studies have shown that the size of the DGB's correspond to the length of the plastic zone ahead of the crack tip, as computed using the Dugdale formulation²⁰:

$$r_y = \pi/8(K_{\max}^2/\sigma_{ys}^2) \quad (1.4)$$

where K_{\max} is the maximum stress intensity factor and σ_{ys} is the yield strength. Skibo et al²¹ and Rimnac et al²² have successfully used Equation 1.4 to infer the yield strength for polystyrene and PVC from DGB measurements and associated stress intensity values.

DGB size and micromorphology are also known to be sensitive to testing parameters. It has been observed that the bands increase in size and also degenerate in appearance with decreasing frequency. Little is known about the effect of temperature on DGB micromorphology; a study of this subject is considered herein for PVC.

Discontinuous growth bands are distinguishable from fatigue striations by a void gradient that exists across the band width. As shown in Figure 1.1, the voids decrease in size in the direction of crack growth, though the void diameter is greatest at a short distance from the crack tip. The location of the maximum void size is believed to correspond to the region associated with the maximum triaxiality of stress.²³ Separating each band is a narrow deformation zone referred to as a stretch zone (see also Figure 1.1), which is thought to represent the location where the crack tip arrests after striking through the previous craze zone.²¹

As shown in Figure 1.2, the stretch zone (i.e., profile of the arrested crack tip, or crack tip radius) is equivalent to one-half the critical crack opening displacement (COD), as given by²⁴

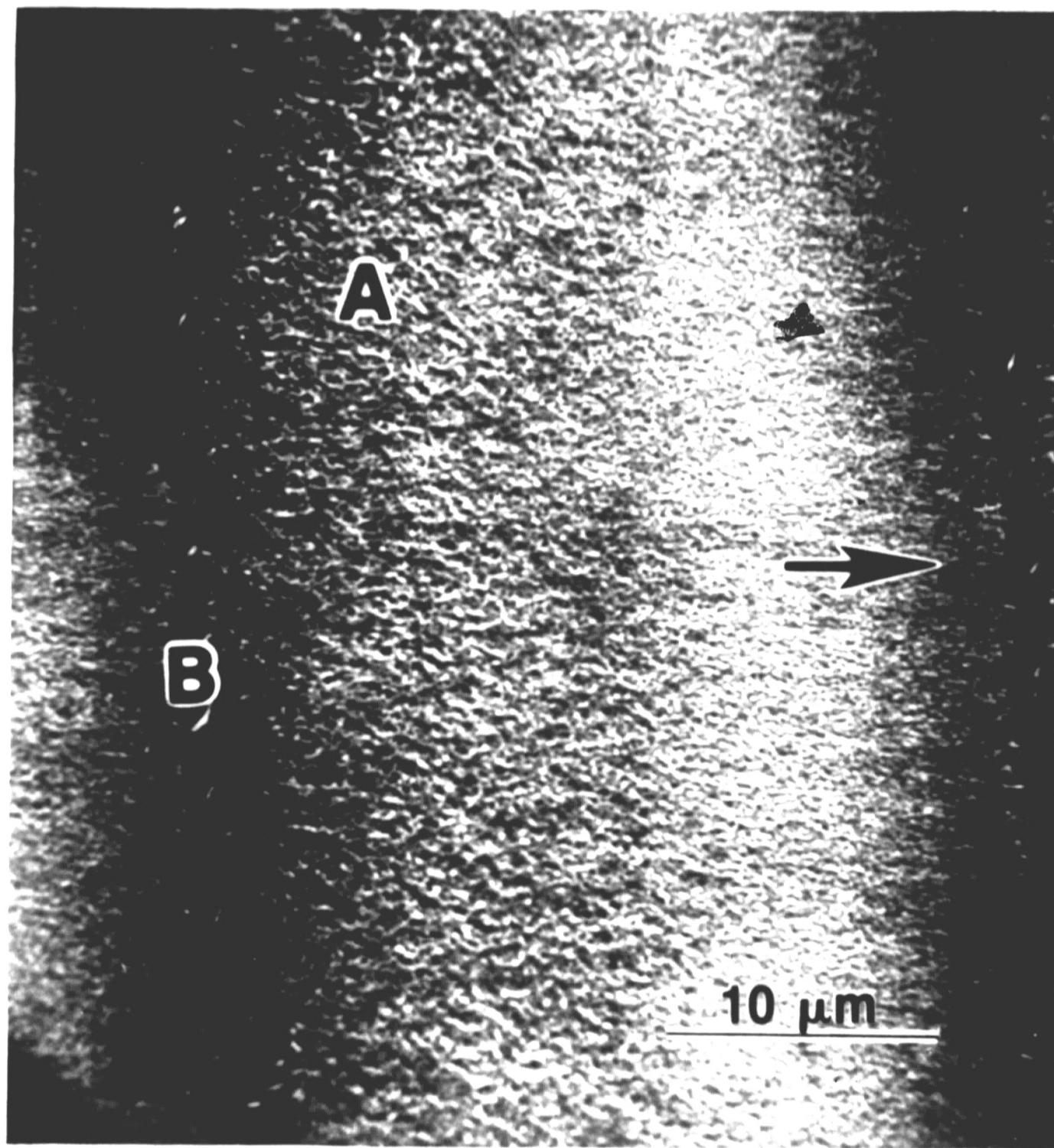


Figure 1-1: Discontinuous Growth Band Morphology at 22°C, 50 Hz, $\Delta K = 0.4 \text{ MPa}\sqrt{\text{m}}$, A) Void Gradient, B) Stretch Zone

$$d = \frac{K_{\max}^2}{2E\sigma_{ys}} \quad (1.5)$$

where

- d = crack tip radius
- K_{\max} = maximum stress intensity factor
- E = Young's Modulus
- σ_{ys} = yield strength

The value of the crack opening displacement as determined from the width of the craze can then be used to infer the J-integral, which is a measure of the elastic-plastic stress-strain fields at the crack tip. Hashemi and Williams have shown that J can be described according to the relationship²⁵ :

$$J = m\sigma_{\text{flow}}d \quad (1.6)$$

where

- J = J-integral
- $\sigma_{\text{flow}} = (\sigma_{ys} + \sigma_{ts})/2$
- d = crack opening displacement
- m = constant = 1.0 - 2.0
(depending upon the stress state)

The J-integral value calculated by this method can then be compared to the value calculated from the Griffith fracture energy criteria; for elastic conditions where J is equivalent to the crack driving force, G.¹⁹ :

$$J = G = \frac{K_{\max}^2}{(1 - \nu^2)E} \quad (1.7)$$

where

- J = J-integral
- ν = Poisson's ratio
- E = Young's Modulus
- K_{\max} = maximum stress intensity factor

1.2 Objectives

The overall objective of this thesis is to study the combined effect of testing temperature and frequency on the fatigue resistance and the kinetics of the FCP process in PVC. Since this material has been reported to develop DGB's over a wide range of ΔK conditions, this study will examine the effects

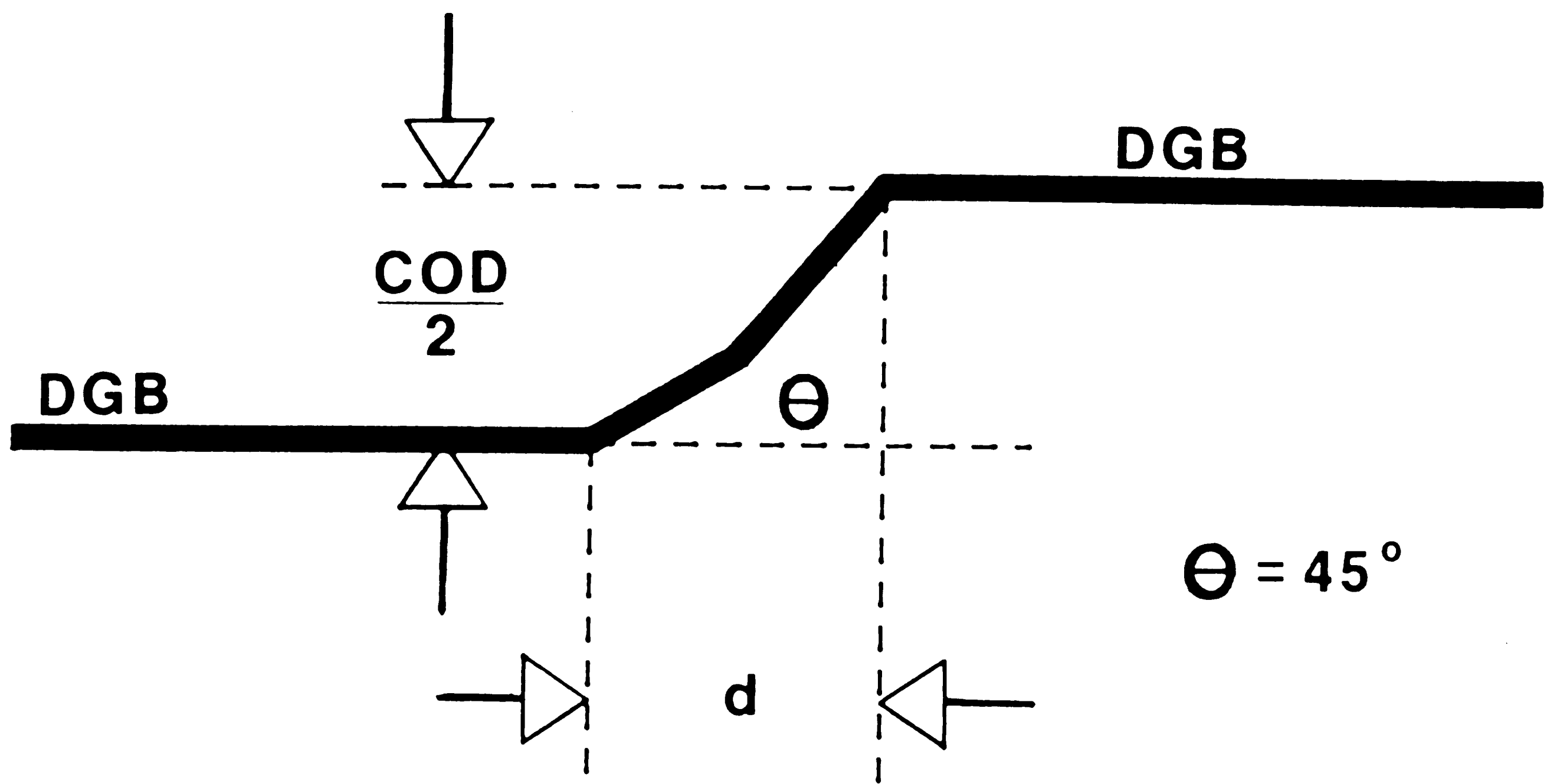


Figure 1-2: Schematic of the Relationship of the Stretch Zone to the Crack Opening Displacement

of testing temperature and frequency on the discontinuous growth band formation process and on DGB morphology. In addition, quantitative measurements of fracture surface features will be used to infer by suitable calculations both material properties and test conditions.

Chapter 2

Experimental Procedure

2.1 Materials and Properties

This research was conducted using a commercial sheet grade of PVC manufactured by Dynamit Nobel [tradename Trovidur[®], ASTM D1784-8, Class 11452-B]. Material specifications are given in Table 2.1. The material is clear in appearance, and comprised of nine layers (each 0.529 mm in thickness), indicative of a calendered sheet.

An automated Rheovibron DDV-III was used to obtain the dynamic mechanical spectrum of the PVC at a test frequency of 110 Hz, with a scan rate of 1°C per minute (see Figure 2.1). The glass transition temperature for this material was found to be approximately 73°C. Tensile specimens were raised to temperatures above ambient through the use of heating tape, and tested in accordance with ASTM Specification D638.* A graph of the yield strength of this grade of PVC as a function of temperature is shown in Figure 2.2.

2.2 Fatigue Crack Propagation (FCP) Testing

Fatigue specimens were cut in the same direction from the PVC sheet in order to avoid any orientation effects on the fatigue behavior of the material. The orientation of the material is unknown. Single-edge-notch and compact tension specimens were used to generate FCP data during the course of this study. Single-edge-notch specimens (50.8 mm in width) were machined according to the diagram given in Figure 2.3.

*Test results provided by Steffanie Sunday, Lehigh University

Table 2-1: Mechanical Property Specifications of Trovidur® 26

Property	ASTM#	Value
Yield Strength	D638	70.33 MPa
Modulus of Elasticity	D638	2.94 GPa
Ultimate Elongation	D638	36 %
Notch Impact Strength	D256	27.76 J/m of notch
Rockwell Hardness	D785	115 "R"

SAMPLE Commercial PVC
FREQUENCY 110 Hz

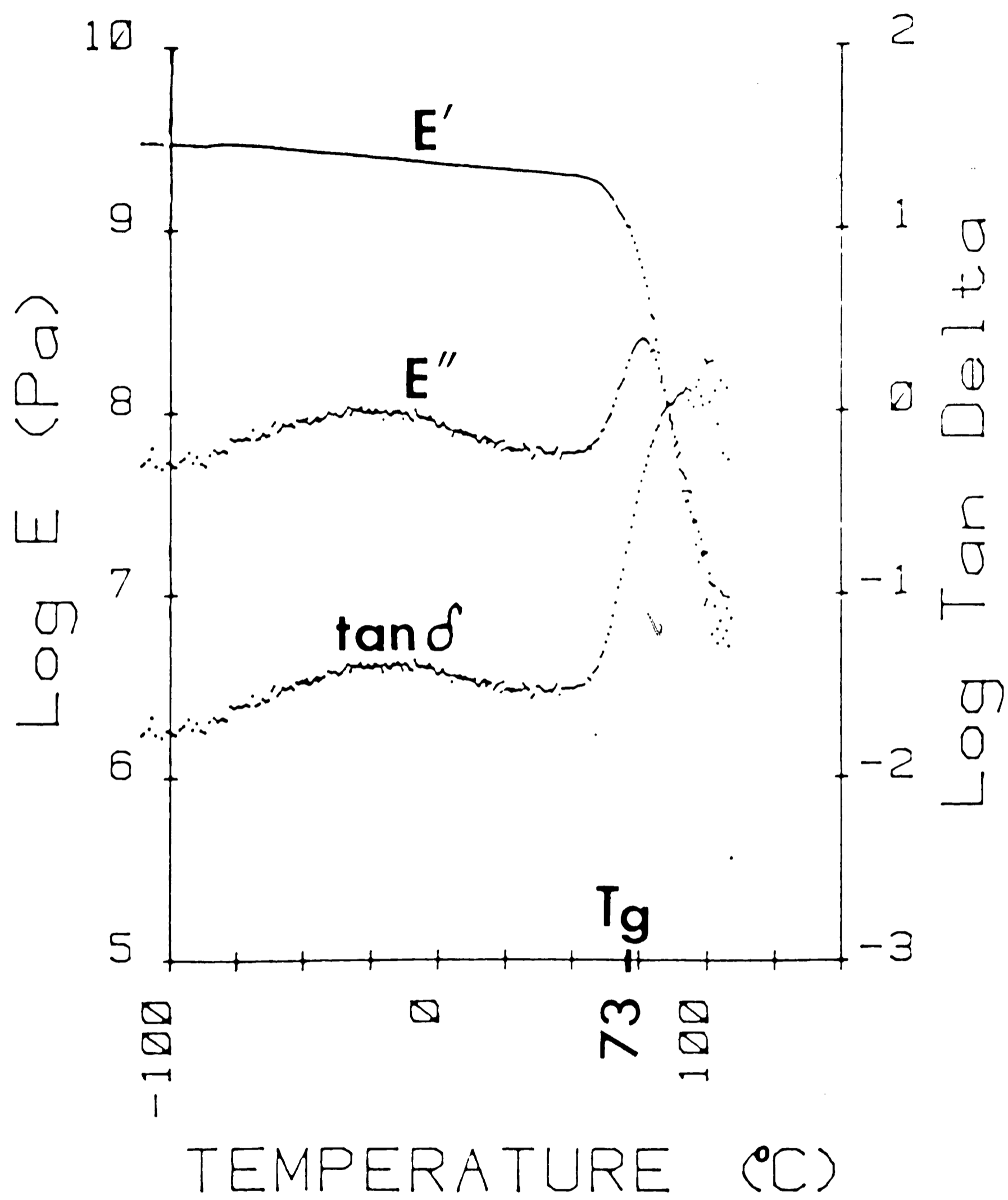


Figure 2-1: The Dynamic Mechanical Spectrum for Trovidur®

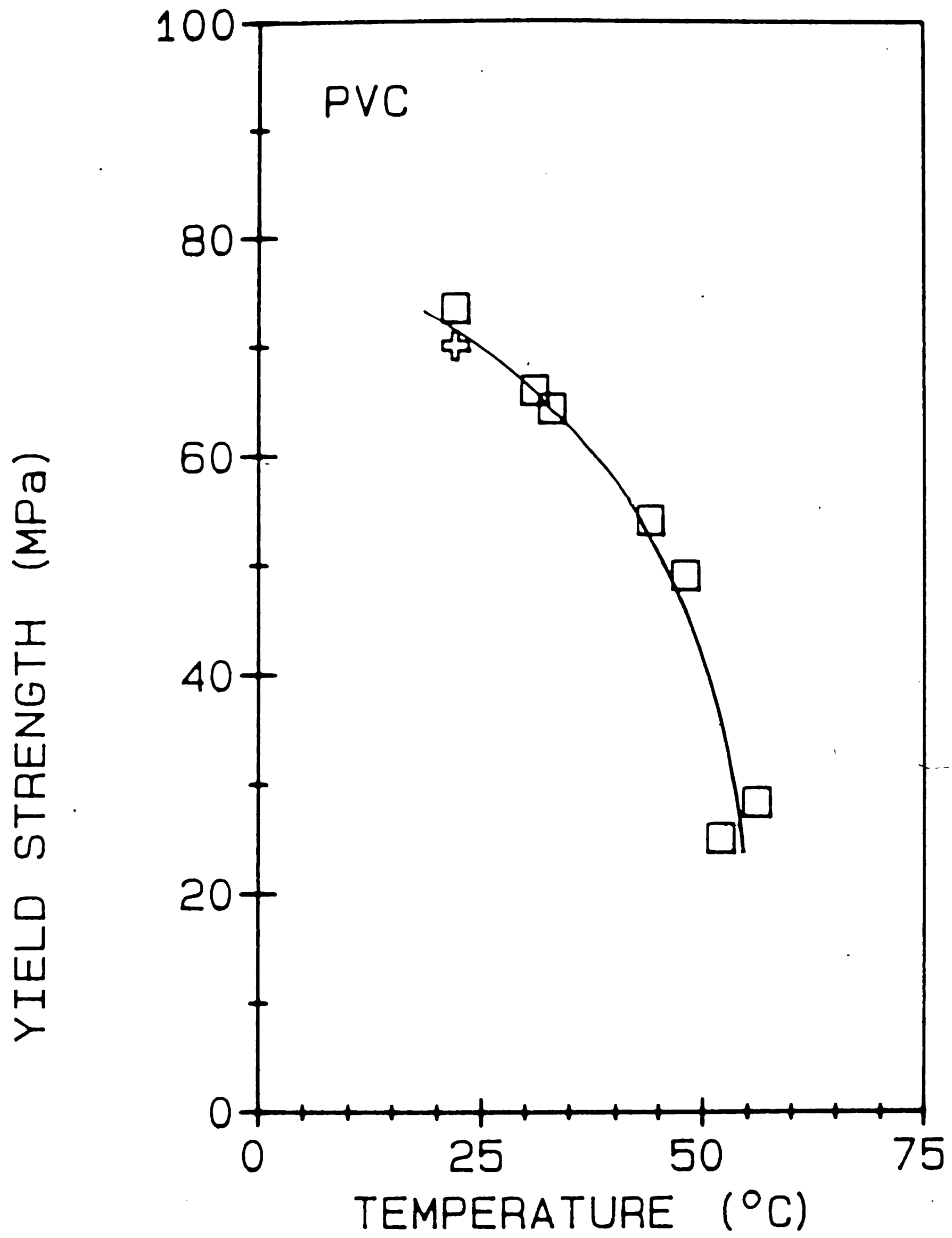


Figure 2-2: The Yield Strength of Trovidur as a Function of Temperature : + Dynamit Nobel, □ Experimental

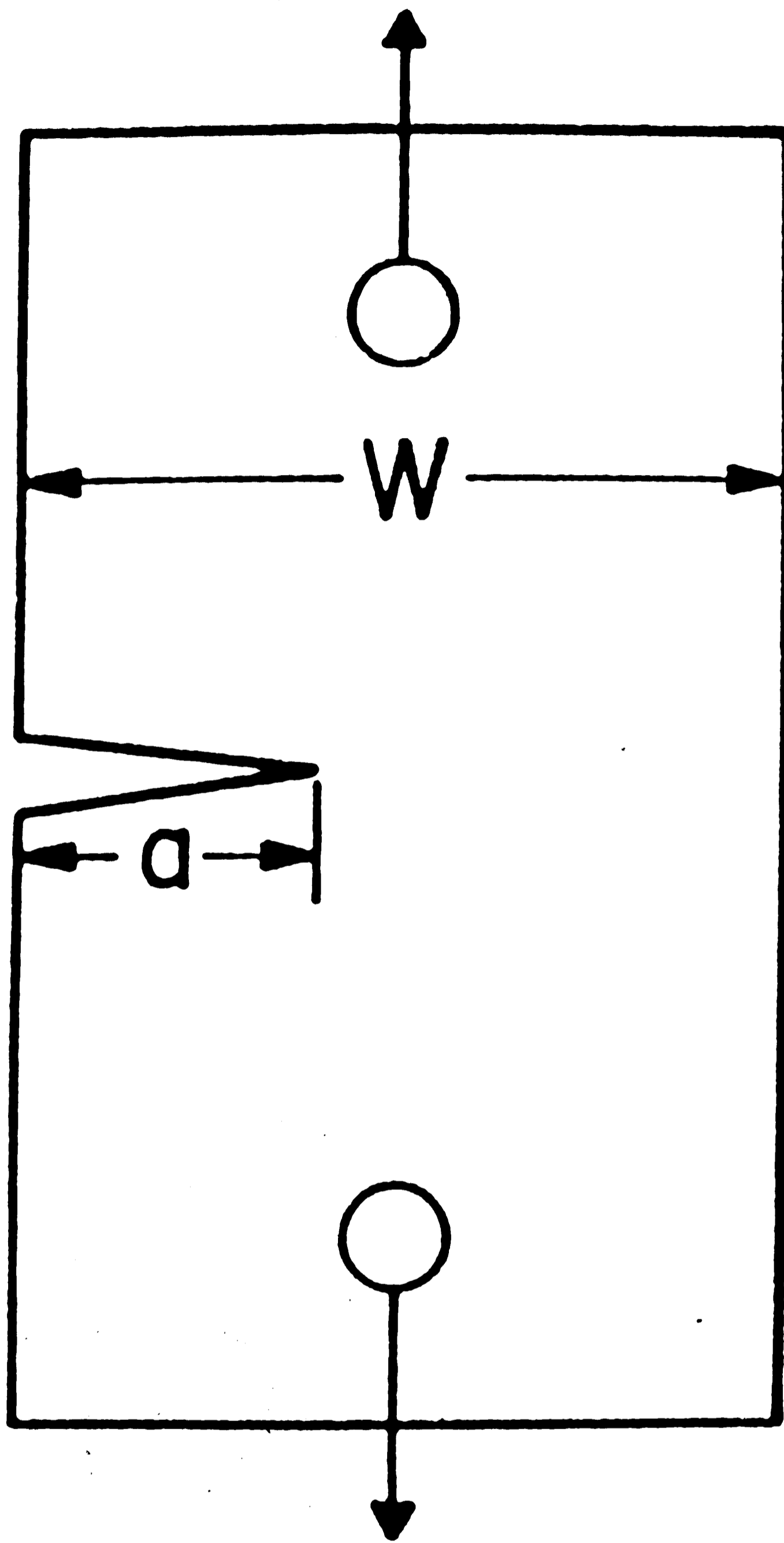


Figure 2-3: Diagram of a Single-Edge-Notch Specimen for the Generation of FCP Data
(a = crack length, w = specimen width)

The stress intensity factor range ΔK for this specimen configuration was determined from the corresponding relationship¹⁹:

$$\Delta K = \sqrt{a}(\Delta P/bW)f[a/W] \quad (2.1)$$

where

ΔP = applied load range

W = specimen width

b = thickness

a = crack length

$$f(a/W) = 1.99 - 0.41(a/W) + 18.7(a/W)^2 - 38.48(a/W)^3 + 53.85(a/W)^4$$

Compact tension specimens, illustrated in Figure 2.4, were machined in accordance with ASTM Specification D647-81T. The stress intensity factor can be calculated for this specimen configuration with the use of the following expression¹⁹:

$$\Delta K = \left[\frac{\Delta P}{B\sqrt{W}} \right] \left[2 + \frac{a/W}{(1-a/W)^{1.5}} \right] f(a/W) \quad (2.2)$$

where

ΔP = applied load range

B = specimen thickness

W = specimen width

a = crack length

$$f(a/W) = 0.886 + 4.64(a/W) - 13.32(a/W)^2 - 14.72(a/W)^3 - 5.6(a/W)^4$$

Fatigue crack propagation tests were conducted under manual control on an Instron Model 1350 servohydraulic unit with a 8896 N load cell. Tests were conducted inside an Applied Test Systems Series 3720 Split Type Oven using a Model 2010 Control System with temperatures inside the oven being monitored with the use of an Omega Model 660 Type J Thermocouple. Subambient temperature tests were conducted in this oven by passing N_2 gas into a 30-liter Dewar flask filled with liquid nitrogen. The chilled gas in the Dewar flask is then fed through a solenoid valve into the oven. Photographs of this apparatus are given in Figure 2.5.

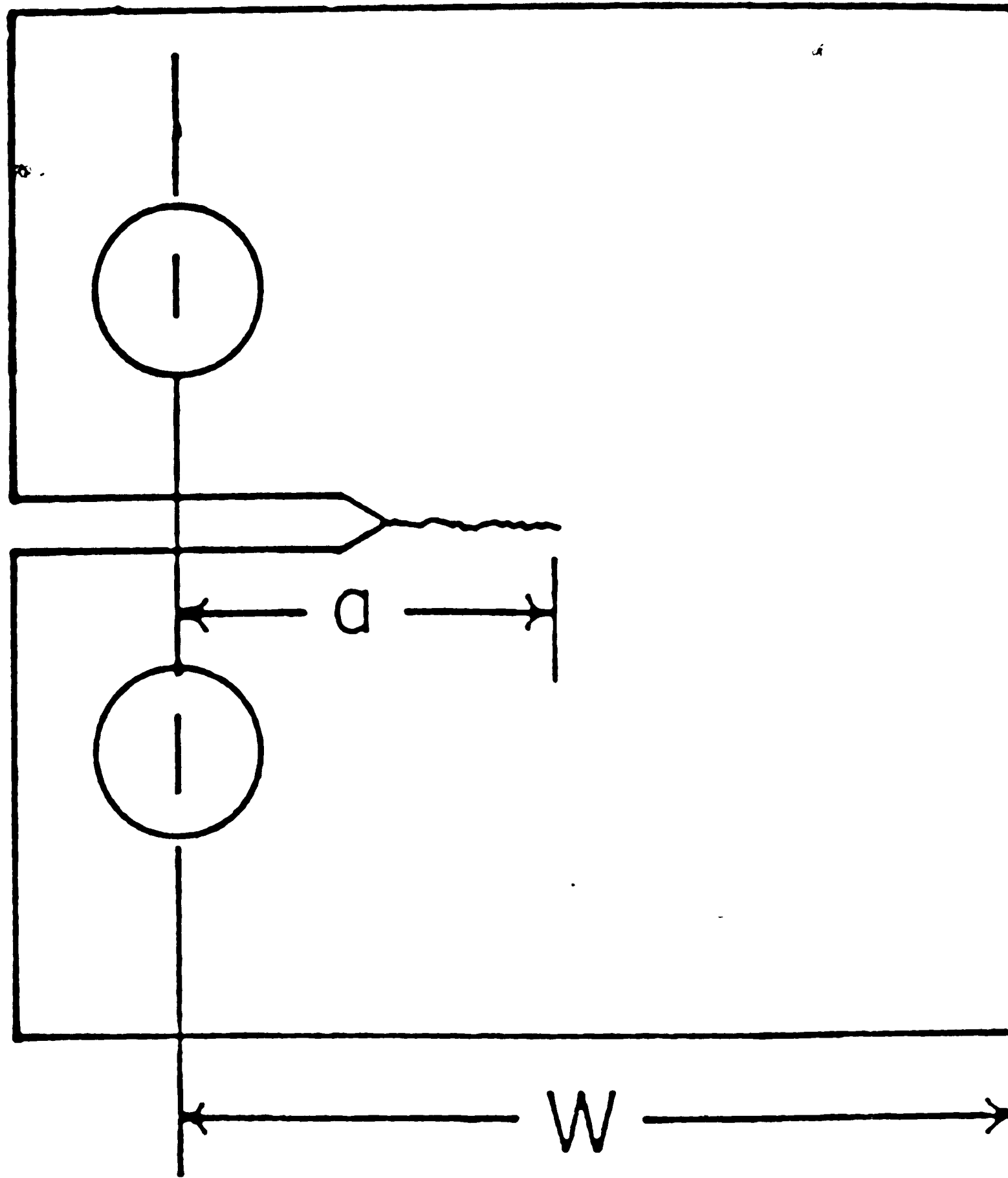


Figure 2-4: Diagram of a Compact Tension Specimen for the Generation of FCP Data
(a = crack length, w = specimen width)

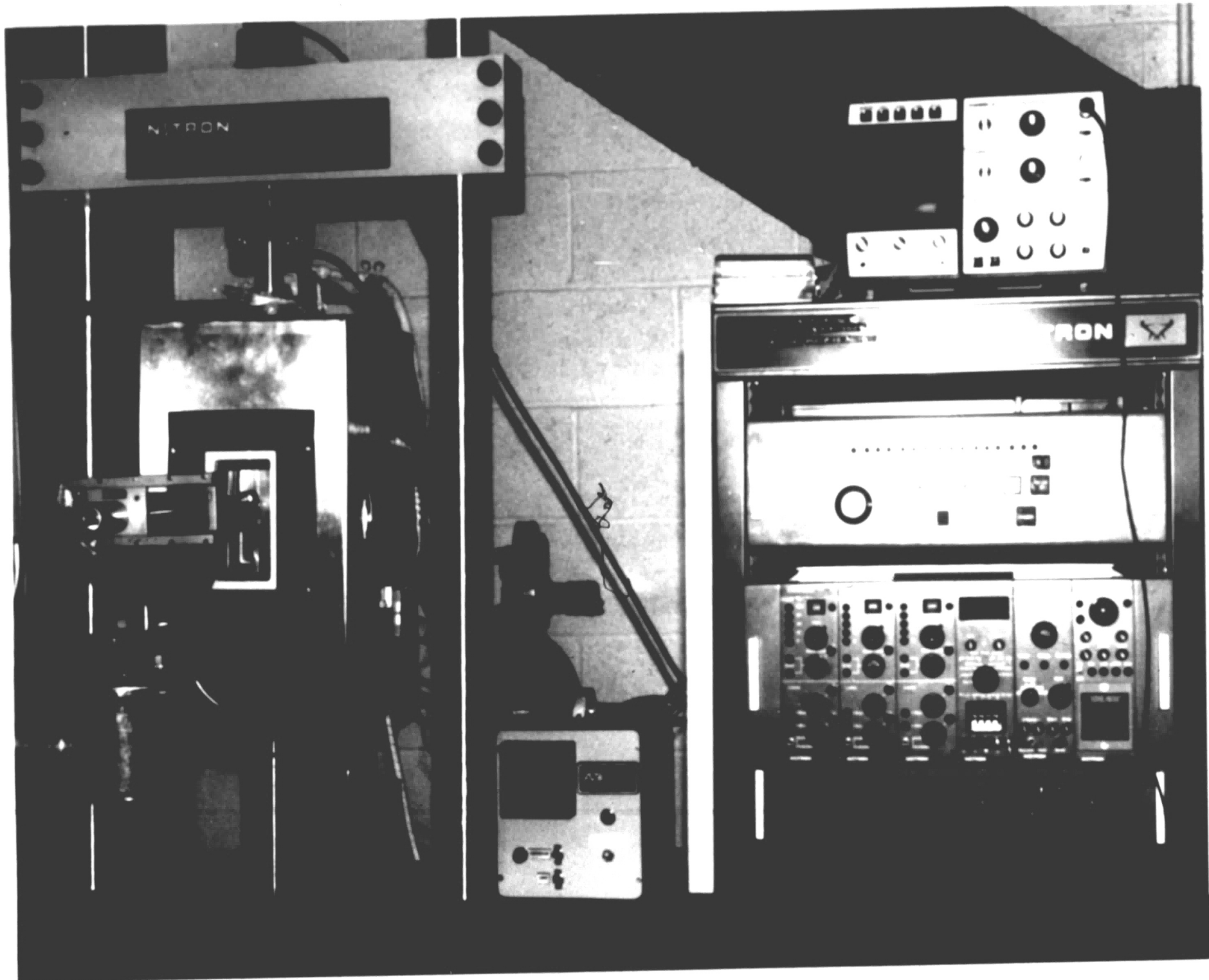


Figure 2-5: The Fatigue Testing and Temperature Control Apparatus

Frequency and temperature conditions were varied with tests being conducted at -30, 0, 22, 35, 45, & 55°C for the frequencies of 1, 10, & 100 Hz. Fatigue experiments were performed under constant load range conditions using a sinusoidal wave form and a load ratio (P_{\min}/P_{\max}) of $R = 0.1$. Precracking of the specimens was completed at 100 Hz and at the testing temperature of study in accordance with ASTM Specification E647-81. Crack lengths were monitored with the use of a Gaertner traveling microscope, and recorded after approximately 0.2 mm of additional crack extension. Crack growth rates, da/dN , were calculated using a modified secant formula

$$(da/dN)_n = (a_{n+1} - a_{n-1}) / (N_{n+1} - N_{n-1}) \quad (2.3)$$

where a_n is the crack length and N_n is the total number of cycles corresponding to the n_{th} crack tip reading.

2.3 Fractography

Fracture surfaces were examined initially with reflected light on a Zeiss Axiomat optical microscope at a magnification of 50 times. Prior to viewing, the fracture surface area was removed from the body of the specimen for easier handling. Fiduciary markings were introduced at 0.2 mm increments to identify specific crack length locations in association with the analysis of particular fracture surface regions. The use of a calibrated microscope eyepiece facilitated the measurement of the widths of discontinuous growth bands.

Microscopic examination of the fracture surfaces was conducted with the use of an ETEC scanning electron microscope. Fracture surfaces were removed from the fatigue specimens, mounted on stubs with carbon paste, and sputter coated with a gold-palladium alloy before viewing. The accelerating voltage

used was 20 kV, and the specimens were oriented horizontally so that vertical fracture lines could be observed without any foreshortening effects. An on-screen micron marker was used to make measurements of fracture surface features.

Chapter 3

RESULTS AND DISCUSSION

3.1 The Effect of Testing Variables on Fatigue Crack Propagation Behavior

In work conducted by previous investigators, it was shown that the FCP resistance of PVC was strongly dependent on testing frequency.²⁷ This was also found to be the case at temperatures both above and below ambient for the present PVC supply (see Figures 3.1 - 3.3). From these results, it is observed that the K_{1C} values increase with increasing testing frequency at each temperature studied; ΔK values required to produce a particular growth rate are plotted against temperature in Figure 3.4 and reveal that ΔK increases linearly with decreasing temperature for a given growth rate at the three frequencies studied.

While not much is known about the effect of temperature on fatigue crack growth in PVC, investigators have noted increased FCP rates with increasing testing temperature in poly(methyl methacrylate) and polystyrene.^{7, 10, 28} The fatigue results for PVC at the various temperatures described above are shown in Figures 3.5 - 3.7 for given test frequencies. It is apparent that the FCP resistance of PVC also improves with decreasing temperature. For those specimens which were tested to failure (all except for two tested at 1 Hz: 0°C and -30°C), the K_{1C} values also increased in value with decreasing temperature, similar to that observed with increasing frequency. The slope of the $da/dN - \Delta K$ curves for PVC and polystyrene¹⁰ (see Figure 3.8) decreased with decreasing temperature, but then rose sharply at temperatures below 0°C.

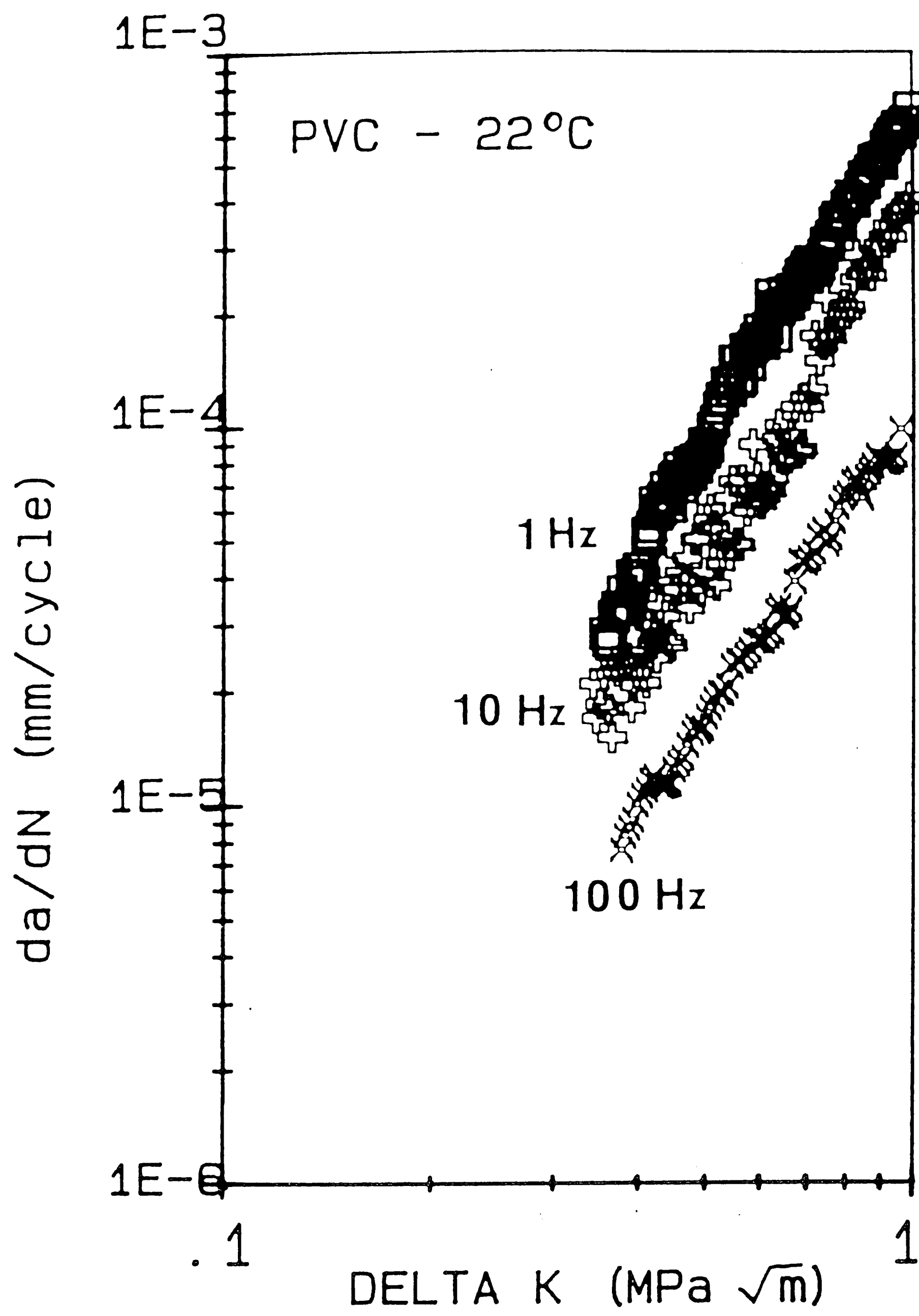


Figure 3-1: The Effect of Testing Frequency on PVC at 22°C

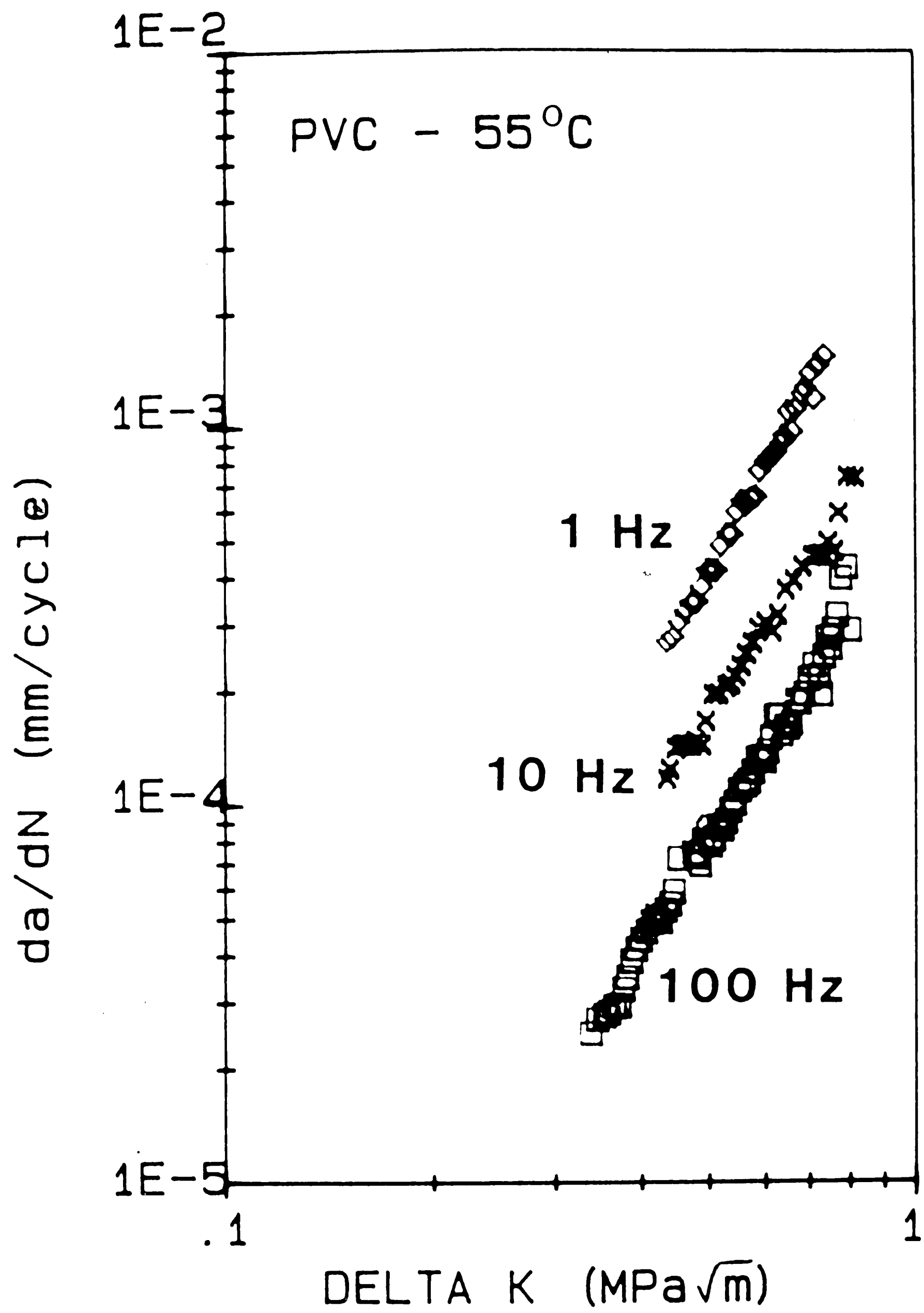


Figure 3-2: The Effect of Testing Frequency on PVC at 55°C

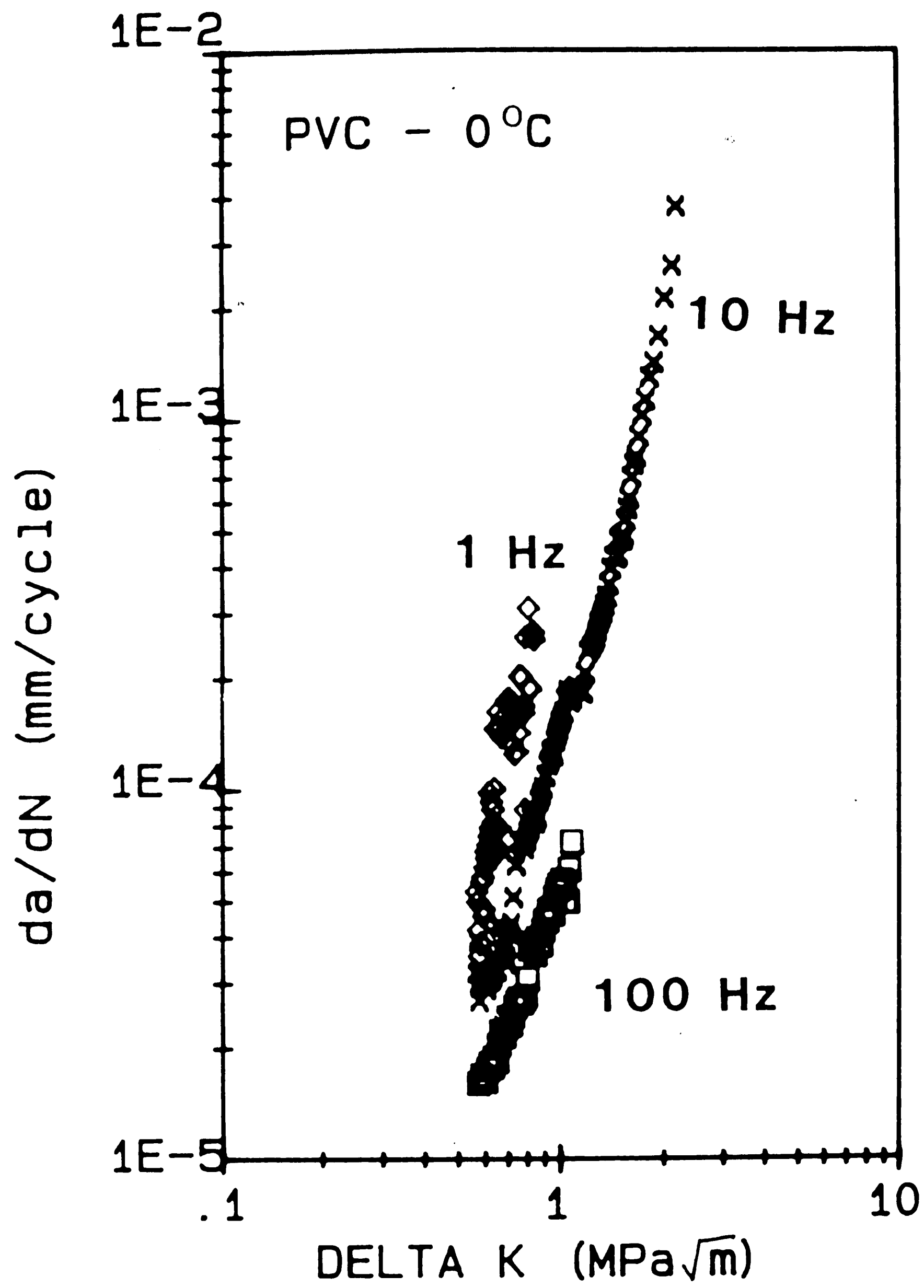


Figure 3-3: The Effect of Testing Frequency on PVC at 0°C

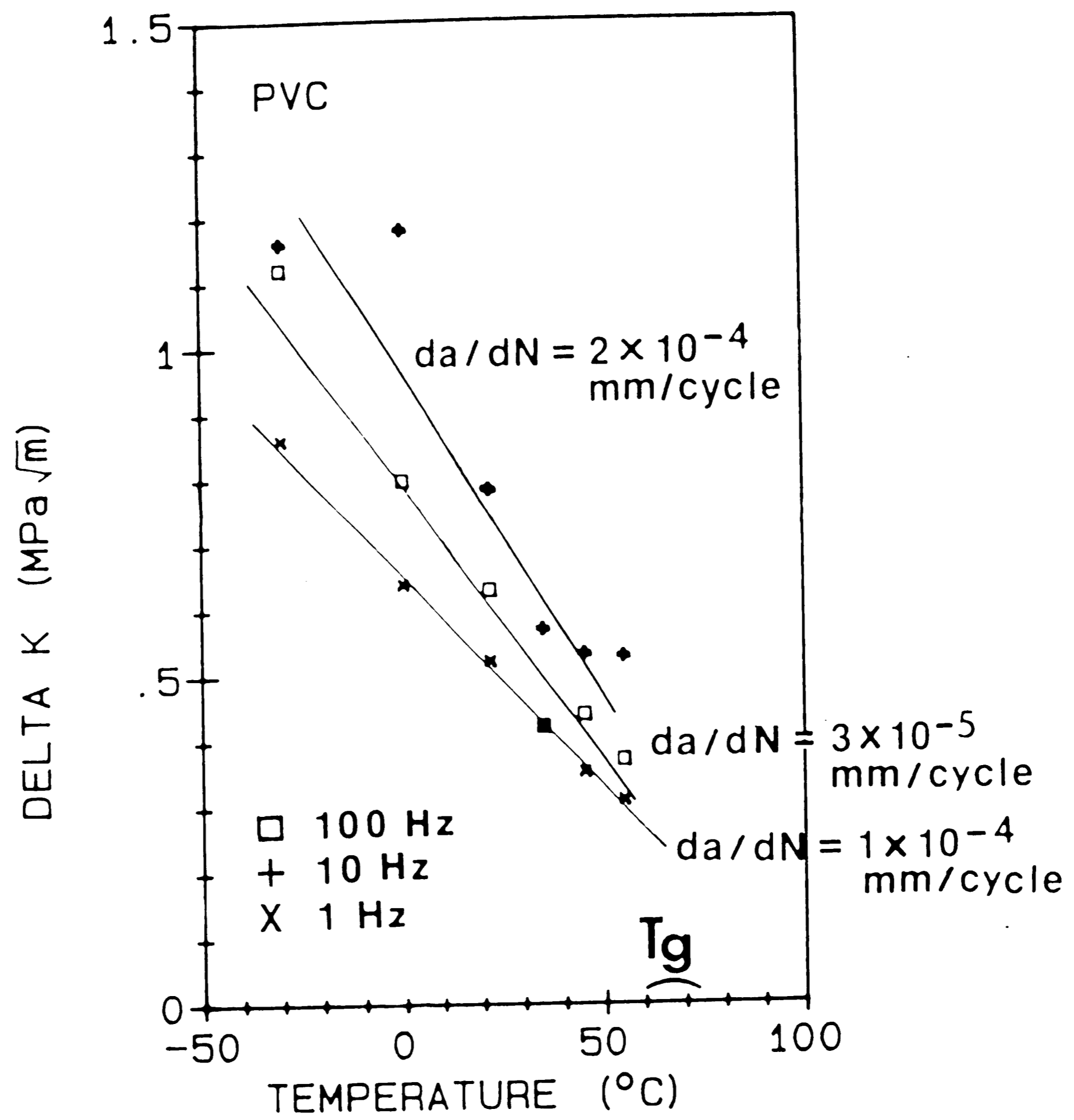


Figure 3-4: The ΔK Level Required to Maintain a Constant Growth Rate at 1, 10, & 100 Hz as a Function of Temperature

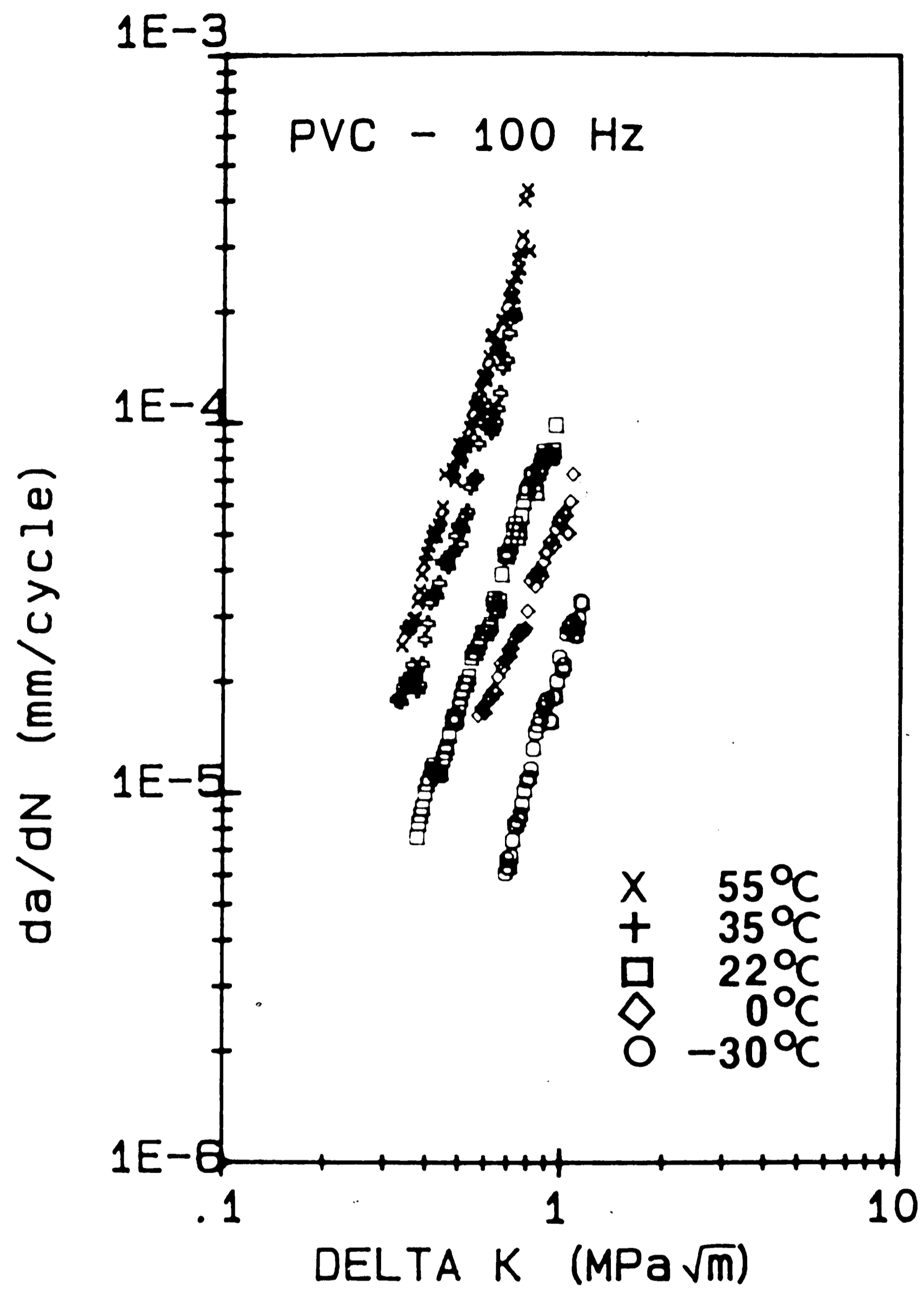


Figure 3-5: The Effect of Temperature on FCP of PVC Fatigue Tested at 100 Hz

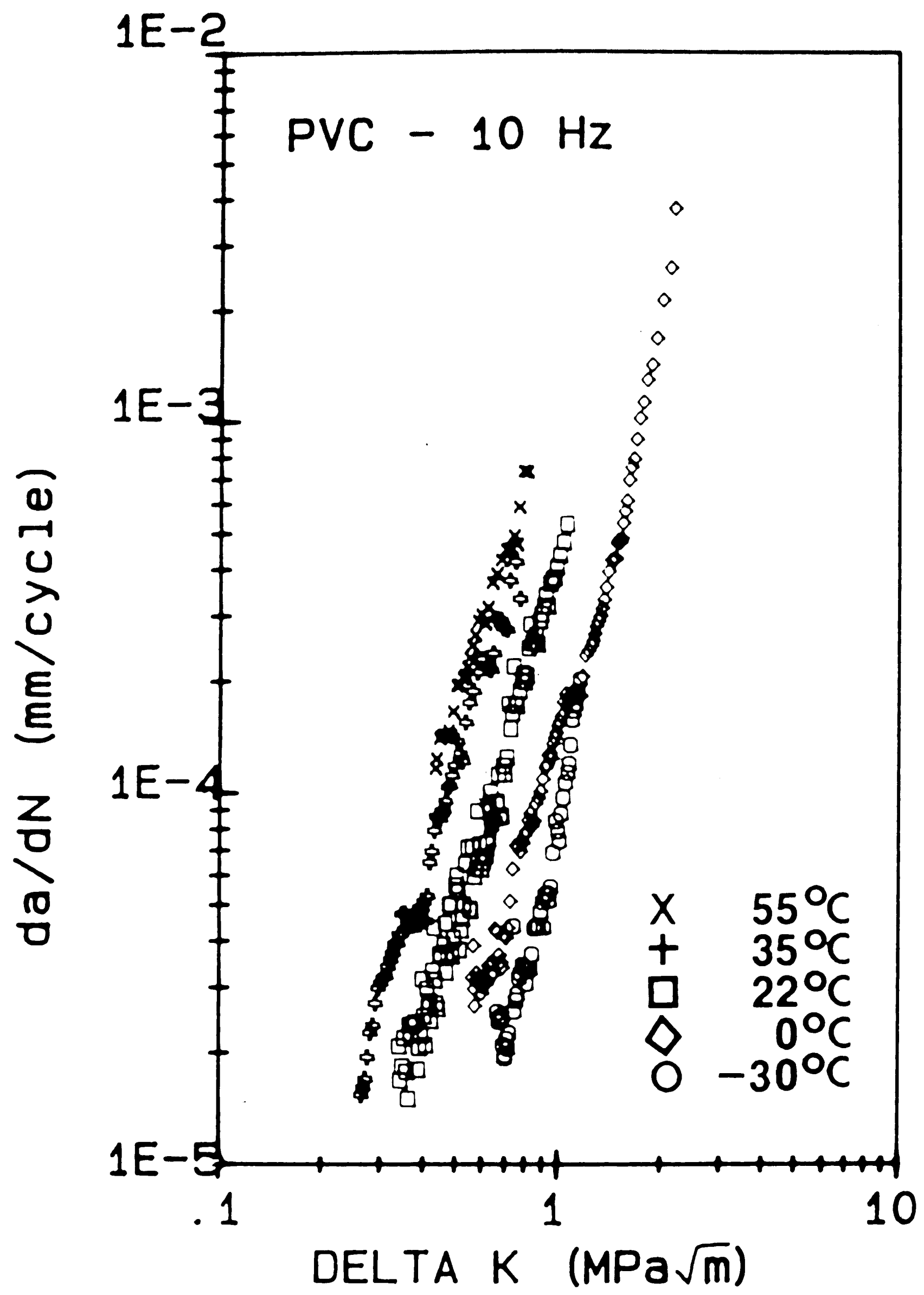


Figure 3-6: The Effect of Temperature on FCP of PVC Fatigue Tested at 10 Hz

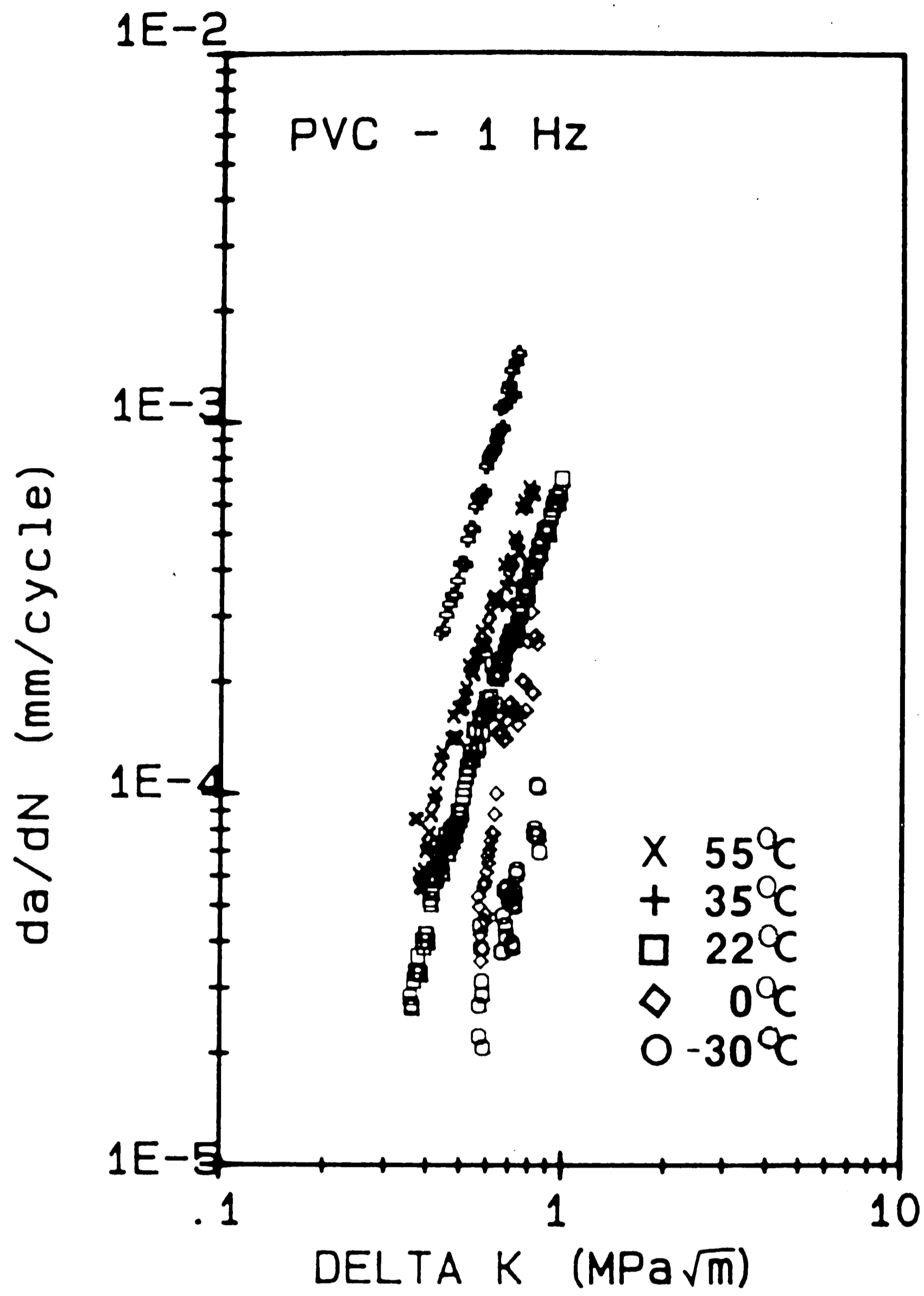


Figure 3-7: The Effect of Temperature on FCP of PVC Fatigue Tested at 1 Hz

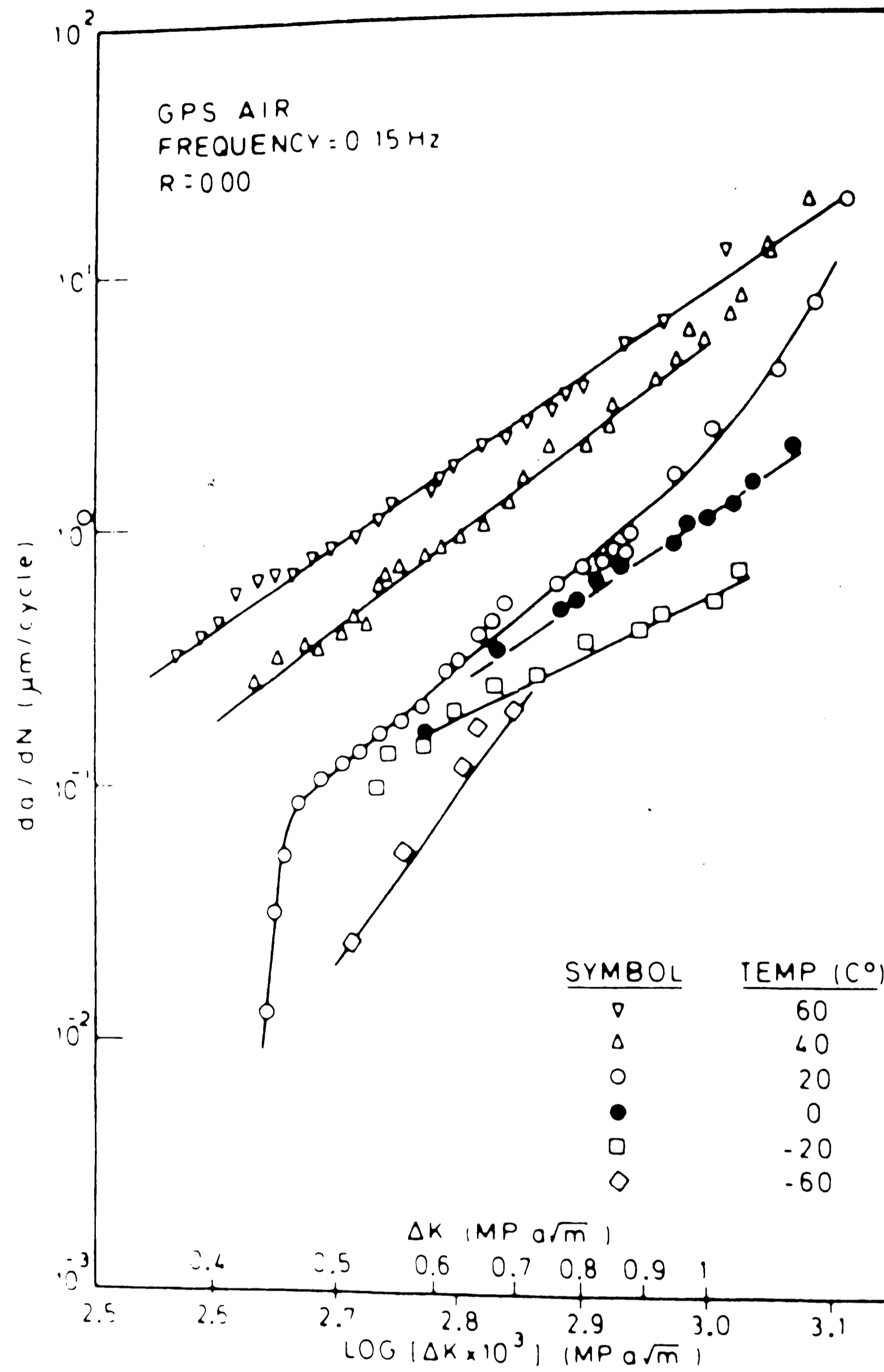


Figure 3-8: The Effect of Temperature on FCP of Polystyrene Fatigue Tested at 0.15 Hz¹⁰

The frequency sensitivity factor (FSF), or the multiple of the change in growth rate per decade increase in frequency, was found to range from 1.5 to 3 for this grade of PVC at the temperatures studied. These values are in general agreement with those observed previously for PVC at room temperature.²⁹ Figure 3.9 shows the frequency sensitivity for the material as a function of testing temperature normalized with respect to the beta transition temperature to be in reasonable agreement with results for other materials except at test temperatures corresponding to 45 and 55°C (i.e. $T - T_{\beta} = -29$ and -19°C , respectively).²⁸ The increase in FSF at these two temperatures may well correspond to test conditions associated with the alpha transition. Accordingly, these data were replotted as a function of the testing temperature normalized with respect to either the beta or alpha transitions, depending on the actual test temperature (see Figure 3.10). It is apparent that a general increase in frequency sensitivity exists at temperatures near both the alpha and beta peaks for this grade of PVC. The increase in FSF values where T_g and T_{β} are minimized can be interpreted as reflecting the influence of enhanced localized hysteretic heating which occurs in association with damping maxima at both the beta and alpha transition peaks (see again Figure 2.1).²⁹

3.1.1 Fatigue as an Activated Process in PVC

A linear relationship was found to exist between the crack growth rate da/dN , and the inverse of the absolute temperature at all frequencies and stress intensity ranges studied (see Figures 3.11 - 3.12). As such, these data are consistent with the Zhurkov/Bueche model, which may be used to describe the fatigue behavior of this grade of PVC.¹¹ Accordingly, crack growth is believed to be thermally dependent with the activation energy Q being reduced by some

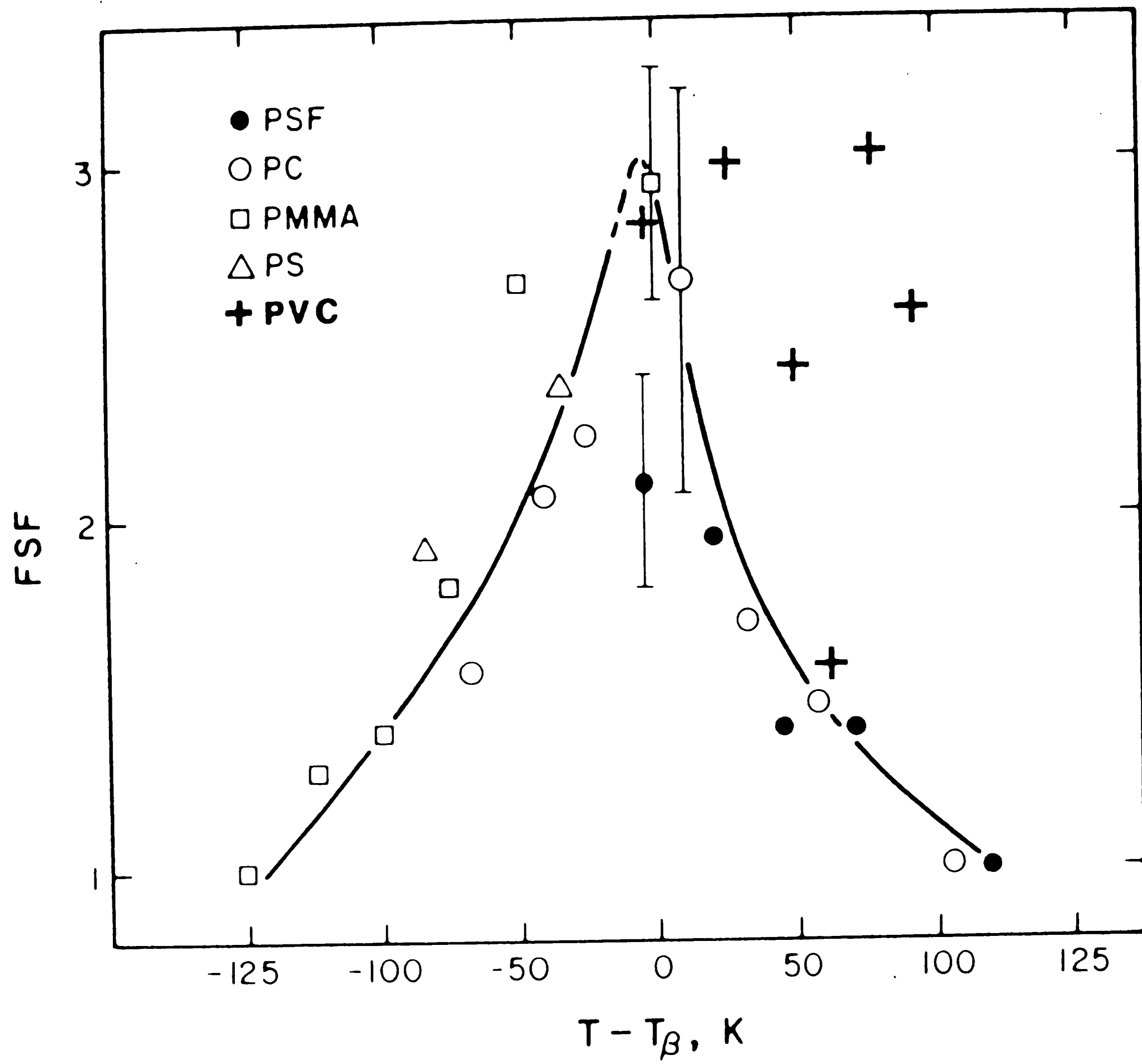


Figure 3-9: The Variation of the Frequency Sensitivity Factor with $T - T_{\beta}$ for Several Polymers

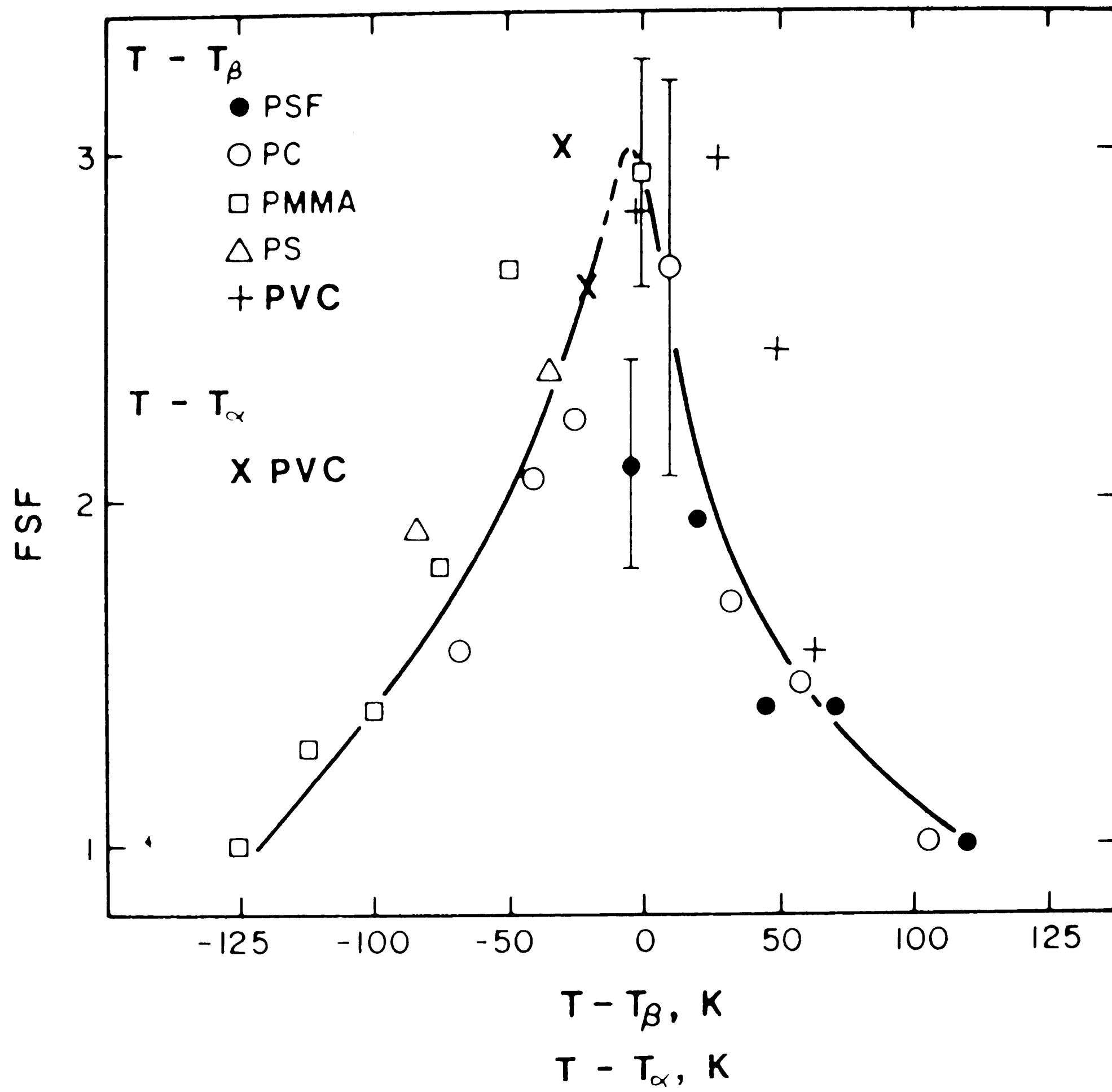


Figure 3-10: The Variation of the Frequency Sensitivity Factor with $T - T_\beta$ and $T - T_\alpha$

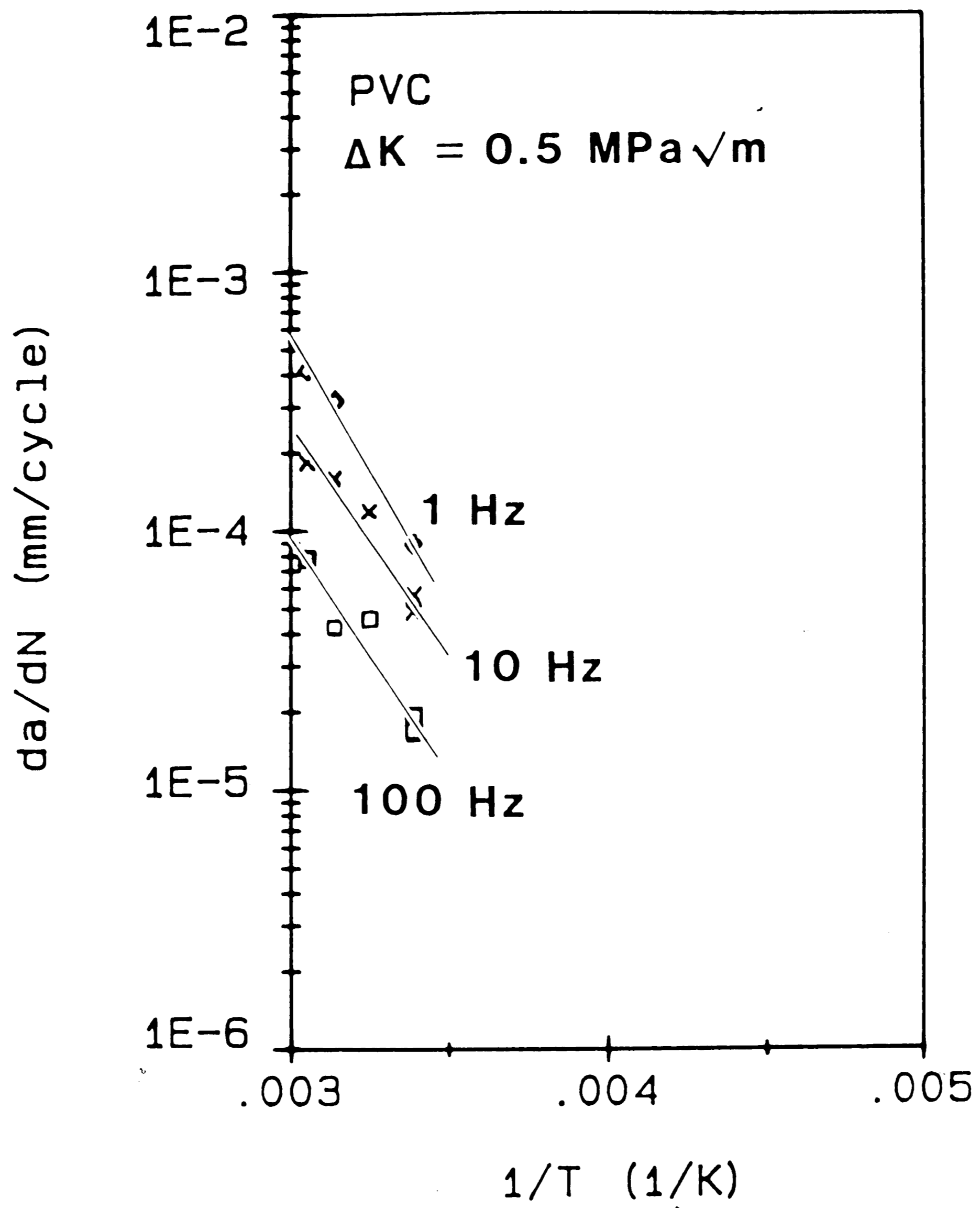


Figure 3-11: The Variation of Growth Rate With the Inverse of Temperature, $\Delta K = 0.5 \text{ MPa}\sqrt{\text{m}}$

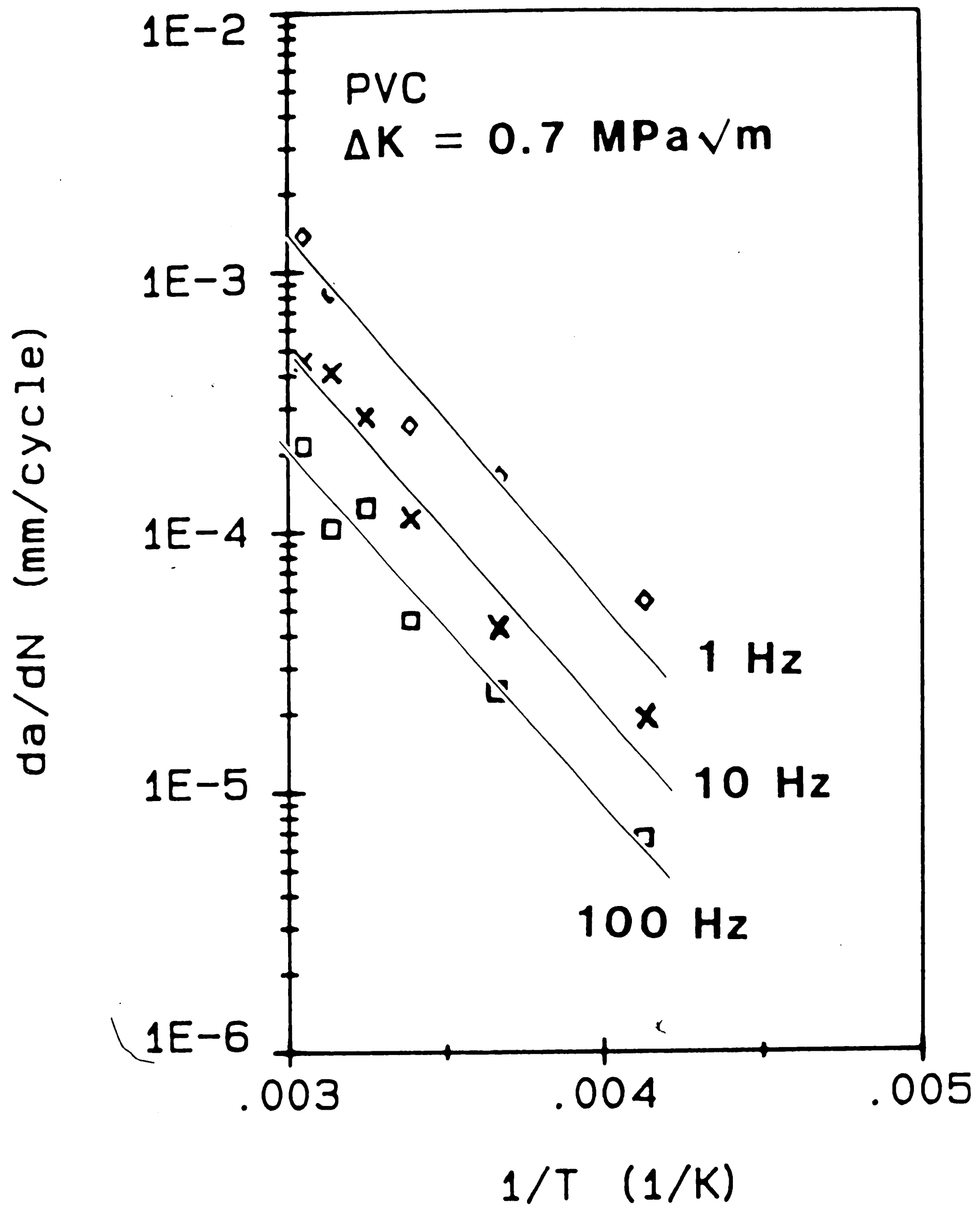


Figure 3-12: The Variation of Growth Rate With the Inverse of Temperature, $\Delta K = 0.7 \text{ MPa}\sqrt{\text{m}}$

appropriate measure of stress (see Equation 1.3).^{12, 13, 14}

Calculated apparent activation energies Q' at various test frequencies and stress intensity conditions are listed in Table 3.1. Note that Q' increases with decreasing frequency and ΔK .

The activation energy for a deformation process often corresponds to a single micromechanism dominant for that process. For example, at $T/T_m > 0.5$, the activation energy for creep in many metals and ceramics corresponds to the activation energy for self-diffusion.^{19, 30} In polymers, the dynamic mechanical spectra characterizes the motion of side chain and backbone segments of the molecules in terms of various damping peaks that occur at temperatures relative to the glass transition temperature (T_g). For PVC, the activation energy values (which have not been corrected to allow for the effect of stress) for the alpha and beta peaks have been reported to be approximately 100 kJ/mol and 60 kJ/mol, respectively.^{11, 31}

It is apparent from Table 3.1, that the activation energies for the alpha and beta peaks are considerably larger than the apparent values associated with the fatigue process. This lack of agreement with most of these activation energy values implies that main chain segment or small main chain axis motions do not dominate the fatigue crack growth process except at the lowest test frequency examined. Despite this general lack of agreement in activation energies, it must be noted that the single value of the activation energy calculated for each of the test frequencies examined and for the two stress intensity conditions studied correspond to the single fracture mechanism observed at these conditions - discontinuous crack extension (see Section 3.2.2) For this reason it is concluded that a common activation process must exist, involving

the motion of molecular segments smaller than would be defined by the beta transition. It is interesting to speculate whether continued reduction in cyclic frequency would reveal an asymptotic value of activation energy comparable to that associated with β -damping peak segmental motion processes. As noted above, the apparent activation energy for the fatigue process in this grade of PVC was observed to decrease with increasing stress intensity level and test frequency despite the presence of the same basic fracture mechanism (i.e. DGB formation). However, differences in the DGB appearance were observed (see Section 3.2.2), which presumably reflect the observed changes in apparent activation energy values. Attempts to analyze the apparent activation energy values further in terms of the activation volume and the effective stress were made, but this investigator was unable to find reasonable combinations of these two parameters.

Table 3-1: The Influence of Frequency on Apparent Activation Energies

$$\Delta K = 0.7 \text{MPa}\sqrt{m}$$

Frequency (Hz)	Time (s)	Apparent Activation Energy, Q' (J/mole)
100	.01	24,100
10	.1	28,700
1	1	29,100

$$\Delta K = 0.5 \text{MPa}\sqrt{m}$$

Frequency (Hz)	Time (s)	Apparent Activation Energy, Q' (J/mole)
100	.01	36,100
10	.1	36,600
1	1	41,700

3.2 The Effect of Testing Variables on Discontinuous Crack Growth in PVC

3.2.1 DGB Macromorphology and Band Size as a Function of ΔK

Previous studies of discontinuous growth band sizes have indicated that these measurements often correspond to values predicted by the Dugdale model.^{21, 22, 32} In the present study, however, the band sizes for this grade of PVC were found to have an other than second power dependence on the quantity $(K/\sigma_{ys})^2$ (see Figure 3.13). Consequently, it was not possible to infer the yield strength of this material from the Dugdale relationship for comparison with the experimental tensile values described above. Rimnac³³ attributed a less than second power dependence of band size on K_{max} to the occurrence of a greater amount of strain hardening which increased with increasing ΔK . Accordingly, the yield strength would be expected to vary moderately with ΔK .

Although the Dugdale model could not be used to predict specific DGB sizes for this grade of PVC, the band sizes did increase, as expected, with decreasing testing frequency (see Figure 3.13) as previously observed for PVC and other plastics.^{27, 32} Band sizes were also observed to increase with increasing temperature, in accordance with time-temperature superposition principles (see Figures 3.14 - 3.16).

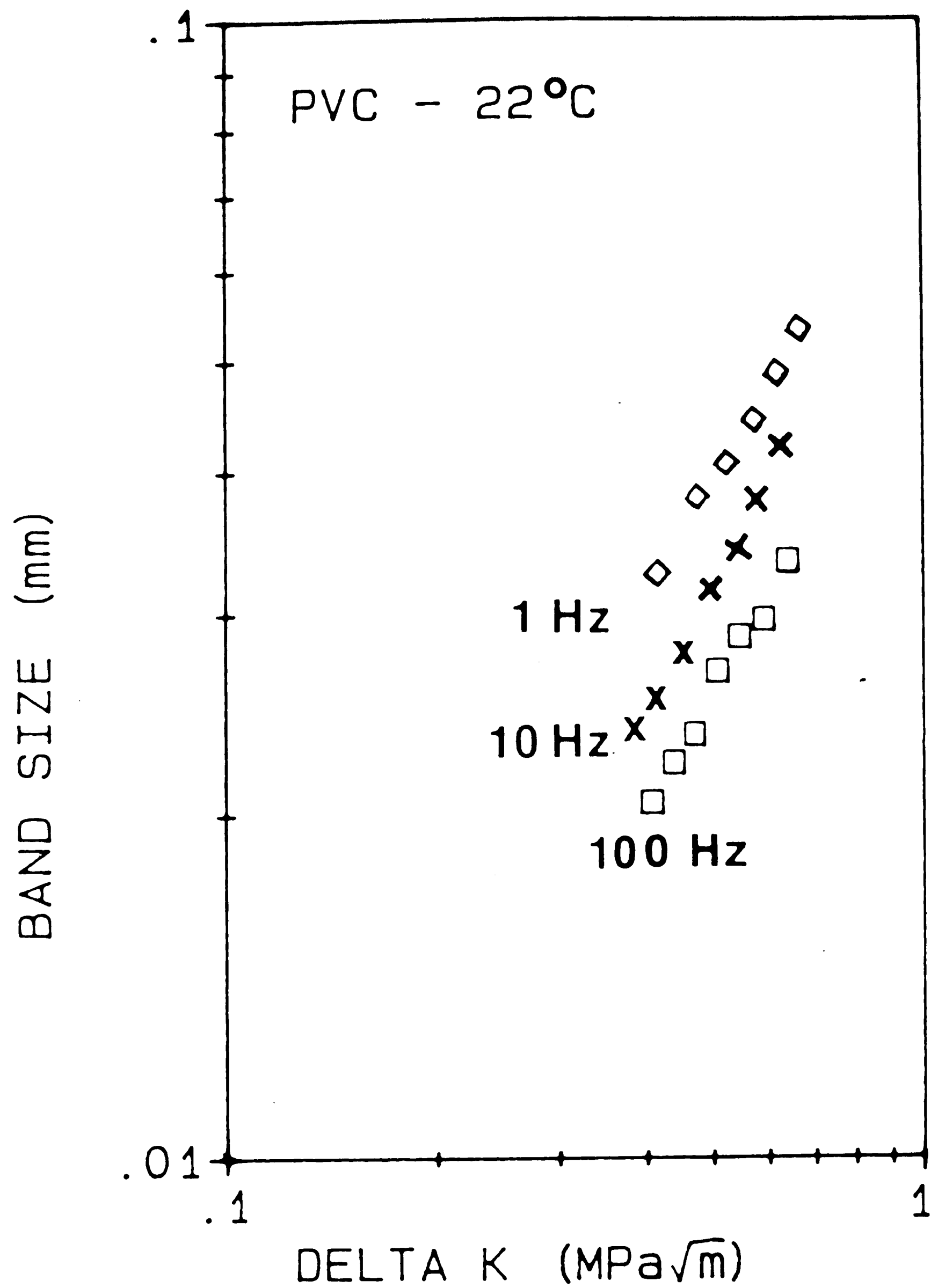


Figure 3-13: DG Band Size as a Function of ΔK and Frequency at Room Temperature
(Slopes: 100 Hz - 1.1, 10 Hz & 1 Hz - 1.35)

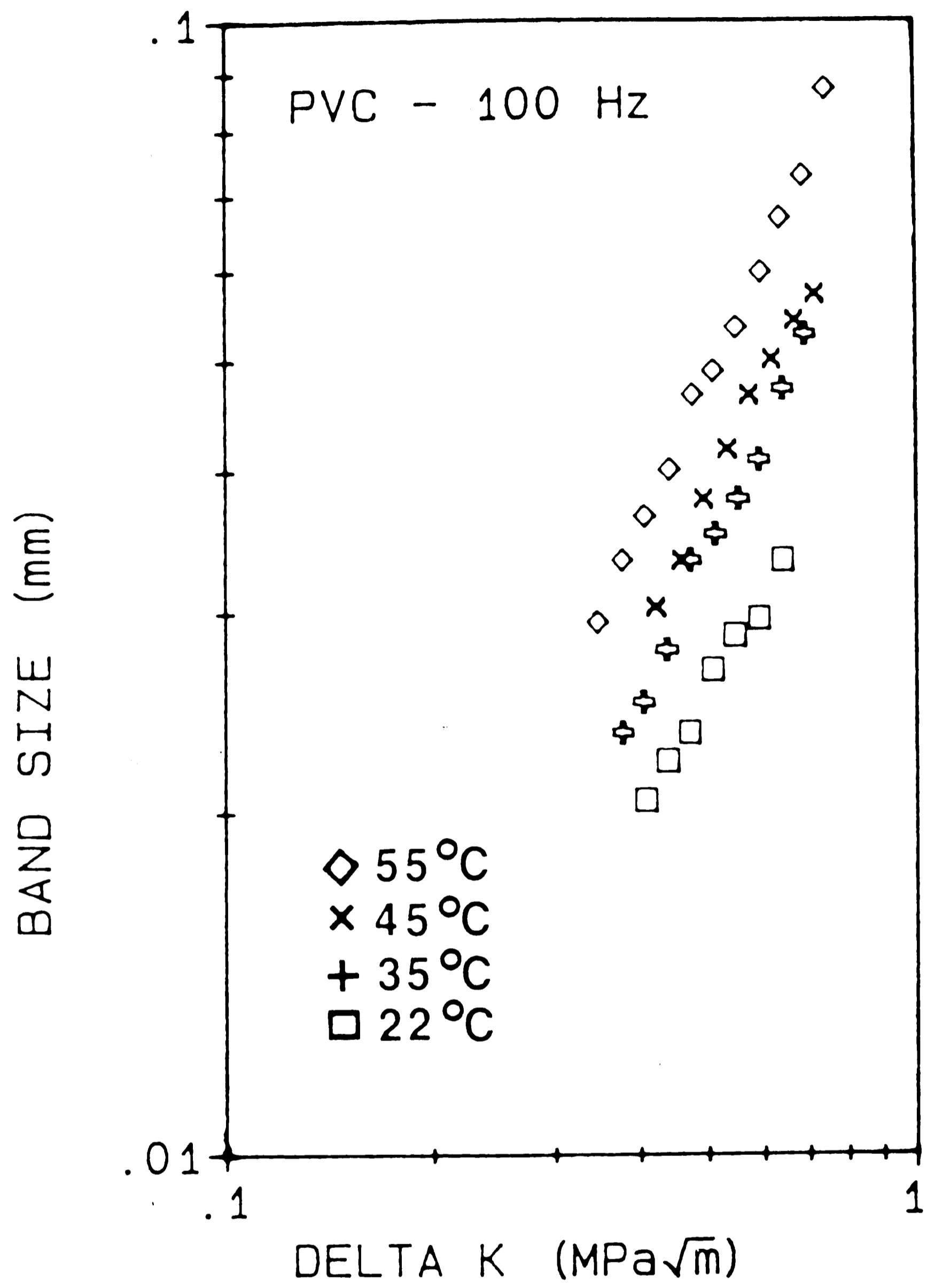


Figure 3-14: DG Band Size as a Function of ΔK and Temperature at 100 Hz

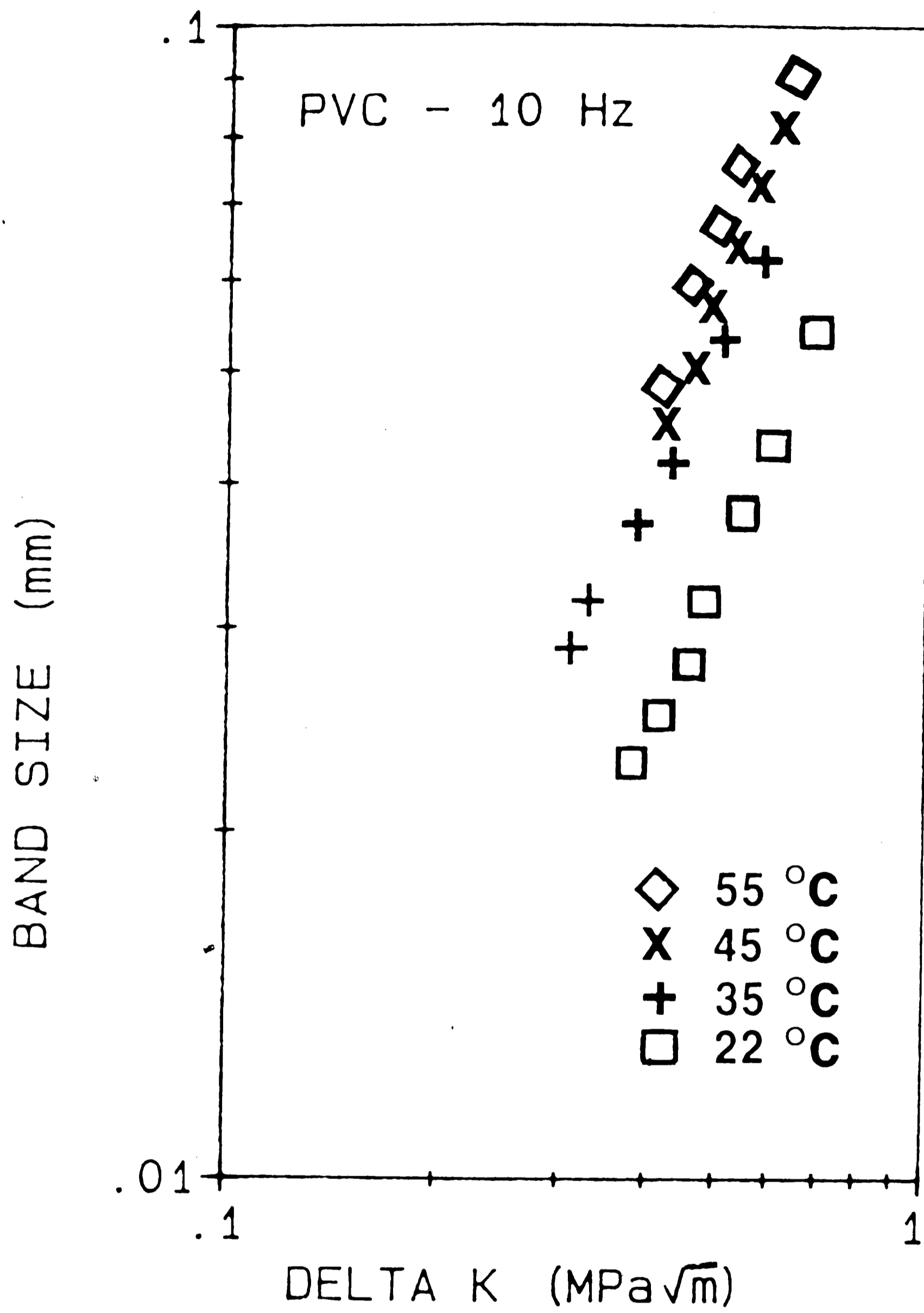


Figure 3-15: DG Band Size as a Function of ΔK and Temperature at 10 Hz

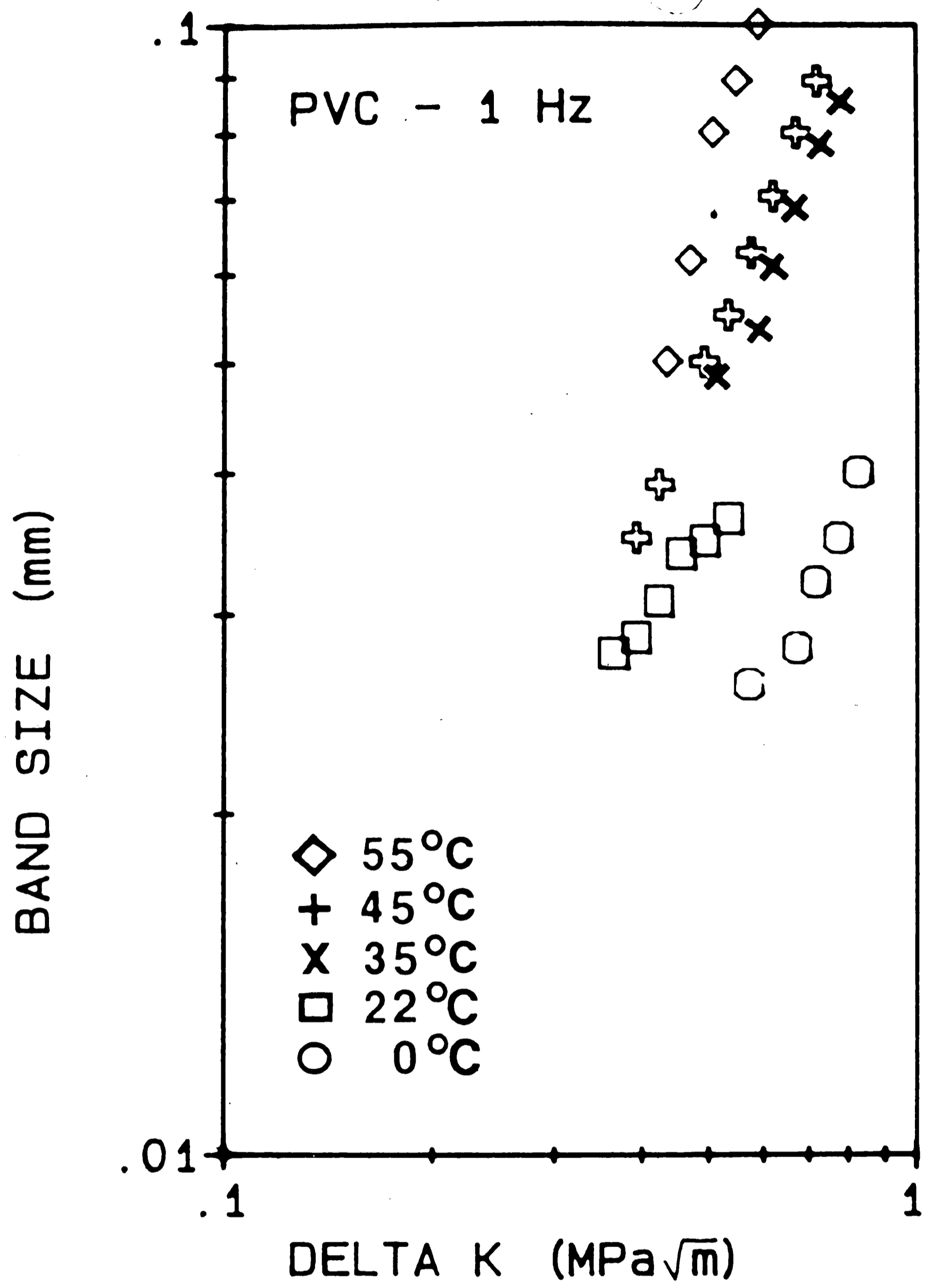


Figure 3-16: DG Band Size as a Function of ΔK and Temperature at 1 Hz

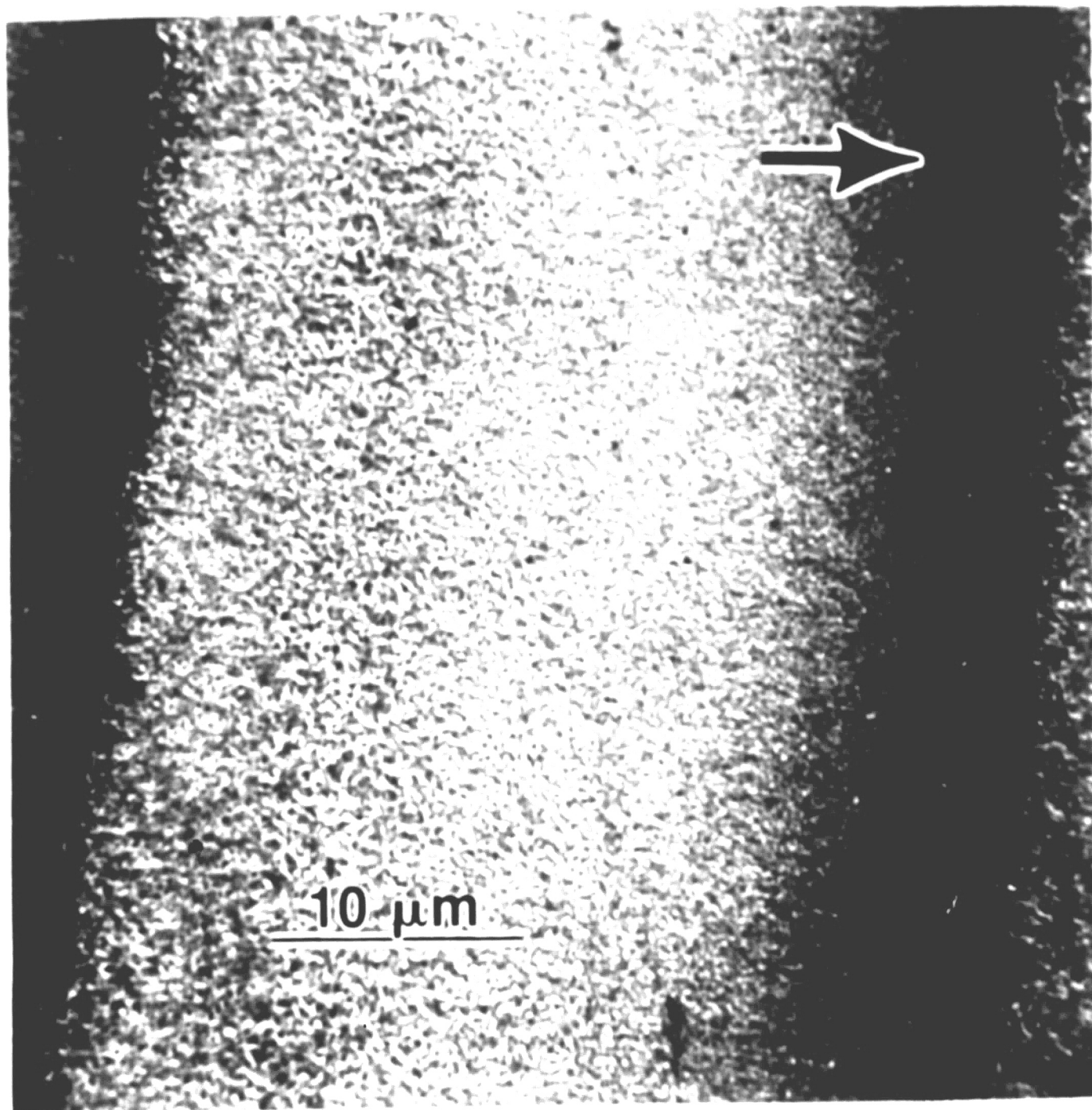
3.2.2 How Testing Conditions Affect DGB Micromorphology

Since test frequency and temperature changes will affect the nature of the craze breakdown process, it is of interest to examine their effect on the fatigue fracture surface micromorphology. As the crack opening displacement (COD) is believed to be the controlling factor in the craze breakdown process, the craze thickening process, and therefore the competition between viscous flow and orientation hardening during fibril growth must be considered.¹⁸ If the dominant flow process is orientation hardening, then fibrillar failure will occur at a COD less than the maximum value associated with the prevailing ΔK level. A DGB would then be expected to form at low ΔK levels, high frequencies, and low temperatures where orientation hardening is dominant. As ΔK increases with increasing crack length, it would be expected that the DGB's will experience a slight breakdown in morphology as the test progresses. If fibrillar growth becomes dominated by viscous flow processes, then craze thickness would likely increase to the prevailing COD level without fracturing. For this condition, DGB formation would not occur; instead, striation formation or some other yielding process(es) would be expected. Since viscous flow is associated with low test frequencies, high temperatures, and high ΔK levels, one would expect to find the above mentioned fracture mechanism transition as was reported previously in polystyrene. However, PVC exhibited DGB's over a wide range of frequencies, temperatures and ΔK levels, though changes in the testing conditions did affect the structure of the DGB. It would then appear that craze thickening in PVC is dominated by orientation hardening with viscous drawing playing a secondary role over a broad range of experimental conditions.

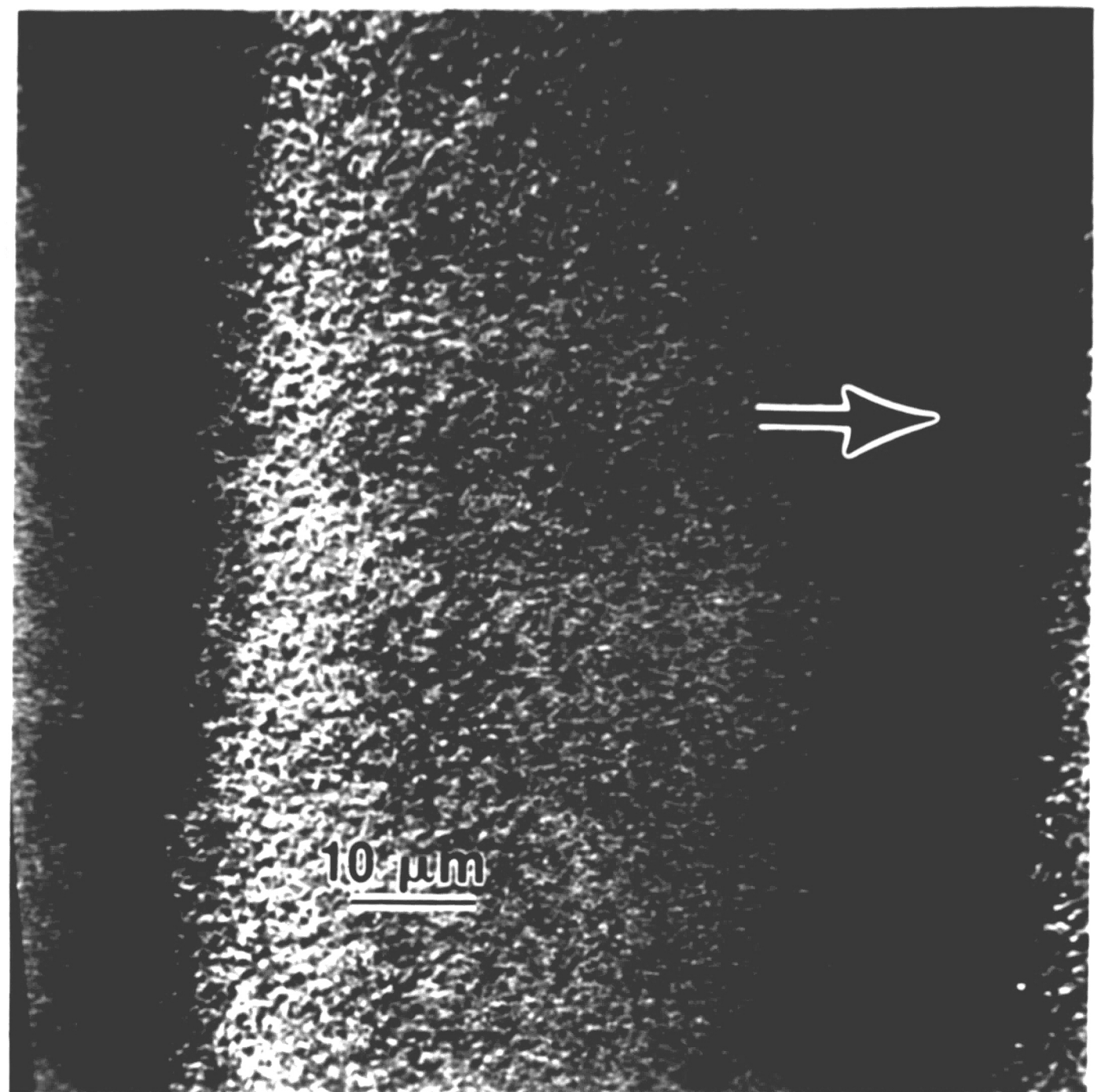
Changes in ΔK , frequency, and testing temperature influenced fracture surface morphology. When the fatigue testing temperature was increased above room temperature, the discontinuous growth band size and stretch zone width increased in size and became more clearly defined. As shown in Figure 3.17, the stretch zone at the higher temperature was larger, clearer and straighter, and the void gradient present across the body of the higher temperature DGB became steeper than that found in association with fracture surfaces produced at room temperature (see also Figure 3.17). A specimen that was fatigue tested at 65°C (i.e. 8°C below T_g) and 100 Hz experienced extensive viscous flow with no DGB formation being noted; due to the amount of viscous flow present, linear elastic fracture mechanics concepts could not be used to describe the crack growth of this material at this temperature.

The fracture surface micromorphology was found to change dramatically when fatigue tests were conducted below room temperature. Figures 3.18 - 3.23 show fracture surfaces produced at progressively lower frequencies below ambient temperatures. For temperatures of 0 and -30°C at the 100 Hz condition, and -30 °C at the 10 Hz condition, it is apparent that major differences in fracture surface appearance exist (see Figures 3.18, 3.19, 3.20). The large smooth bands (Figures 3.18 and 3.19) that are widely spaced correspond to the Δa increments at which the test was stopped to take crack length measurements. The narrower and irregularly spaced bands found at these two test temperature conditions lie between the large smooth bands and are 1 - 10 X smaller than the macroscopic growth rate; these small bands are rough in appearance. Although the large smooth bands are approximate in size to that which would be expected for fatigue striations, these bands possess a void gradient and are

probably bands of creep damage corresponding to the load-hold periods.



a



b

Figure 3-17: DGB Morphology With Increasing Temperature
(22°C and Above) at 10 Hz, $\Delta K = 0.5 \text{ MPa}\sqrt{\text{m}}$
a) 22°C, b) 55°C

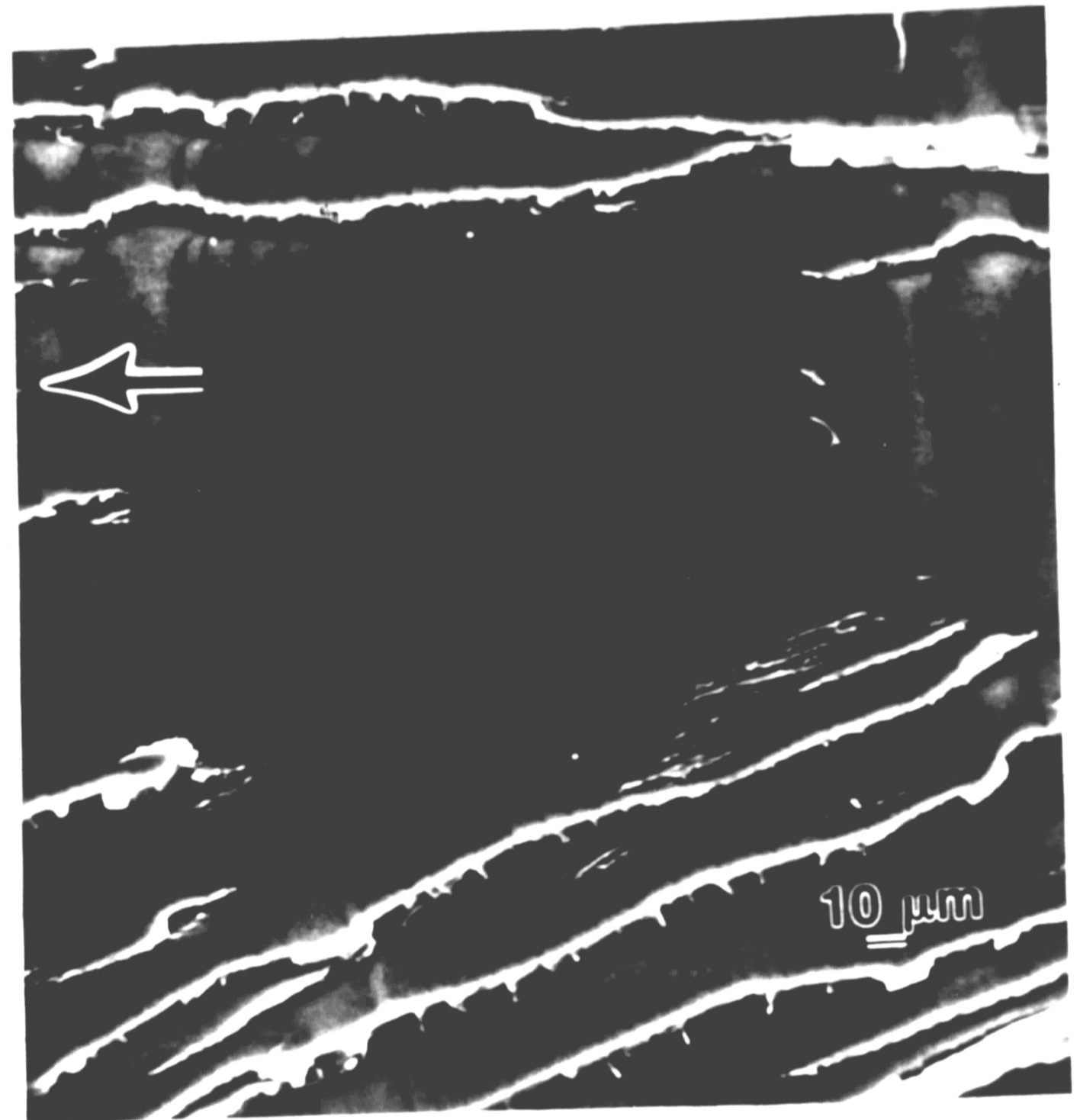


Figure 3-18: Fracture Surface Morphology at 0°C, 100 Hz
 $\Delta K = 0.7 \text{ MPa}\sqrt{\text{m}}$

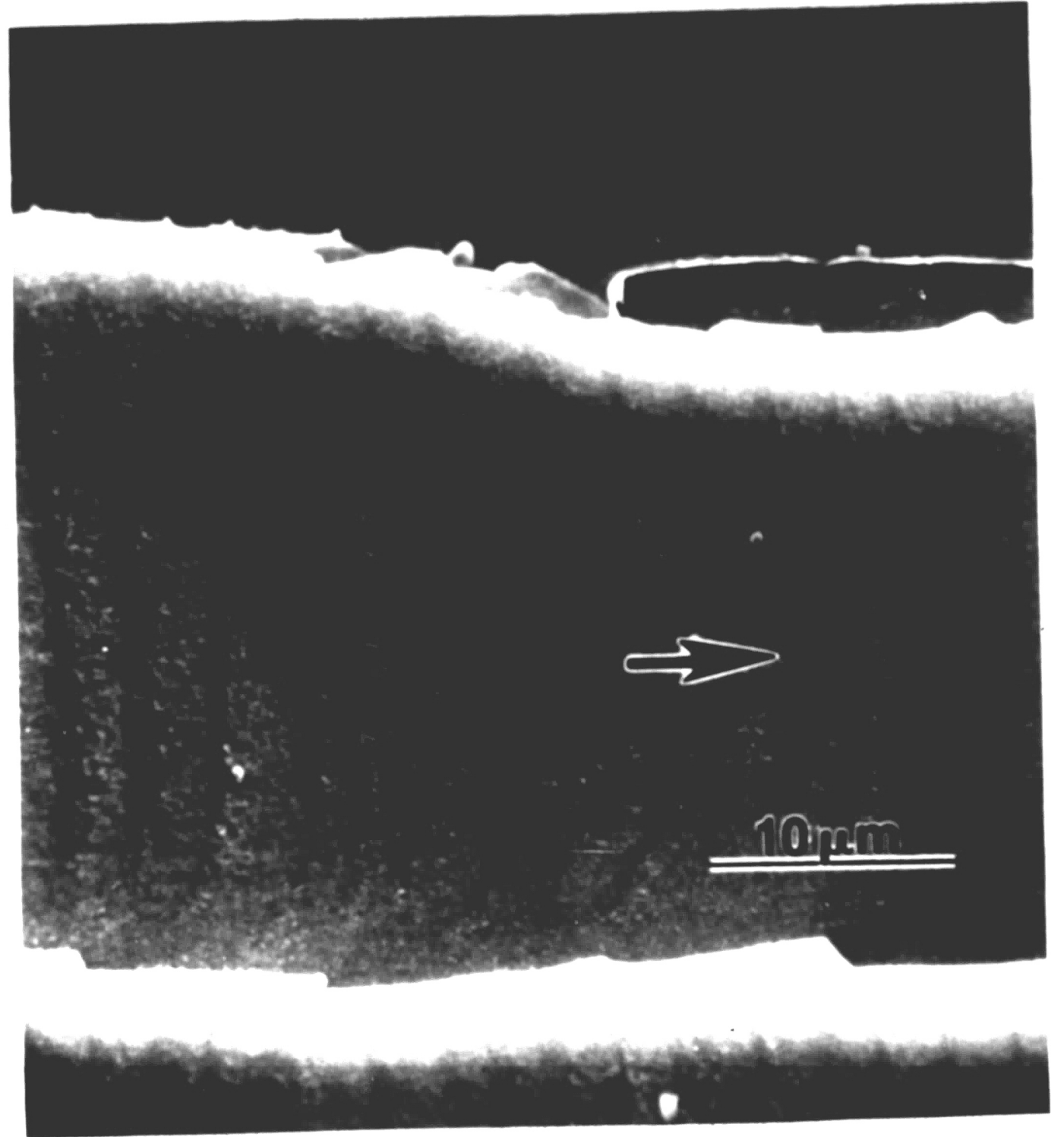
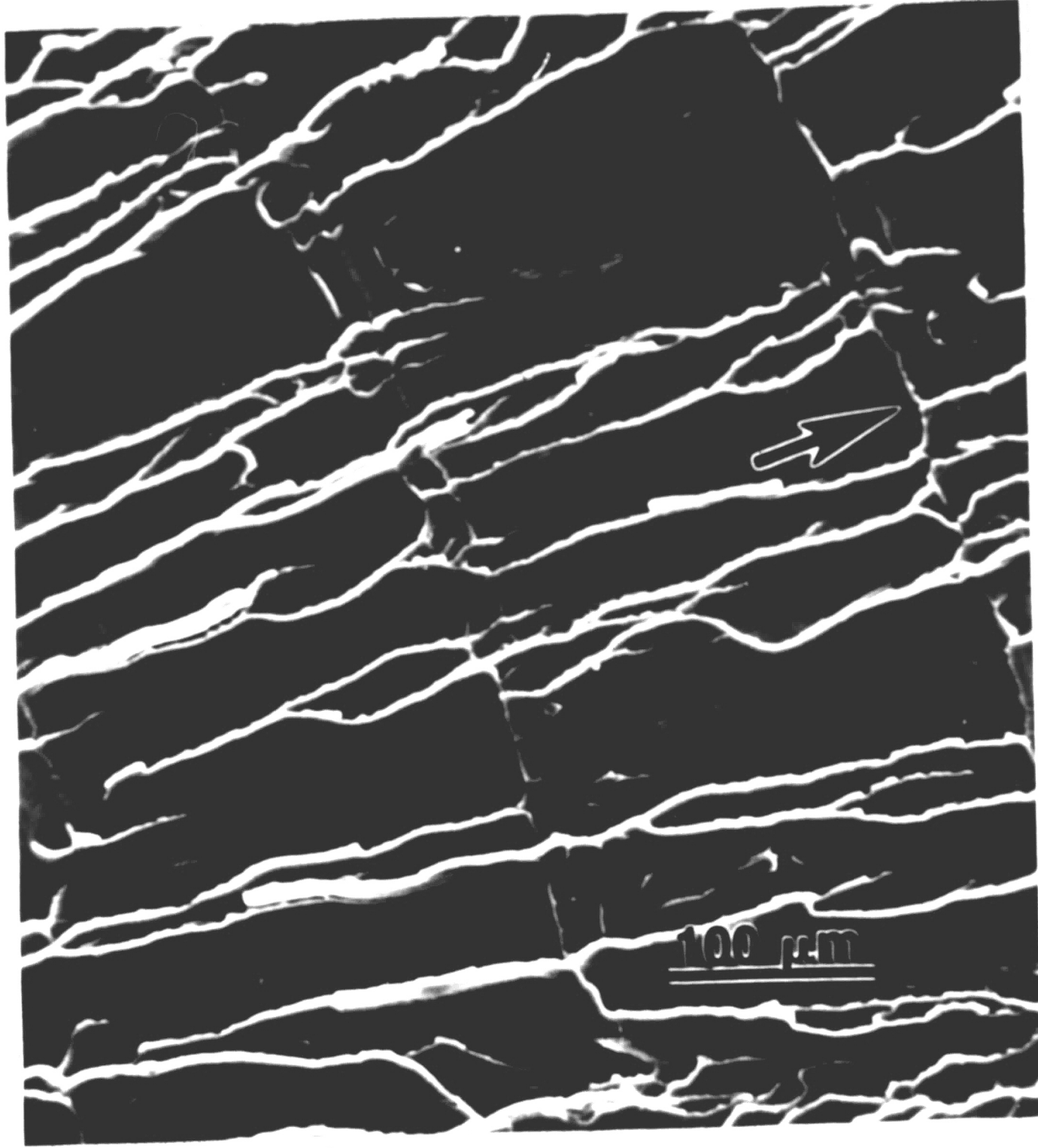


Figure 3-19: Fracture Surface Morphology at -30°C , 100 Hz,
 $\Delta K = 0.7 \text{ MPa}\sqrt{\text{m}}$

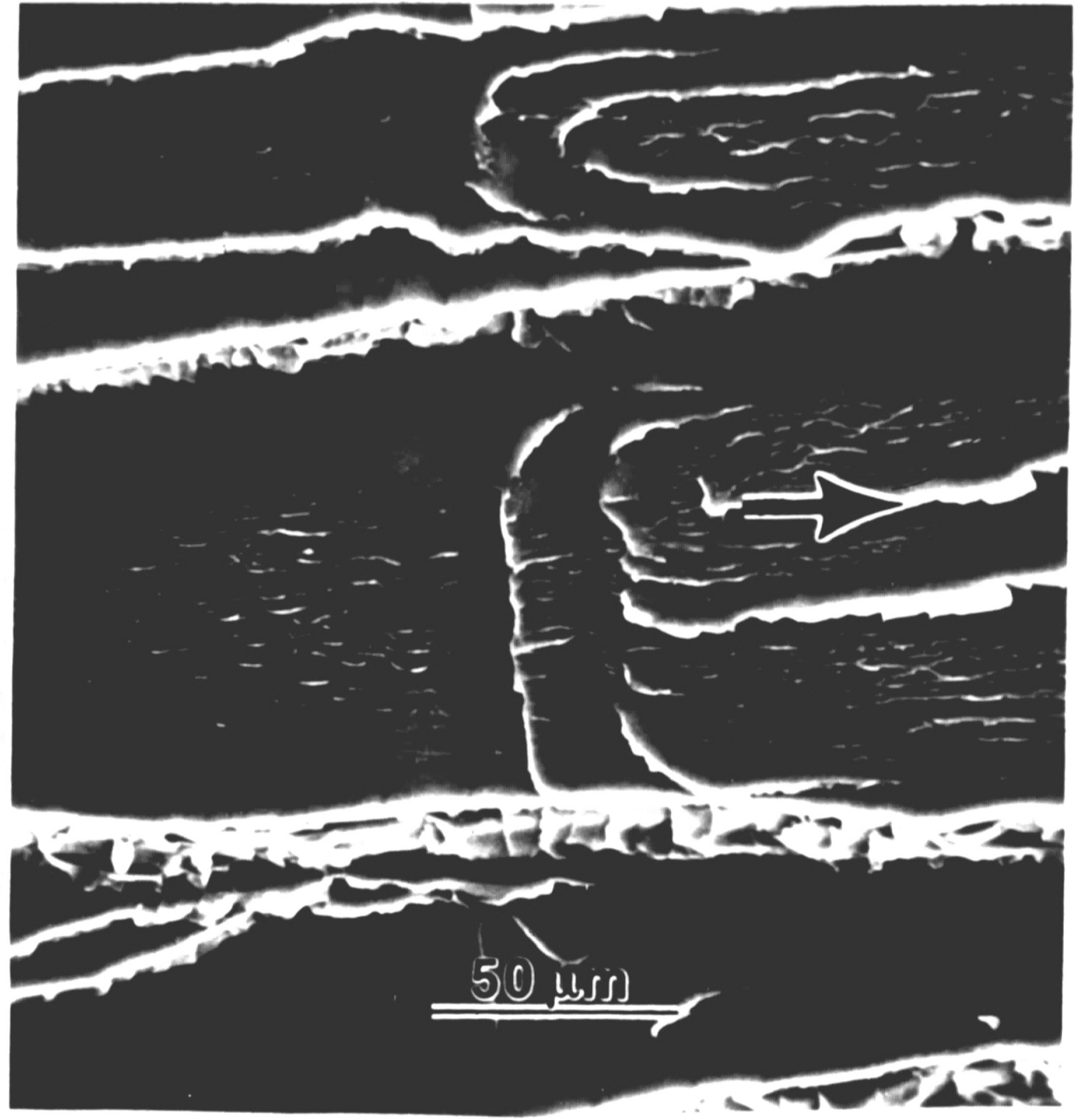
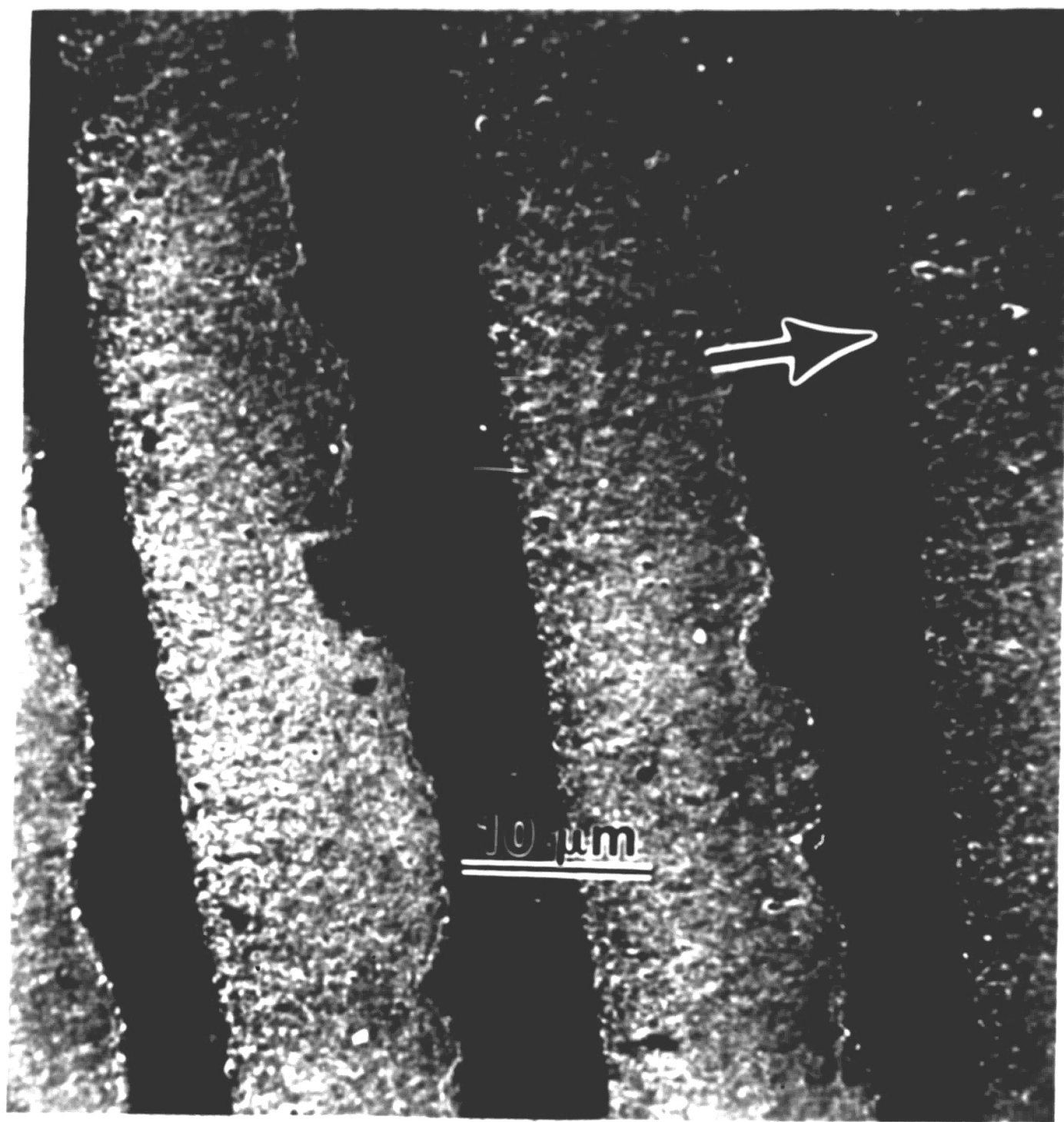


Figure 3-20: Fracture Surface Morphology at -30°C , 10 Hz
 $\Delta K = 0.7 \text{ MPa}\sqrt{\text{m}}$

For the testing conditions of 0°C and 10 Hz (see Figure 3.21) flat bands with a wavy trailing edge are apparent, with a size smaller than that of the macroscopic growth rate at low ΔK levels. The wavy, scalloped edge appears to be similar to the morphology described by the meniscus instability mechanism, and suggests that these irregular bands represent cracking through incompletely formed crazes that form at the advancing crack tip.³⁴ As ΔK increases, these bands increase in size, but deteriorate in shape. The fracture surface takes on a morphology similar to that observed at the conditions of 0 & -30°C, 100 Hz and -30°C, 10 Hz as previously described. Similarly, at the -30°C and 1 Hz condition (see Figure 3.22), bands are observed which are smaller in size than da/dN at the low ΔK levels, and deteriorate to the flat band appearance with a wavy trailing edge as noted previously at the 0°C and 10 Hz condition. The fracture surface morphology then again changes to that of small irregular bands which lie inbetween large smooth ones. The only bands which were found to be larger than the macroscopic growth rate in size were those produced at 0°C and 1 Hz (see Figure 3.23). These bands appear to be very similar to classical DGB's, but gradually break down as ΔK increases to a morphology similar to that of the flat bands described above.

From the above, a series of fracture surface morphologies are observed which depend on different testing conditions and stress levels. DGB's are favored at temperatures equal to and above room temperature. As the temperature is decreased, and the frequency and stress intensity range is increased, the DGB's first break down into numerous scalloped flat bands, and then into a combination of two band types where small bands lie between the large ones, the latter corresponding to crack extension during the time period

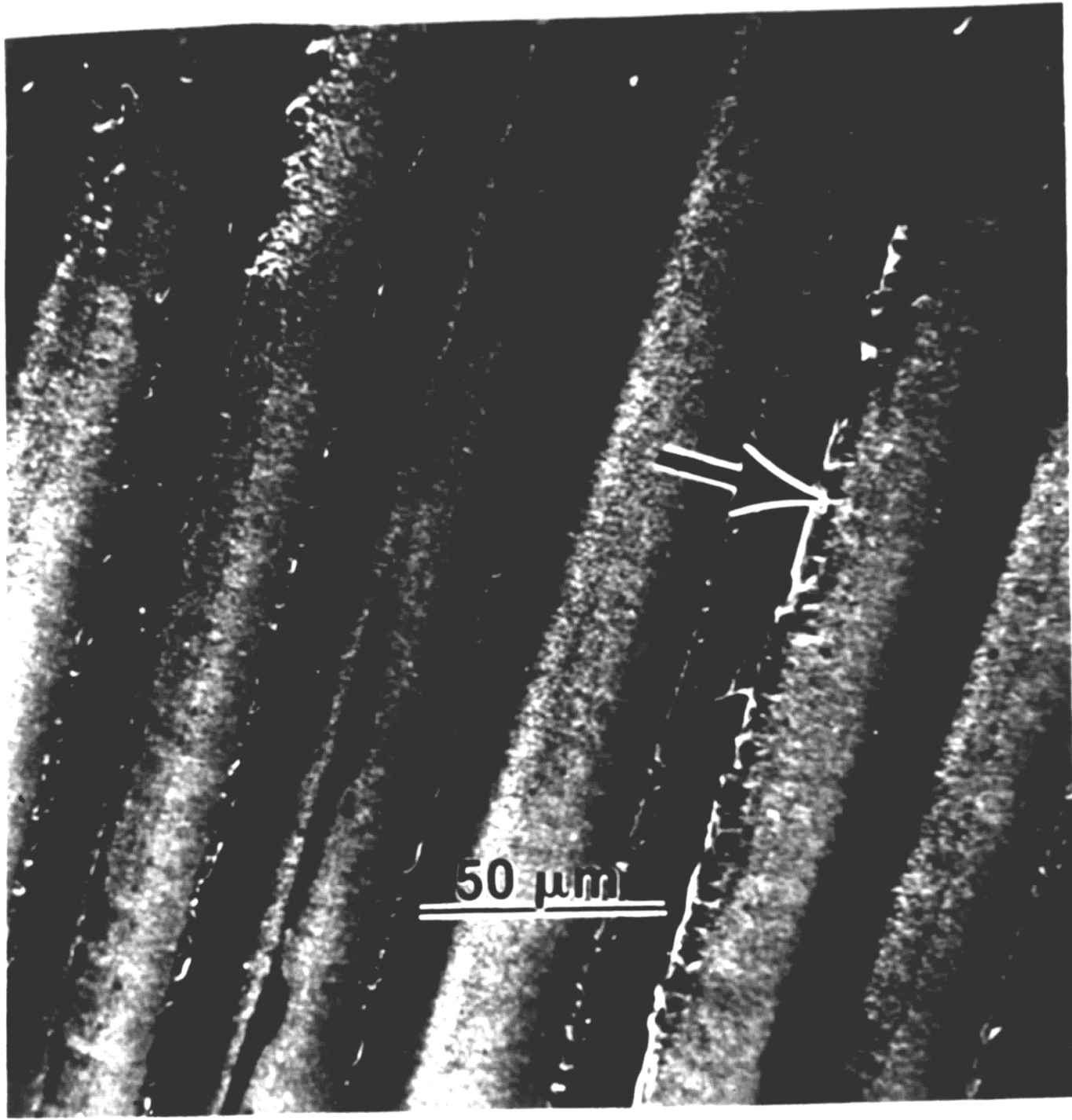


a

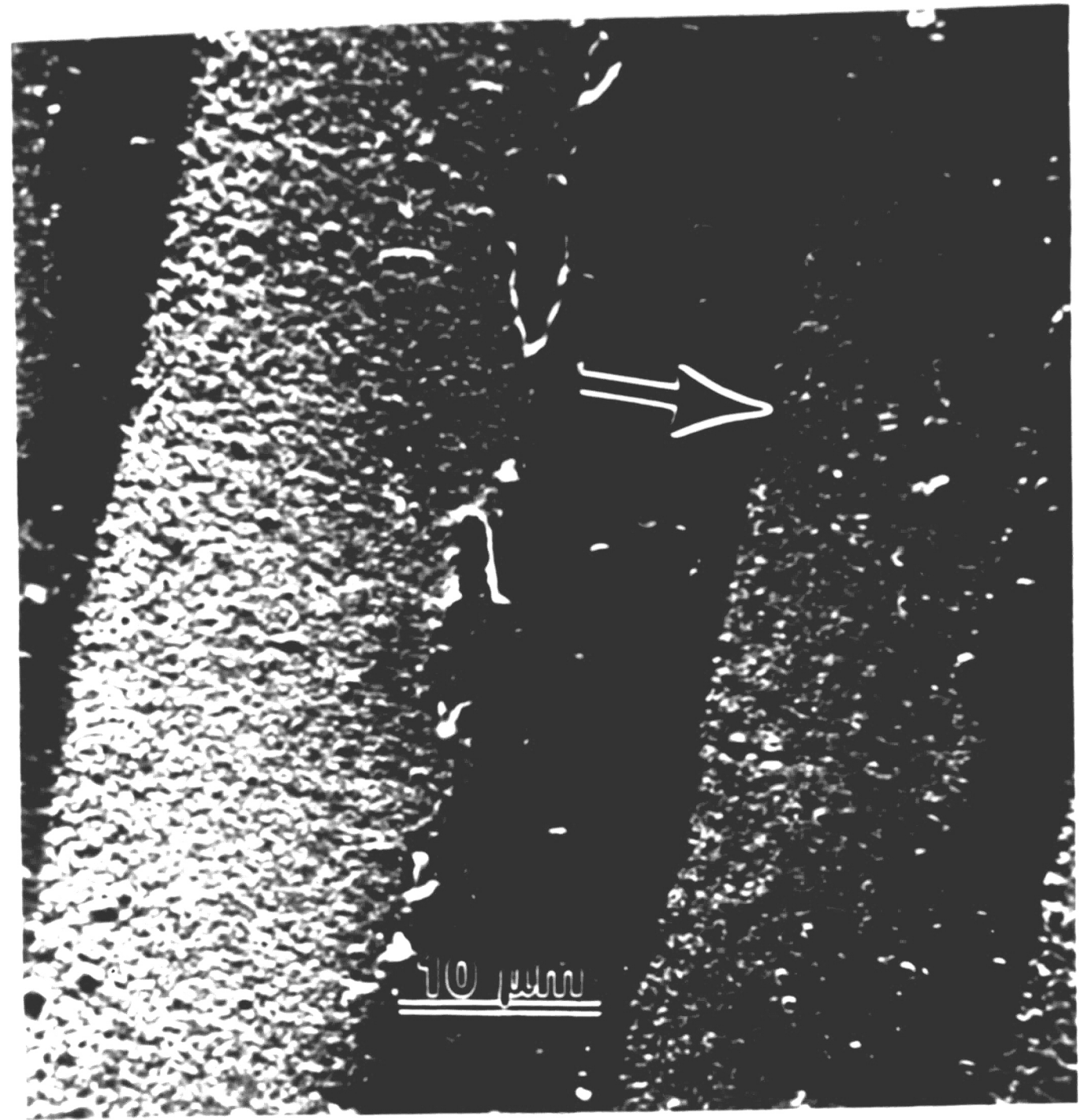


b

Figure 3-21: Fracture Surface Morphology at 0°C, 10 Hz
a) $\Delta K = 0.7 \text{ MPa}\sqrt{\text{m}}$, b) $\Delta K = 1.1 \text{ MPa}\sqrt{\text{m}}$

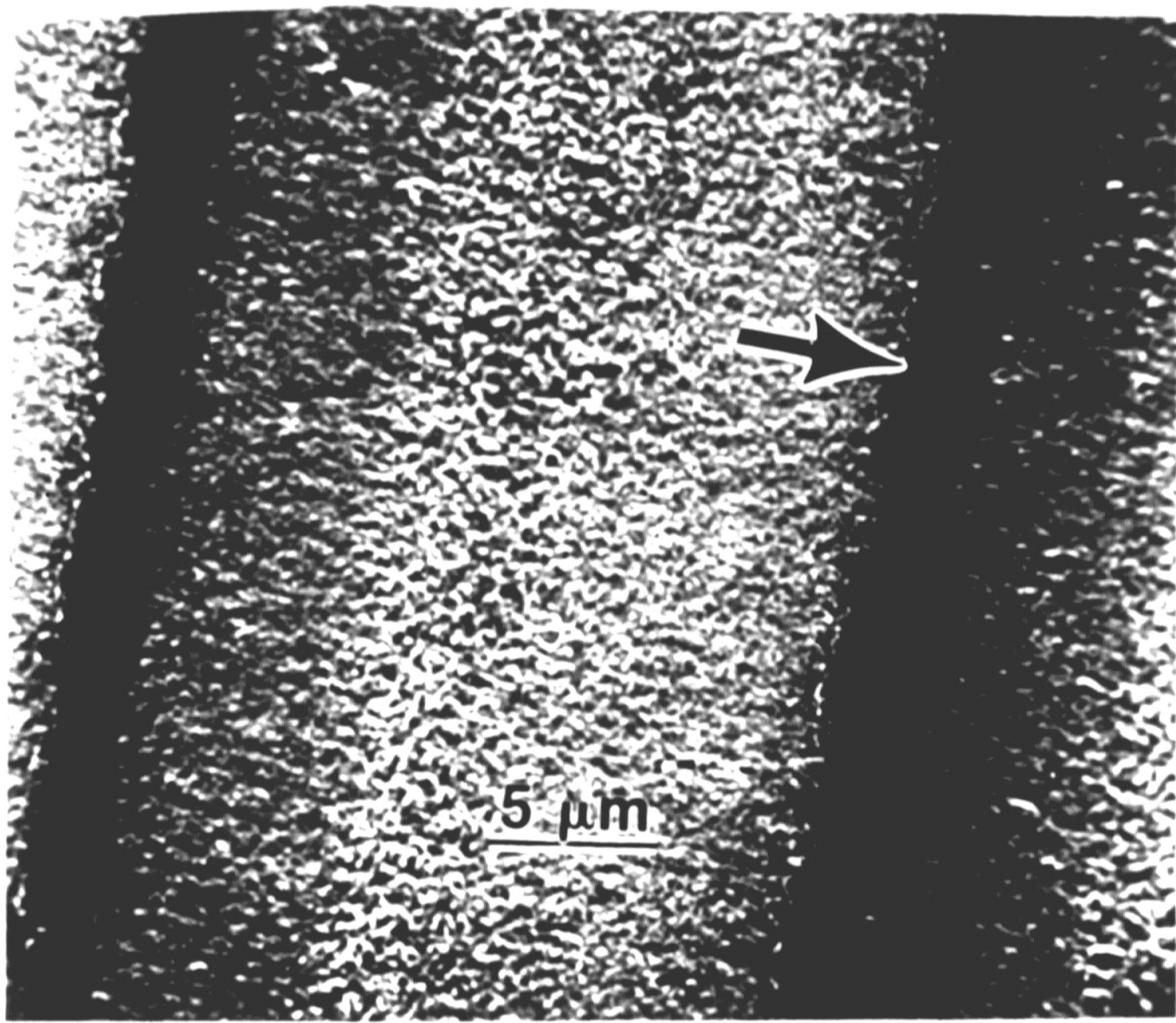


a

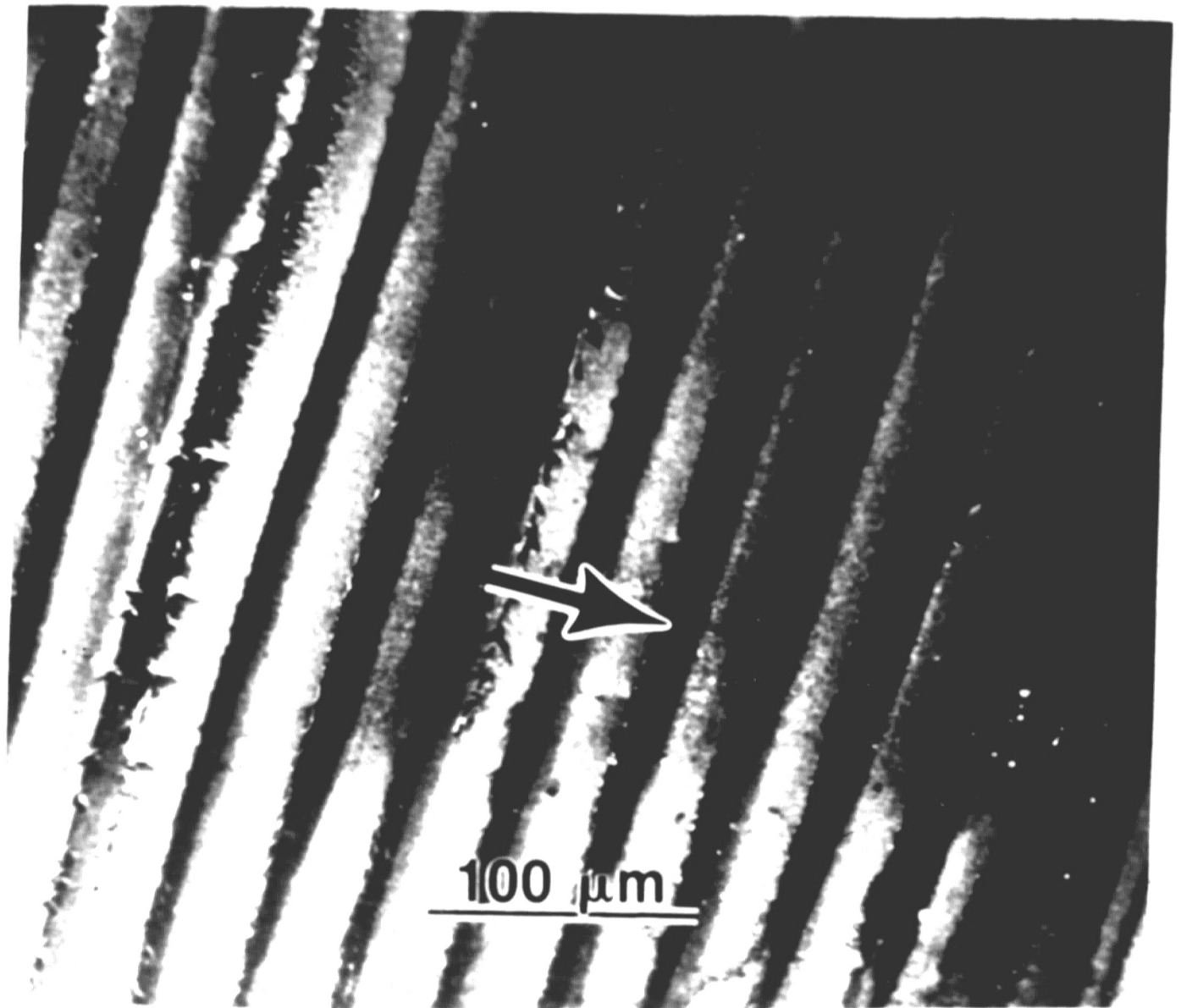


b

Figure 3-22: Fracture Surface Morphology at -30°C , 1 Hz
a) $\Delta K = 0.6 \text{ MPa}\sqrt{\text{m}}$, b) $\Delta K = 0.7 \text{ MPa}\sqrt{\text{m}}$



a



b

Figure 3-23: Fracture Surface Morphology at 0°C, 1 Hz
a) $\Delta K = 0.7 \text{ MPa}\sqrt{\text{m}}$, b) $\Delta K = 0.8 \text{ MPa}\sqrt{\text{m}}$

when crack tip readings were made. It is interesting to note that these bands are formed at low test temperatures in association with high test frequencies. Since creep crack extension during load-hold time periods would be expected to be more pronounced at high temperatures and low frequencies, the observed presence of these bands at low temperatures and high frequencies is most surprising. It is speculated that creep crack expansion is, indeed, responsible for the presence of these bands but that they form preferentially under test conditions near T_{β} where hysteretic heating occurs in the crack tip region.

Steps were observed on the fracture surface of all specimens tested below ambient, except at the 1 Hz 0°C condition, indicative of the occurrence of multiple crazing during the deformation process. From band life calculations taken from fracture surfaces generated at testing temperatures of ambient and above (see Table 3.2), it is shown that the band life increased dramatically with decreasing temperature and ΔK . This reflects the fact that craze growth and breakdown kinetics become more sluggish at lower temperatures and stress intensities, as would be expected. Therefore, it may be more energetically favorable for the deformation energy imparted into the system during the course of each loading cycle to be dissipated by the formation of additional crazes. This is analogous to the nucleation and growth of precipitates observed in metallic alloys. Under high temperature conditions, the growth of precipitates is more thermodynamically favorable as opposed to their nucleation, and vice versa. There is, however, an optimum temperature where the driving force for craze nucleation and growth processes are equivalent. Likewise, a testing temperature approximate to 0°C can be thought of as a cross-over temperature between single craze (DGB formation) and multiple craze (non-DGB formation)

deformation behavior. Figure 3.24 shows that for neat PVC with various notch sizes, the ductile to brittle transition for this material is in the 0°C range.³⁵ It is speculated, that below this temperature, the nucleation of multiple crazes is dominant, while at temperatures of ambient and above, single craze nucleation and subsequent growth is dominant.

Table 3-2: The Effect of Temperature, Frequency, & ΔK on DG Band Life

$$\Delta K = 0.5 \text{ MPa}\sqrt{m}$$

55°C

Frequency (Hz)	DG Band Life, N* (cycles)
1	180
10	305
100	613

22°C

Frequency (Hz)	DG Band Life, N* (cycles)
1	422
10	640
100	1250

0°C

Frequency (Hz)	DG Band Life, N* (cycles)
1	1625

$$\Delta K = 0.7 \text{ MPa}\sqrt{m}$$

22°C

Frequency (Hz)	DG Band Life, N* (cycles)
1	200
10	392
100	720

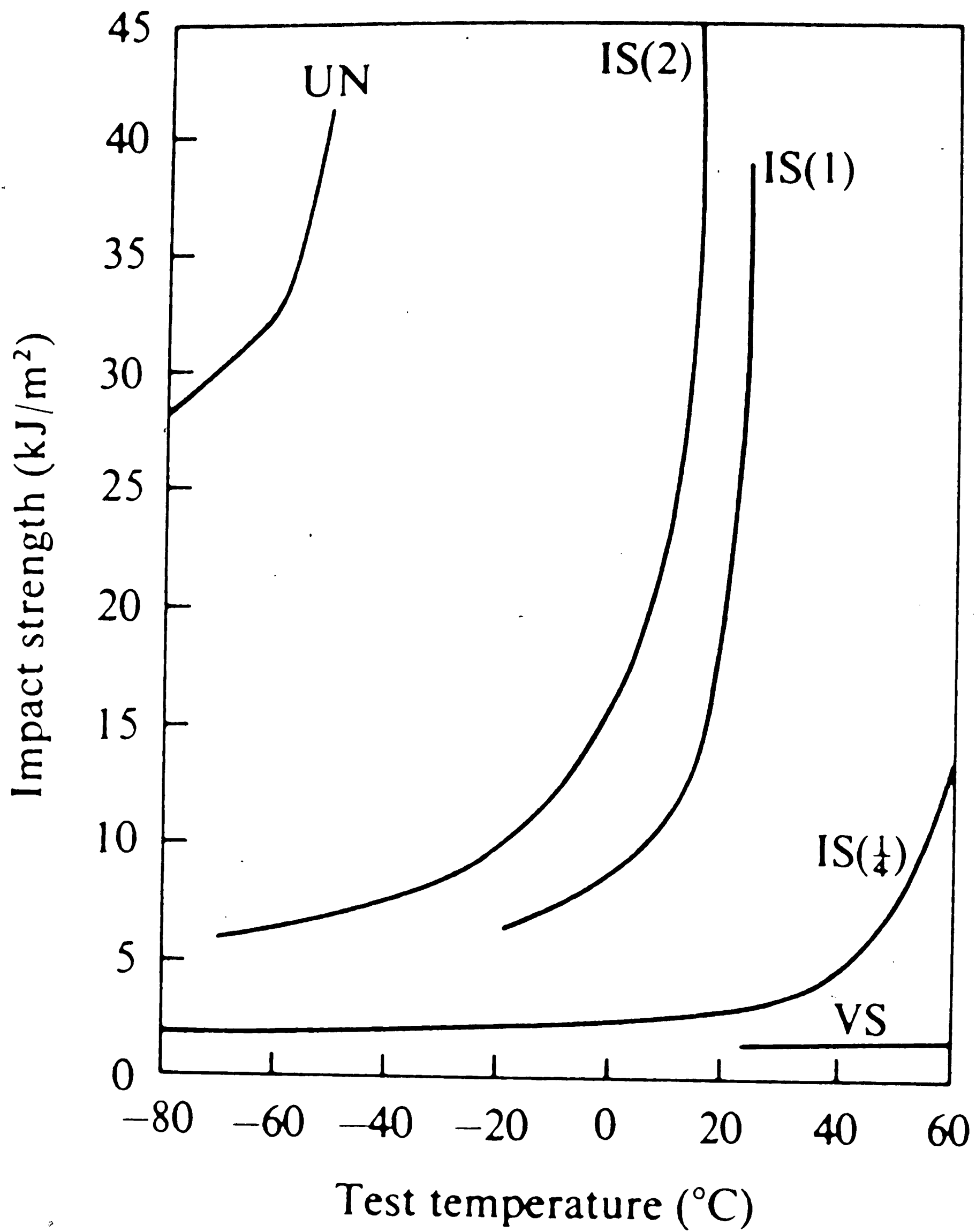
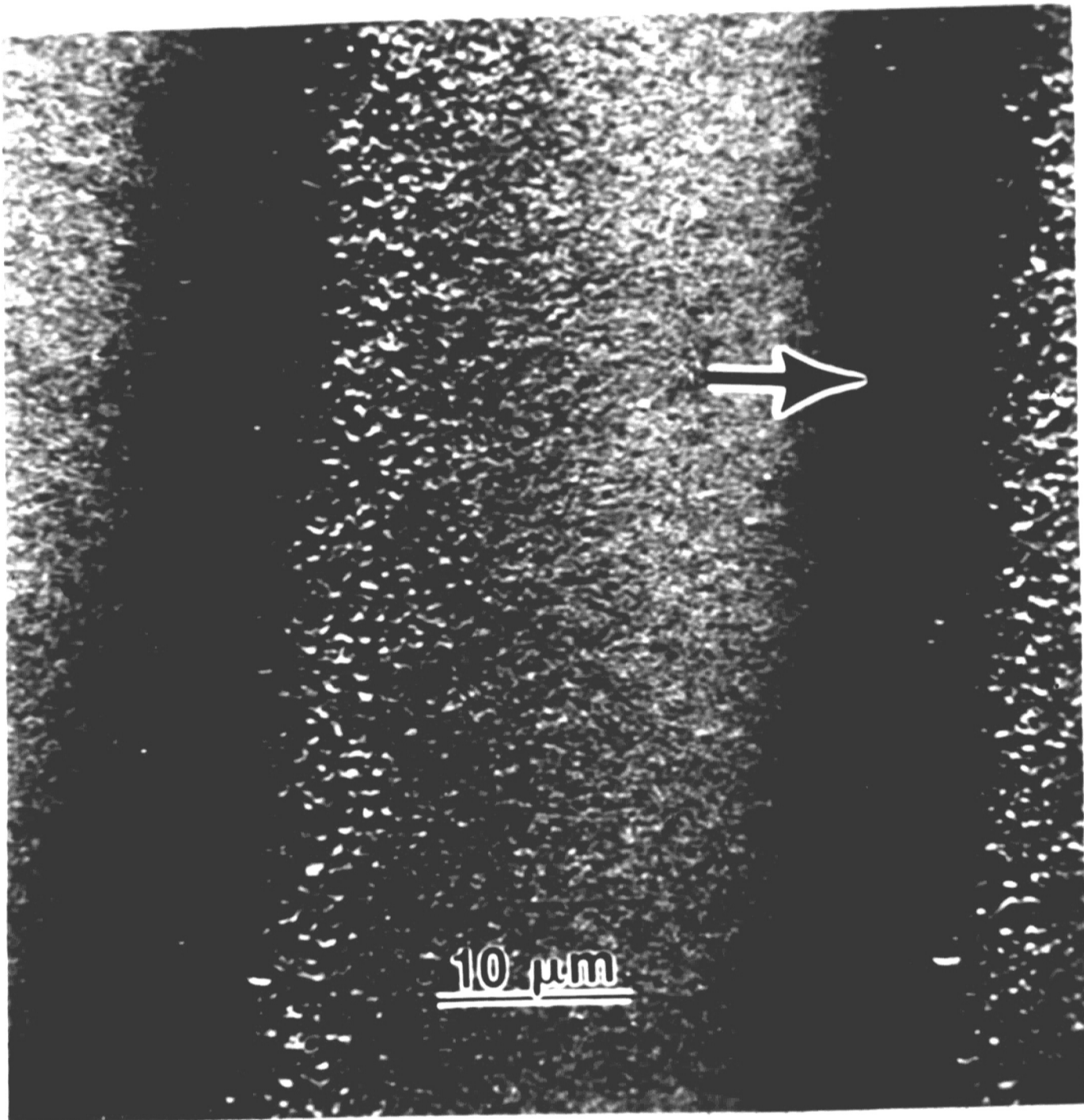


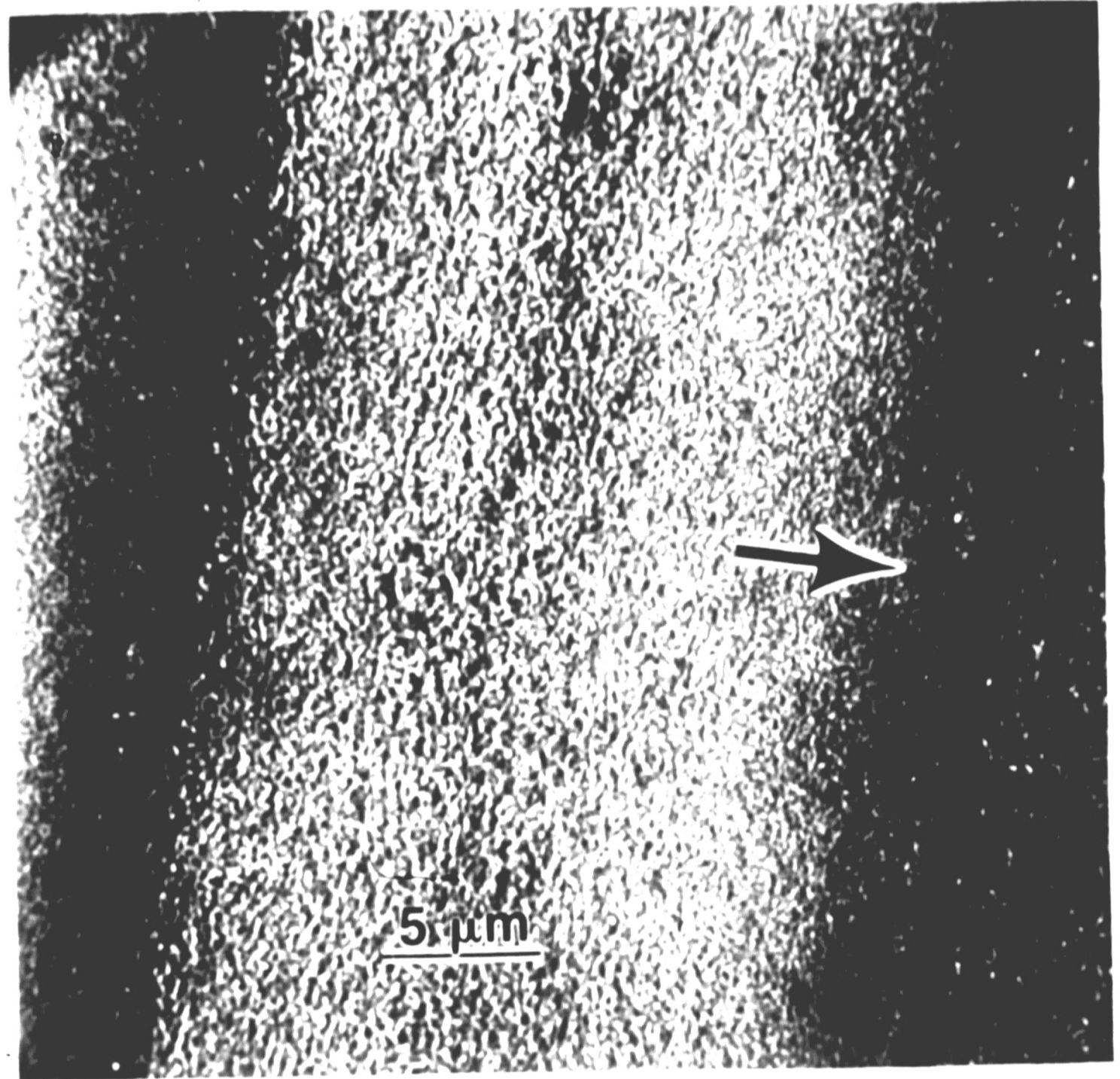
Figure 3-24: The Effect of Temperature on the Impact Behavior of Neat PVC : UN = Unnotched Specimens, IS(2), IS(1), IS(1/4) = Notch Tip Radius of 2, 1, 1/4 mm, VS = Very Sharp Notches (~10 μm)

DGB formation is also favored by conditions associated with increased testing frequencies (see again Table 3.2).^{7, 18} In accordance with previously observed behavior, discontinuous growth band structure was also observed to change with increasing frequency for this grade of PVC for specimens tested at room temperature. It is apparent from Figure 3.25 that the void gradient becomes steeper at lower test frequency. This was also observed for a given frequency when the testing temperature was increased, suggesting that a time-temperature relationship exists for DGB morphology as well. No significant frequency effects on the stretch zone appearance were noted.

At temperatures above ambient, the discontinuous growth bands were observed to become rougher in appearance with increasing crack length and corresponding stress intensity level, as illustrated in Figure 3.26. This observation is in agreement with known DGB behavior.⁷ As previously mentioned, DGB formation is favored at low ΔK levels. It then follows that the bands will experience a breakdown in appearance as the stress intensity level increases.

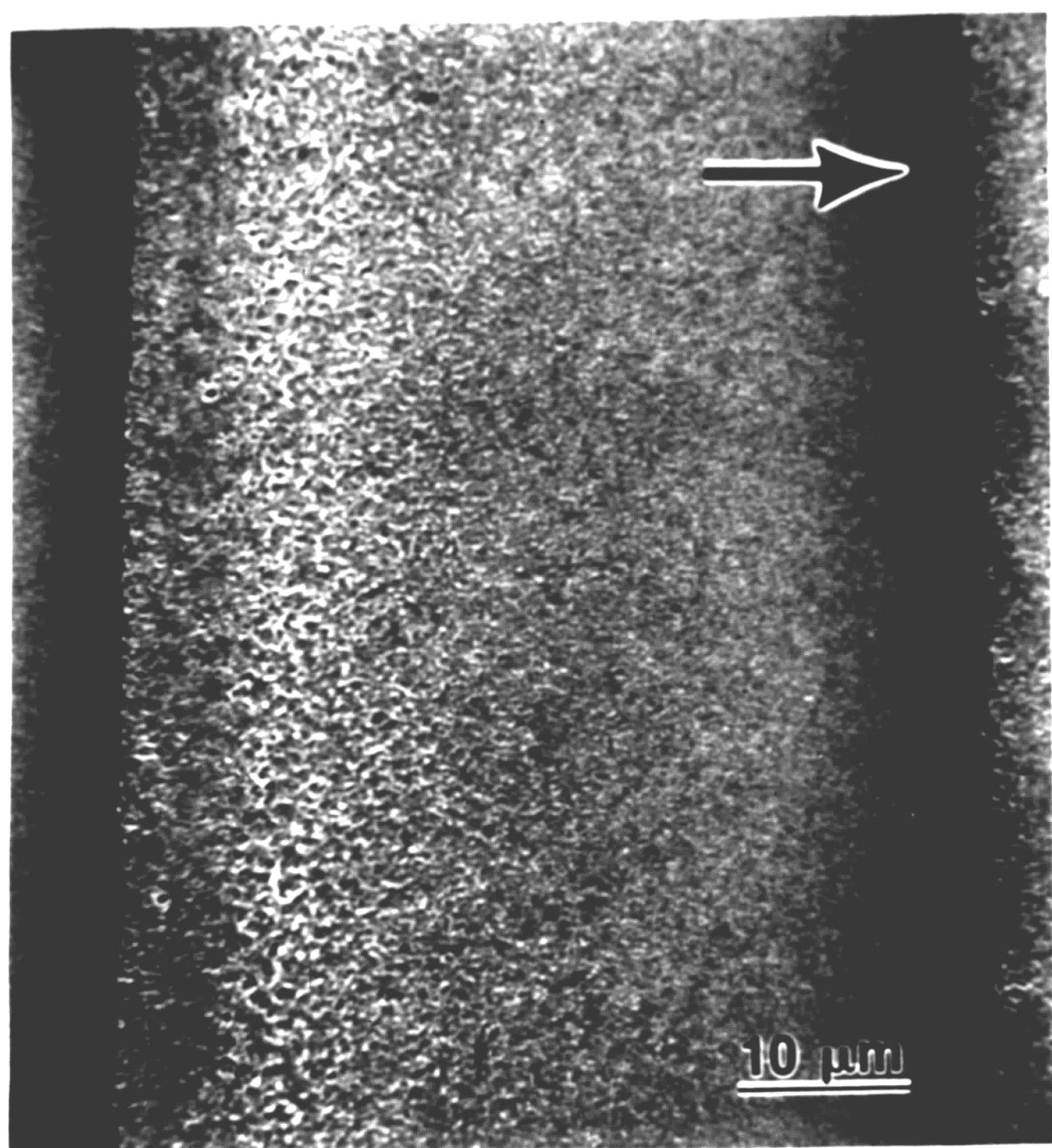


a

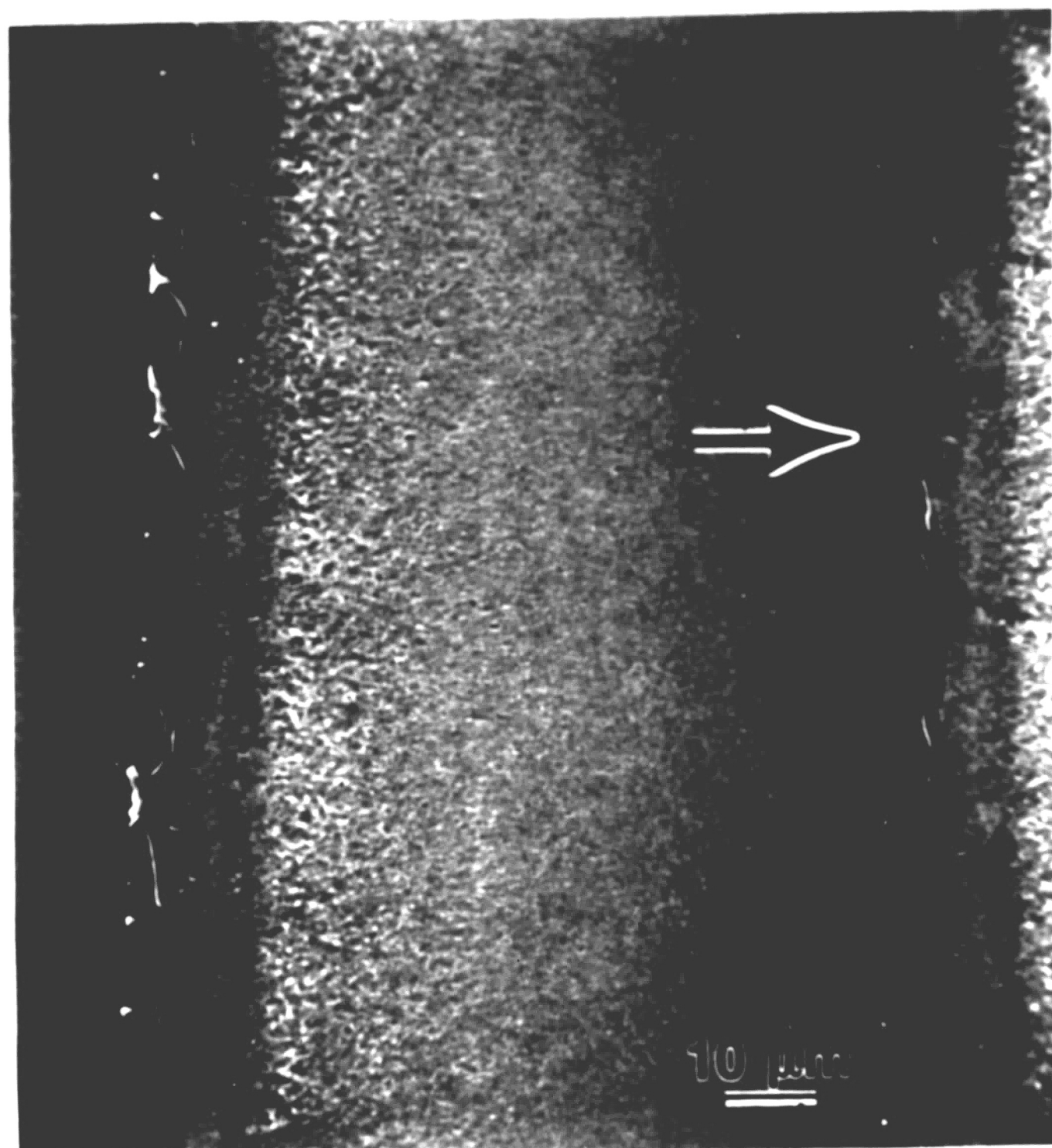


b

Figure 3-25: The Effect of Frequency on DGB Morphology at 22°C
 $\Delta K = 0.5 \text{ MPa}\sqrt{\text{m}}$, a) 1 Hz, b) 100 Hz



a



b

Figure 3-26: DGB Morphology as a Function of ΔK at 35°C
a) 1 Hz, $\Delta K = 0.5 \text{ MPa}\sqrt{\text{m}}$, b) 1 Hz, $\Delta K = 0.7 \text{ MPa}\sqrt{\text{m}}$

3.2.3 The DGB Stretch Zone

As previously indicated, the stretch zone separating each DGB is thought to represent the blunted profile of the crack tip after it has passed through the craze and arrested in fresh material.²¹ Since the stretch zone is a measure of the crack tip radius (see again Figure 1.2), then the crack opening displacement (COD) should correspond to twice this value and describe the extent of plastic straining at the crack front.²⁴ Accordingly, the yield strength and the COD are interrelated.

In order to determine if quantitative fracture surface measurements can be used to estimate the COD, stretch zone measurements were compared to corresponding values calculated from the stress intensity conditions and known material properties. In Figure 3.27, a one-to-one relationship is noted for measured and calculated values of the crack opening displacement for specimens tested at ambient temperatures and above at 100 Hz. For the frequency conditions of 1 & 10 Hz, however, observed stretch zone values were found to be approximately two times larger than those calculated (see Figures 3.28 - 3.29). No convenient explanation for this diminished correlation is available at this time. Although there is an effect of frequency/strain rate on the yield strength of most plastics, it was felt that such a correction in σ_{ys} would have had little effect on the room temperature data.³⁶ In addition, the correction for the effect of frequency on PVC at temperatures above room temperature was not available.

It is speculated that the additional time for deformation available at the lower frequencies enables the material to behave in a more viscous fashion, thereby resulting in greater stretch zone dimensions than those observed at the

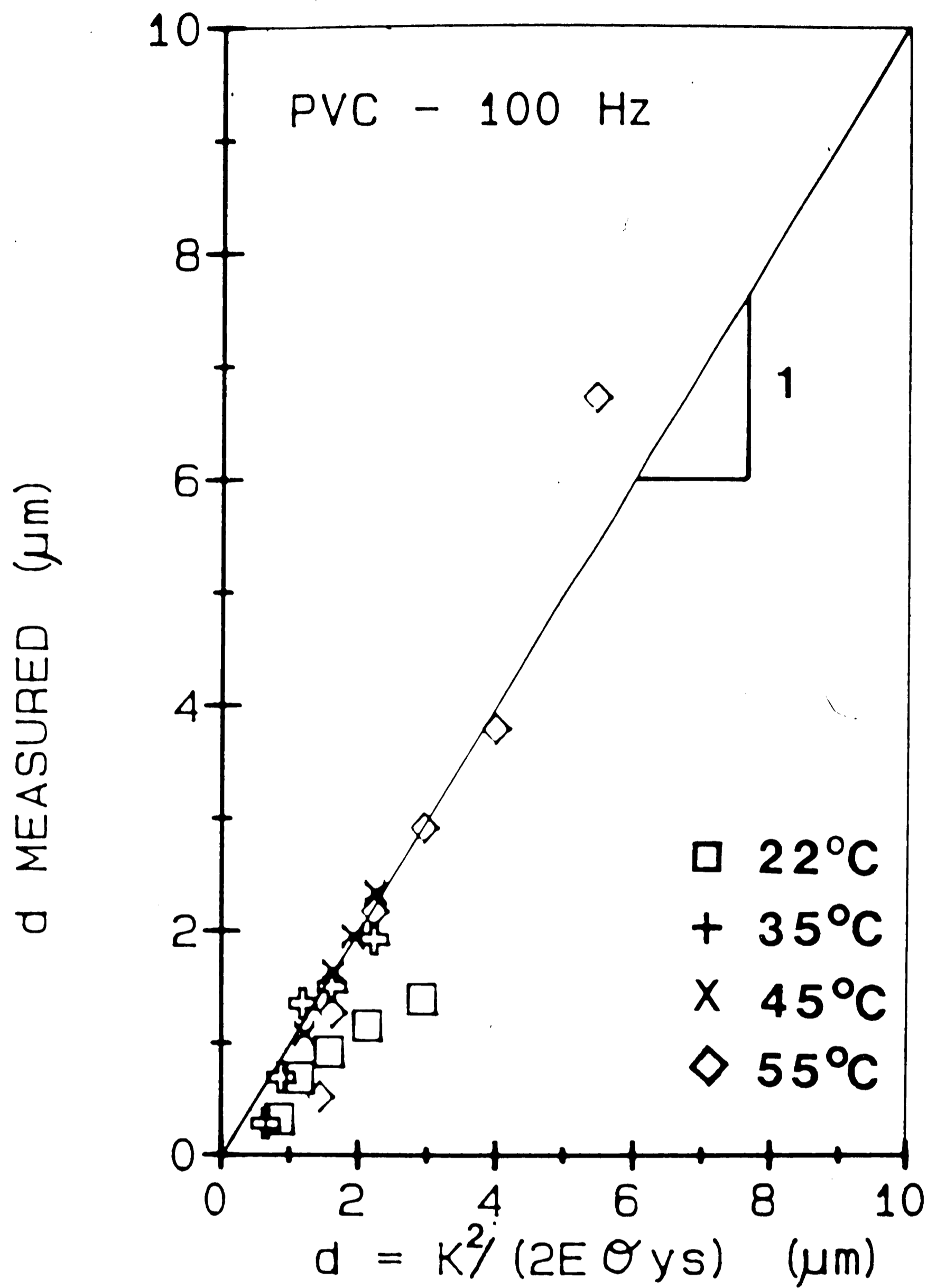


Figure 3-27: Correspondence of Measured and Calculated Stretch Zone Sizes at 100 Hz

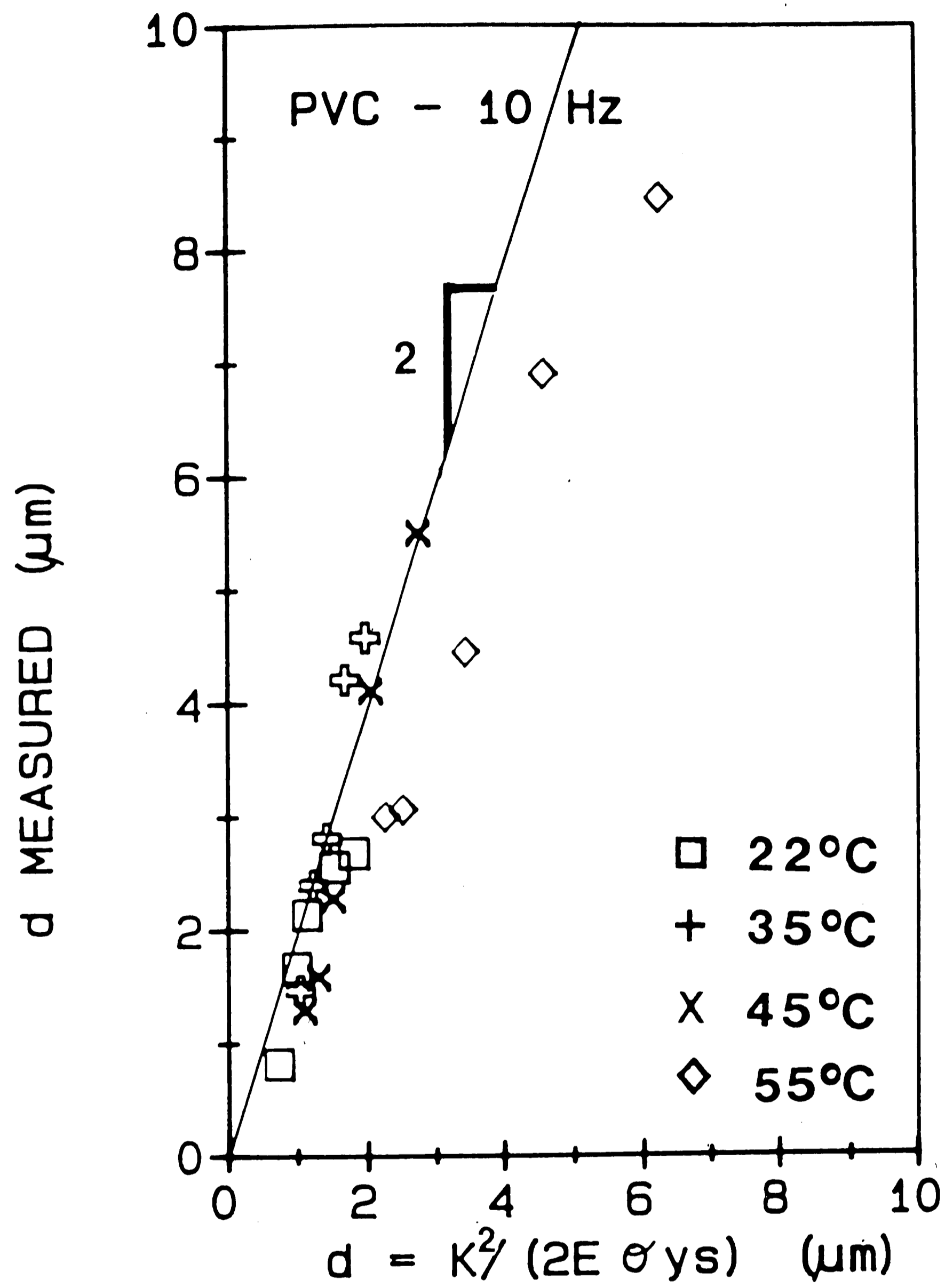


Figure 3-28: Comparison of Measured and Calculated Stretch Zone Sizes at 10 Hz

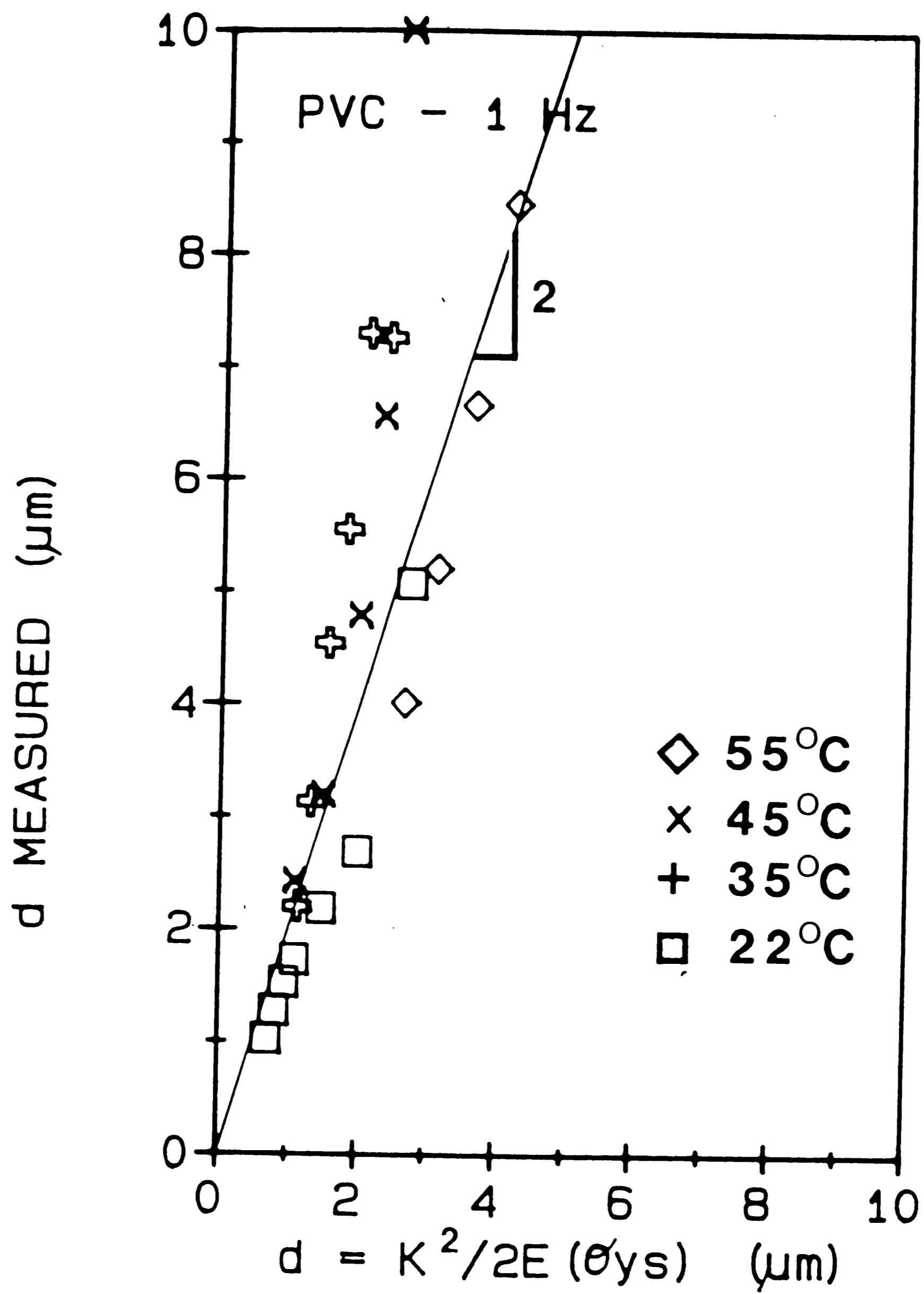


Figure 3-29: Comparison of Measured and Calculated Stretch Zone Sizes at 1 Hz

high frequency. At 100 Hz, the material is restricted in its deformation response, and therefore, exhibits a more elastic response. The one to one correspondence observed at 100 Hz is significant because it confirms that at this frequency (i.e. for elastic conditions) the stretch zone is indeed a measure of the crack tip radius and is equivalent to one-half the value of the COD.

The J-integral is another parameter that is used to describe fracture conditions in a component experiencing both elastic and plastic deformation. J is the energy made available at the crack tip per unit extension, and can be approximated by the crack driving force, G (i.e. fracture toughness) under elastic conditions.¹⁹ Therefore, J can be computed from either the Griffith energy criteria or from COD considerations (see Equations 1.6 and 1.7). The constant m in Equation 1.6 is used to allow for changes from the plane stress to plane strain state induced by changes in testing temperature.²⁵ In order to compare these two methods of calculating J, stretch zone measurements taken from samples tested at temperatures above ambient were used to infer the value of the J-integral. The inferred values were then compared to values computed from the Griffith energy criteria. A good correlation was seen between J values computed by the two different methods only at the 22°C, 100 Hz condition, similar to that observed in Figure 3.27 (see Figure 3.30). It is once again speculated that this is due to the predominately elastic behavior of this material in association with testing at 100 Hz.

J values calculated from COD considerations were found to be much larger than values calculated from Griffith energy criteria for frequency conditions at 1 & 10 Hz for temperatures at ambient and above, as illustrated in Figures 3.31 - 3.32. This suggests that at the frequencies of 1 and 10 Hz, the comparisons of

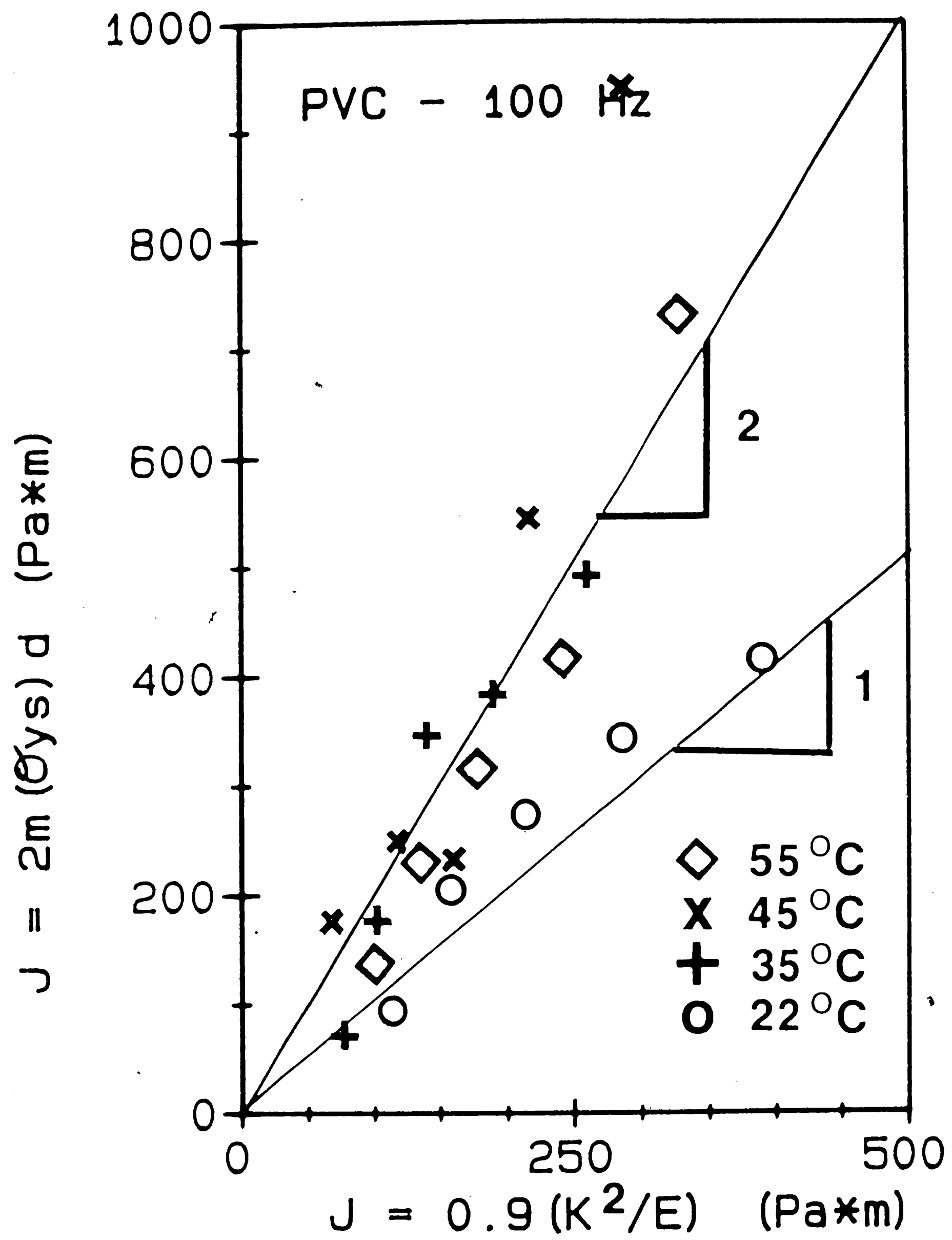


Figure 3-30: Relationship Between Calculated and Fractographically Inferred Values of the J-integral at 100 Hz

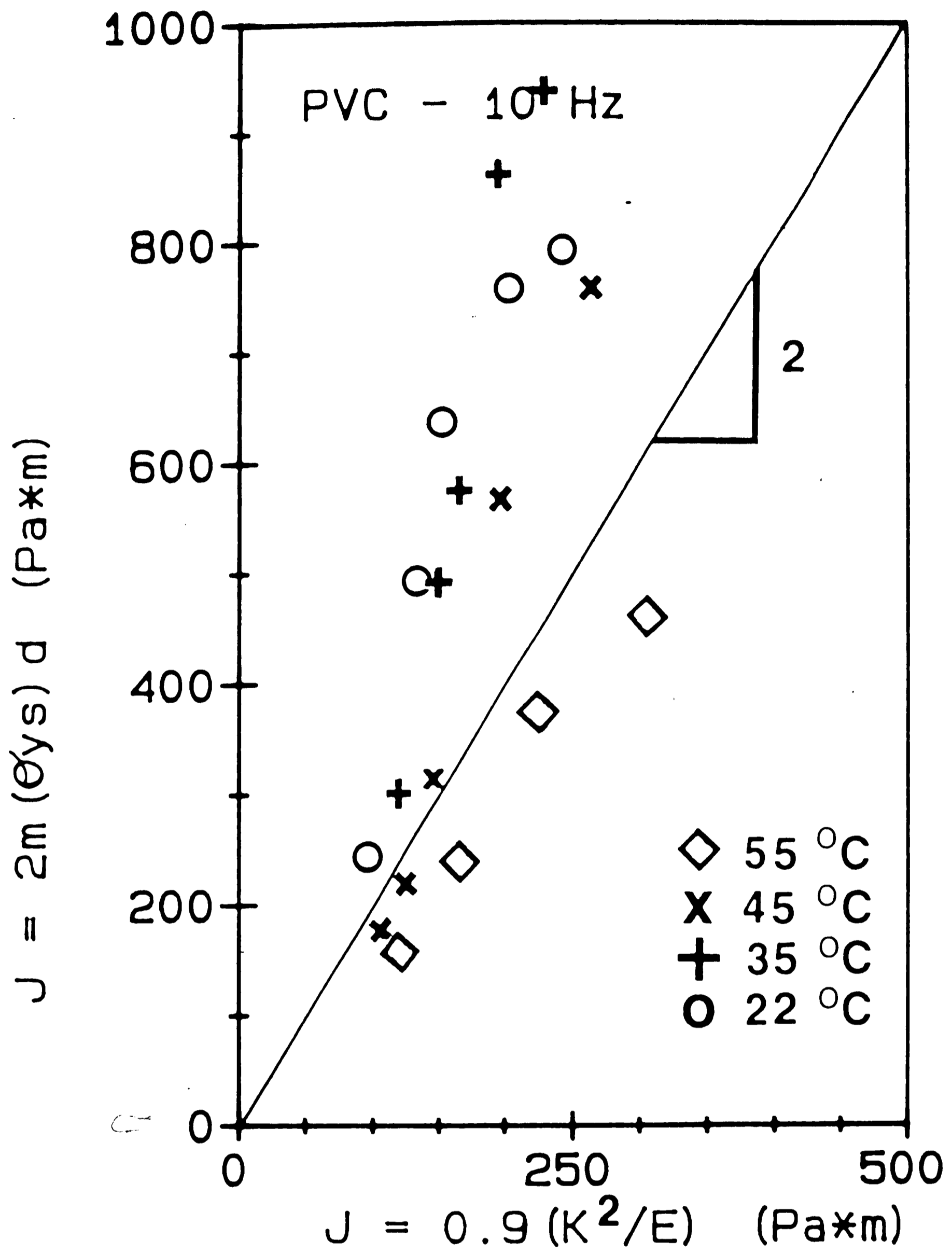


Figure 3-31: Comparison of Calculated and Fractographically Inferred Values of the J-integral at 10 Hz

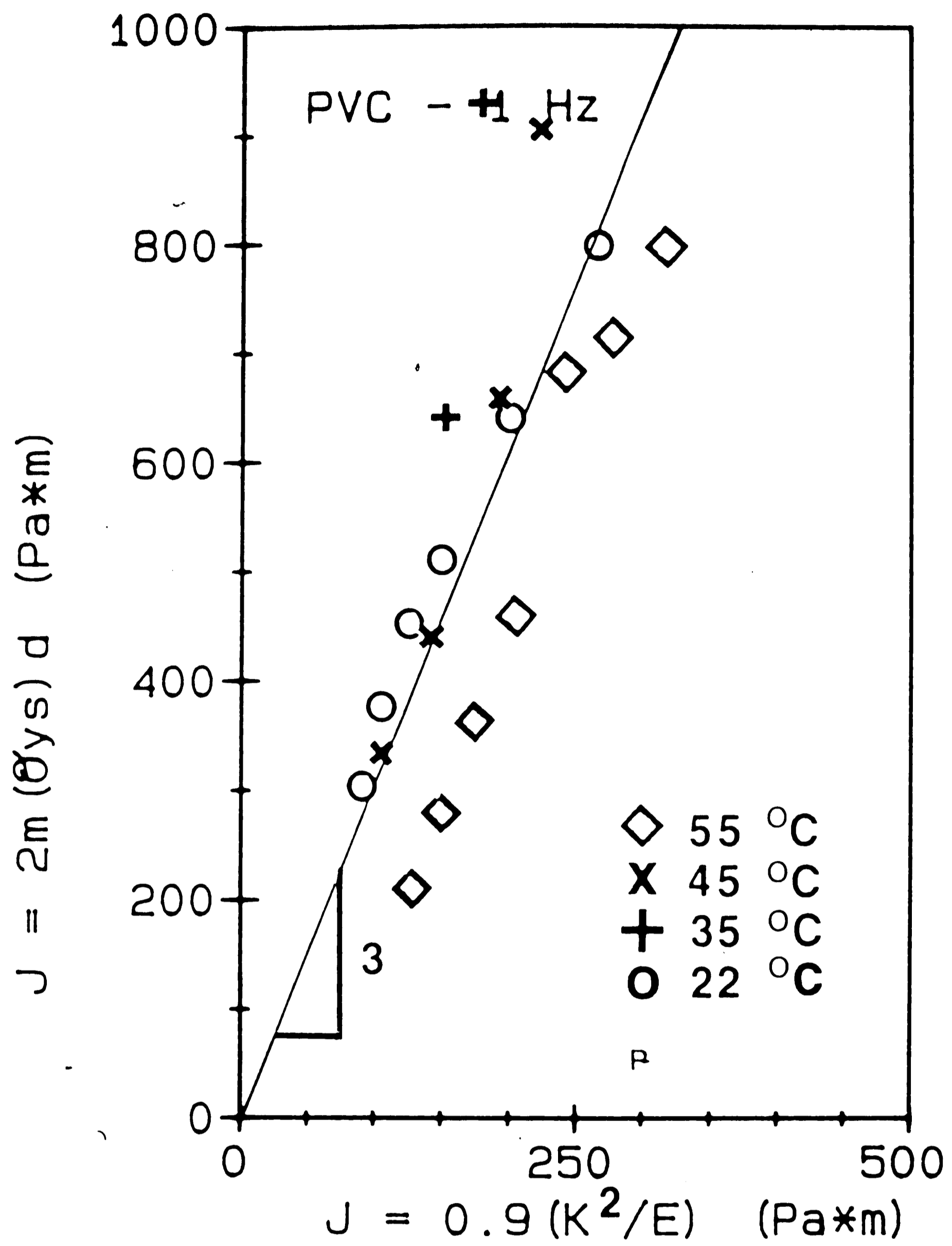


Figure 3-32: Comparison of Calculated and Fractographically Inferred Values of the J-integral at 1 Hz

inferred and calculated J values as well as measured and calculated stretch zone sizes are invalid due to the increased time-dependent plasticity of the material in association with longer testing times.

Chapter 4

Conclusions

1. The FCP resistance of this grade of poly(vinyl chloride) was found to improve with increasing frequency, as had been previously observed for PVC. As implied from time-temperature superposition principles, the FCP resistance of PVC improved with decreasing temperature as well.
2. An Arrhenius relationship is shown to exist between the fatigue crack growth rate and the inverse of the absolute temperature at the testing frequencies and stress intensity levels studied. The value of the apparent activation energy calculated using the Zhurkov/Bueche model was observed to be lower than the reported values of the activation energies for the alpha and beta peaks. However, the single value of the apparent activation energy found corresponds with a single type of fracture surface morphology observed - discontinuous crack extension.
3. Discontinuous growth band measurements revealed that the DGB sizes increased with increasing temperature and decreasing frequency, also in accordance with time-temperature superposition principles. A power of two relationship was not observed between the band size and the stress intensity range. This was attributed to strain hardening effects in this grade of PVC.

4. The expected influences of frequency and ΔK on DGB morphology was noted for specimens tested at room temperature and above. DGB's were produced at temperatures up to 55°C. When the testing temperature was increased above ambient, it was observed that the DGB void gradient became steeper and the stretch zone width became clearer. For specimens tested at temperatures below ambient, it appears that there is a series of fracture surface morphologies that are dependent on different testing conditions and stress levels. It is speculated that at 0 °C (the lowest temperature at which classical DGB's were observed) there is a transition between single craze and multiple craze deformation kinetics analogous to nucleation and growth in metals.

5. Measured DGB stretch zone sizes of specimens tested at 100 Hz for temperatures at ambient and above were found to correspond to calculated values of the crack opening displacement, confirming the hypothesis that the stretch zone represents the radius of the crack tip which blunts in fresh material upon passing through the craze. Subsequently, values of the J-integral calculated from measurements of the stretch zone at 100 Hz and temperatures at ambient and above were found to reasonably correspond to values calculated from material properties. Modifications are necessary when the above comparisons are made for specimens tested at frequencies of 1 and 10 Hz at the same temperature conditions.

REFERENCES

1. Hutchinson, S. J., Benham, P. P., *Plast. Polym.*, **102**, 1970, p. 102.
2. Sauer, J. A., Richardson, G. C., *Int. J. Fracture*, **16**, 1980, p. 449.
3. Manson, J. A., Hertzberg, R. W., *CRC Crit. Rev. Macromol. Sci.*, **1**, 1973, p. 433.
4. Brown, W. F., Strawley, J. E., *ASTM STP 410*, 1966.
5. Paris, P. C., *Proc. Sagamore Army Mater. Res. Conf.*, 10th Ed., 1964.
6. Hertzberg, R. W., Skibo, M. D., Manson, J. A., *ASTM STP 700*, 1980.
7. Skibo, M. D., Ph. D. Dissertation, Lehigh University, 1977.
8. Lang, R. W., Ph. D. Dissertation, Lehigh University, 1984.
9. Lang, R. W., Hahn, M. T., Hertzberg, R. W., Manson, J. A., *ASTM STP 833*, 1984.
10. Mai, Y. W., Williams, J. G., *J. Mater. Sci.*, **14**, 1979, p. 1933.
11. Kausch, H. H., *Polymer Fracture*, Springer-Verlag, Berlin, 1978.
12. Bueche, F., *J. Appl. Physics*, **26**, 1955, p. 1133.
13. Bueche, F., *J. Appl. Physics*, **28**, 1957, p. 784.
14. Bueche, F., *J. Appl. Physics*, **29**, 1958, p. 1231.
15. Donald, A. M., Kramer, E. J., *Phil. Mag. A*, **43**, 1981, p. 857.
16. Verheulpen-Heymans, N., *Deformation, Yield, and Fracture of Polymers*, Plastics and Rubber Institute, London, 1979, p. 35 - 1.
17. Verheulpen-Heymans, N., *Polymer*, **20**, 1979, p. 356.
18. Hertzberg, R. W., Manson, J. A., *Fatigue 1981*, England, 1981, p. 185.
19. Hertzberg, R. W., *Deformation and Fracture Mechanics of Engineering Materials*, Second Edition, Wiley, New York, 1983.
20. Dugdale, D. S., *J. Mech. Phys. Sol.*, **8**, 1960, p. 100.
21. Skibo, M. D., Hertzberg, R. W., Manson, J. A., Kim, S. L., *J. Mater. Sci.*, **12**, 1977, p. 531.

22. Rimnac, C. M., Hertzberg, R. W., Manson, J. A., ASTM STP 733, 1981.
23. McMeeking, R. M., *J. Mech. Phys. Sol.*, **25**, 1977, p. 357.
24. Amouzouvi, K. F., Bassim, M. N., *Mater. Sci. Eng.*, **55**, 1982, p. 257.
25. Hashemi, S., Williams, J. G., *Polymer*, **27**, 1986, p. 384.
26. Dynamit Nobel of America, Inc., "Properties of Trovidur 151 Rigid Extruded Clear PVC Sheets".
27. Hertzberg, R. W., Manson, J. A., Skibo, M. D., *Poly. Eng. Sci.*, **15**, 1975, p. 338.
28. Hertzberg, R. W., Manson, J. A., Skibo, M. D., *Polymer*, **19**, 1978, p. 358.
29. Hertzberg, R. W., Manson, J. A., *Fatigue of Engineering Plastics*, Academic Press, New York, 1980.
30. Weertman, J., *Trans ASM*, **61**, 1968, p. 681.
31. McCrum, N. G., Read, B. E., Williams, G., *Anelastic and Dielectric Effects in Polymeric Solids*, Wiley, New York, 1967.
32. Skibo, M. D., Hertzberg, R. W., Manson, J. A., *J. Mater. Sci.*, **11**, 1976, p. 479.
33. Rimnac, C. M., Ph. D. Dissertation, Lehigh University, 1983.
34. Argon, A. S., Hannoosh, J. G., *Phil. Mag.*, **36**, 1977, p. 1195.
35. Vincent, P. I., *Short-Term Strength and Impact Behavior*, Wiley, New York, 1974, p. 76.
36. Skibo, M. D., Unpublished Research.

Vita

Jill Denise Phillips was born on August 26, 1963 in Elizabeth, NJ to Darrell K. and Lorraine A. Phillips. She received her elementary and secondary education in the Union, NJ School District, and graduated from Union High School in 1981, where she was a member of the National Honor Society and voted to Who's Who Among American High School Students.

In June of 1985, Ms. Phillips graduated from Lafayette College with a Bachelor of Science degree in Metallurgical Engineering. While at Lafayette, she participated in several activities which included tutoring, peer counseling, involvement in the John Markle Metallurgical Society, and in her sorority, Pi Beta Phi. During the summer of 1984, she also participated in Bethlehem Steel Corporation's Summer Engineering Program.

Since August of 1985, Ms. Phillips has been a Research Assistant in the Department of Materials Science and Engineering at Lehigh University. During that time, she investigated the effects of temperature and frequency on the fatigue crack propagation behavior of PVC and has published several papers concerning this topic. Her course work has included the study of fracture mechanics and the deformation behavior of engineering materials.

Ms. Phillips joined Carpenter Technology Corporation in March of 1987 as an Assistant Metallurgist in the Laboratory Services area.